

Developmental plasticity at glutamatergic synapses in
mouse somatosensory cortex

Inaugural-Dissertation

zur

Erlangung des Doktorgrades der
Mathematisch-Naturwissenschaftlichen Fakultät
der Heinrich-Heine-Universität Düsseldorf

vorgelegt von

Corinna Gabriele Walz

aus Castrop-Rauxel

Februar 2008

Aus dem Institut für Neuro- und Sinnesphysiologie
der Heinrich-Heine-Universität Düsseldorf

Gedruckt mit der Genehmigung der
Mathematisch-Naturwissenschaftlichen Fakultät der
Heinrich-Heine-Universität Düsseldorf

Referent: Prof. Dr. K. Gottmann

Koreferent: Prof. Dr. C. Rose

Tag der mündlichen Prüfung: 23. April 2008

Abstract

The formation of synaptic networks in the developing neocortex is thought to involve the activity-dependent stabilization of presynaptically immature transmitter release sites. To study the maturation of glutamatergic synapses on layer Vb pyramidal neurons in mouse barrel cortex evoked AMPA receptor mediated excitatory postsynaptic currents were recorded. Paired-pulse minimal stimulation in acute slices at P7 revealed a high initial failure rate and a strong paired-pulse facilitation in about 25% of all synapses tested, indicating that a subset of synapses has a very low release probability. At P14 all synapses studied showed a low failure rate and paired-pulse depression suggesting a developmental maturation of the low release probability synapses observed at P7. The analysis of corresponding NMDA receptor mediated excitatory postsynaptic currents suggested a coupling of functional presynaptic maturation and postsynaptic maturation of NMDA receptor subunit composition. At P7, selective block of either NR2B or NR2A subunits revealed a larger amount of NR2A subunits in synapses with a high release probability, whereas synapses with a low release probability exclusively contained NR2B subunits. Additionally NMDA receptor only synapses were present, which contained mainly NR2B subunits. In summary, we obtained evidence for presynaptically immature glutamatergic synapses in layer Vb pyramidal neurons at P7 and for a tight coupling of pre- and postsynaptic maturation processes.

A candidate molecule to modulate synaptogenesis and network formation in the developing brain is the neurotrophin BDNF, which is known to play a crucial role in synaptic development and plasticity in the mammalian central nervous system. To study a possible involvement of BDNF as a retrograde messenger, single BDNF-deficient or wildtype neurons (EGFP expressing) were transplanted to organotypic slice cultures of the mouse neocortex. The transplanted cells were functionally integrated into the cortical tissue and showed no differences in their morphology and basic electrophysiological properties compared to endogenous slice culture neurons. A spatial mapping of the synaptic inputs on BDNF deficient neurons using *caged* glutamate photolysis revealed a strong influence of postsynaptic BDNF expression on the formation of inhibitory inputs, which were reduced as compared to transplanted wildtype neurons. Recordings of spontaneous, GABA_A receptor mediated miniature postsynaptic currents confirmed a reduction of functional GABAergic synapses on transplanted BDNF-deficient neurons. Therefore, the postsynaptic release of BDNF might promote the formation or functional maturation of GABAergic synapses through local retrograde actions.

Zusammenfassung

Die Bildung synaptischer Netzwerke im Neokortex während der Entwicklung schließt eine aktivitätsabhängige Stabilisierung präsynaptischer unreifer Freisetzungstellen ein. Um die Reifung glutamaterger Synapsen auf Pyramidenzellen der Schicht Vb im somatosensorischen Kortex der Maus zu untersuchen, wurden evozierte AMPA Rezeptor-vermittelte postsynaptische Ströme gemessen. „Paired pulse“-Stimulationen in akuten Hirnschnitten am postnatalen Tag 7 (P7) ließen eine hohe initiale Fehlerrate und eine starke Faszilitierung in 25% der synaptischen Antworten erkennen. Dies deutet auf eine extrem niedrige Freisetzungswahrscheinlichkeit in einem Teil der Synapsen hin. Ab P14 zeigten alle Synapsen im Gegensatz zu Beobachtungen an P7 eine sehr niedrige Fehlerrate und eine deutliche Depression in Antworten auf die „paired pulse“-Stimulation, was auf eine Reifung der Synapsen schließen lässt. Dazugehörige NMDA Rezeptor-vermittelte Antworten ließen eine Kopplung von präsynaptischer und postsynaptischer Reifung vermuten. Ein daraufhin durchgeführter selektiver Block der NR2B bzw. NR2A Untereinheiten des NMDA Rezeptors zeigte bei Synapsen mit einer sehr hohen Freisetzungswahrscheinlichkeit einen großen Anteil an NR2A Untereinheiten. Synapsen mit einer niedrigen Freisetzungswahrscheinlichkeit enthielten ausschließlich NMDA Rezeptoren mit NR2B Untereinheiten. Zusätzlich konnten Synapsen beobachtet werden, die ausschließlich funktionelle NMDA Rezeptoren aufwiesen, welche aus NR2B Untereinheiten bestanden. Diese Resultate deuten auf eine enge Kopplung von präsynaptischen und postsynaptischen Reifungsprozessen hin.

Als modulierender Faktor während der Synaptogenese des sich entwickelnden Gehirns wird das Neurotrophin BDNF diskutiert, welchem eine wichtige Rolle bei der synaptischen Entwicklung und Plastizität im zentralen Nervensystem der Säugetiere zugesprochen wird. Um den Einfluss von BDNF als retrograder Botenstoff zu untersuchen, wurden BDNF-defiziente Neurone in organotypische Hirnschnittkulturen transplantiert. Die transplantierten Zellen waren voll funktionsfähig integriert und zeigten keine Unterschiede bezüglich ihrer Morphologie und elektrophysiologischer Eigenschaften. Eine räumliche Kartierung der synaptischen Eingänge dieser Neurone mittels *caged* Glutamat Photolyse verdeutlichte einen starken Einfluss auf die Ausbildung inhibitorischer Eingänge. Die Messung spontaner postsynaptischer Miniaturströme bestätigte eine Reduktion funktioneller GABAerger Synapsen auf die transplantierten BDNF-defizienten Neurone. Daraus lässt sich schließen, dass die Freisetzung von BDNF die Bildung oder Proliferation GABAerger Synapsen durch eine lokale retrograde Wirkung fördert.

Contents

1.	Introduction	3
1.1	Development and organization of the neocortex.....	3
1.2	Principles of synaptic transmission.....	5
1.3	The glutamatergic synapse (Gray type I).....	6
1.4	The GABAergic synapse (Gray type II).....	9
1.5	Long-term plasticity of glutamatergic synapses.....	11
1.5.1	Plasticity at presynapses.....	13
1.5.2	Plasticity at postsynapses.....	13
1.5.3	Plasticity at „silent“synapses.....	13
1.6	Neurotrophins.....	15
1.7	Aims of the study.....	17
2.	Materials and Methods	19
2.1	Chemicals.....	19
2.2	Media and Solution.....	19
2.3	Creation and genotyping of genetically modified mice.....	22
2.4	Slices of the mouse neocortex.....	24
2.4.1	Preparation of acute slices.....	24
2.4.2	Preparation of neocortical slice cultures.....	26
2.4.3	Coculture of neocortical slices and EGFP-expressing neurons.....	26
2.5	Principles of the patch clamp technique.....	27
2.6	Experimental setup for patch clamp experiments in acute slices.....	30
2.7	Production of glass pipettes.....	32
2.8	Electrophysiological experiments.....	32
2.8.1	Recordings of postsynaptic currents evoked by extracellular stimulation	32
2.8.2	Recordings of spontaneous miniature postsynaptic currents.....	33
2.8.3	Recordings of synaptic activity in single EGFP-expressing neurons.....	33

2.9	Analysis of electrophysiological recordings.....	33
2.9.1	Analysis of postsynaptic currents evoked by extracellular stimulation.....	33
2.9.2	Analysis of spontaneous miniature postsynaptic currents.....	34
2.9.3	Analysis of synaptic activity in single EGFP-expressing neurons	34
2.10	Principles of „caged glutamate“ photolysis.....	35
2.11	Experimental setup for photolysis induced activity in cocultures.....	36
2.12	Mapping of photolysis induced activity.....	37
2.13	Analysis of photolysis induced activity.....	37
2.14	Data analysis and statistics.....	39
2.15	Histology	39
2.15.1	Histological staining of cortical slices.....	39
2.15.2	Visualization and reconstruction of single neurons.....	40
3.	Results	42
3.1	Characterization of AMPA receptor-mediated EPSCs in layer Vb pyramidal neurons.....	42
3.1.1	Morphology and basic electrophysiology of layer Vb pyramidal neurons at P7.....	42
3.1.2	Presynaptic properties of immature glutamatergic synapses on layer Vb pyramidal neurons.....	44
3.1.3	Developmental changes of presynaptic properties of glutamatergic synapses on layer Vb pyramidal neurons.....	48
3.2	Characterization of NMDA-receptors in immature layer Vb pyramidal neurons.....	52
3.2.1	NMDA-receptor only synapses on immature layer Vb pyramidal neurons.....	54
3.2.2	NMDA-receptor subunit composition at immature and mature synapses on layer Vb pyramidal neurons at P7.....	55
3.2.3	Differences in release probability as indicated by MK801 block of NMDA receptors.....	59
3.2.3	Pairing-induced potentiation of immature synapses in layer Vb pyramidal neurons.....	61

3.3	Spatial mapping of synaptic inputs onto BDNF-deficient neurons transplanted to wildtype organotypic slice cultures.....	64
3.3.1	Morphology and basic electrophysiology of transplanted BDNF-deficient neurons.....	64
3.3.2	Properties of photolysis-induced synaptic activity.....	67
3.3.3	Synaptic inputs on transplanted BDNF-deficient neurons.....	70
3.3.4	Comparison of transplanted wildtype and endogenous neurons in organotypic slice cultures.....	75
3.3.5	Quantitative analysis of synaptic inputs on transplanted BDNF-deficient neurons.....	77
3.3.6	GABA _A -receptor mediated miniature postsynaptic currents in transplanted BDNF- deficient neurons.....	79
4.	Discussion	81
4.1	Presynaptic maturation of glutamatergic synapses in layer Vb pyramidal neurons.....	81
4.1.1	Morphology and basic electrophysiology of immature layer Vb pyramidal neurons.....	81
4.1.2	Presynaptic properties of immature glutamatergic synapses on layer Vb pyramidal neurons.....	82
4.1.3	Changes of presynaptic properties in layer Vb pyramidal neurons during postnatal development.....	84
4.2	Developmental changes of postsynaptic NMDA-receptor properties in layer Vb pyramidal neurons.....	85
4.2.1	NMDA receptor only synapses on immature layer Vb pyramidal neurons.....	87
4.2.2	Changes in NMDA-receptor subunit composition during developmental maturation of glutamatergic synapses.....	87
4.2.3	Changes in release probability at different developmental stages.....	89
4.3	Pairing-induced potentiation of immature synapses in layer Vb pyramidal neurons.....	90
4.4	Spatial mapping of synaptic inputs onto single BDNF-deficient neurons transplanted to wildtype organotypic slice cultures.....	92

4.4.1	Morphology and basic electrophysiology of transplanted BDNF-deficient neurons.....	92
4.4.2	Properties of photolysis-induced synaptic activity.....	93
4.4.3	Comparison of transplanted and endogenous neurons in organotypic slice cultures.....	95
4.4.4	Synaptic inputs on transplanted BDNF-deficient neurons.....	95
4.4.5	Quantitative analysis of synaptic inputs onto transplanted BDNF-deficient neurons.....	96
4.4.6	GABA _A -receptor mediated miniature currents in transplanted BDNF-deficient neurons.....	97
5.	References	101
6.	Appendix	121
6.1	Abbreviations	121
6.2	List of figures and tables.....	122
6.3	TIDA Makrofunktionen.....	124
6.4	Rasterprogramm.....	126
6.5	Curriculum Vitae.....	128
6.6	Publications	129
7.	Acknowledgements	130

1. Introduction

In the present study early developmental changes of central synapses at the presynaptic as well as the postsynaptic side were investigated in neocortical slices of mice. Furthermore, the coordination between presynaptic and postsynaptic maturation was analysed and a possible function of the neurotrophic factor BDNF was studied. Therefore, the introduction will focus on development and organization of the neocortex and plasticity at the pre- and postsynaptic side. Besides the current basic knowledge on synaptic transmission, also a short overview of the structure and function of glutamatergic and GABAergic synapses will be given. In addition, the neurotrophins in general and especially BDNF will be introduced. Finally, the aim of the study will be defined.

1.1 Development and organization of the neocortex

The study of neural development describes the cellular and molecular mechanisms by which complex nervous systems emerge during embryonic development and that underlie plasticity throughout life. Some landmarks of embryonic neural development include the birth and differentiation of neurons from stem cells, the migration of immature neurons to their final positions, outgrowth of axons from neurons and guidance of the motile growth cone towards postsynaptic partners, the generation of synapses between these axons and their postsynaptic partners, and finally the lifelong changes in synapses which are thought to underlie learning and memory. Typically, these neurodevelopmental processes can be broadly divided into two classes: activity-independent mechanisms, which are generally believed to represent processes that are determined by genetic programs (like differentiation, migration or axon guidance), and activity-dependent mechanisms. Activity-dependent mechanisms include for example the stabilization of newly formed synapses by neural activity and sensory experience, as well as synaptic plasticity, which will be responsible for the refinement of the nascent neural circuits.

The cerebral cortex develops from the cortical plate that is itself embedded in the primordial cortical preplate (fig. 1.1). As the cortical plate expands, it splits the preplate into a superficial layer (marginal zone) and a Subplate that lies beneath the cortical plate at its boundary with the white matter. Finally, the cortical plate differentiates into cortical layers II to VI (Supér and Uylings, 2001; Kageyama and Robertson, 1993) that can be distinguished by the appearance of different cell-types (Peters and Kara, 1985; Sur and Cowey, 1995). The formation of layers occurs in an inside-out order, i.e. first the deep layers are formed, the

layers above are built afterwards as has been shown with the BrdU-method (Takahashi et al., 1999). As an exception layer I (so-called “*molecular layer*”) is found already at the start of corticogenesis (Rakic, 1972) and consists largely of glia cells and axons, respectively dendrites from neurons from deeper layers. Layer II (“*external granular layer*”) has a high density of small pyramidal neurons and numerous stellate neurons, whereas layer III (“*the external pyramidal layer*”) predominantly contains small and middle-sized pyramidal neurons. In contrast to that, layer IV (“*the internal granular layer*”) includes mainly non-pyramidal cells and has a broad appearance in the sensory cortex. Characteristically, layer V (“*the internal pyramidal layer*”) neurons are the biggest pyramidal cells found in the cortex and layer VI (“*the multiform layer*”) contains few big pyramidal neurons as well as many small spindle-like pyramidal and multiform neurons and projects to the thalamus. Below these layers the white matter is found, which consists for the most part of myelinated axons. All of these cortical layers are not simply stacked one over the other; characteristic connections between different layers and neuronal types exist, which span all the thickness of the cortex. These cortical microcircuits are functionally regrouped into cortical columns, which have been proposed to be the basic functional units of the cortex (Mountcastle, 1997). Later work has provided evidence for the presence of functionally-distinct cortical columns in the visual cortex (Hubel and Wiesel, 1959), auditory cortex and associative cortex (Tanaka, 2003).

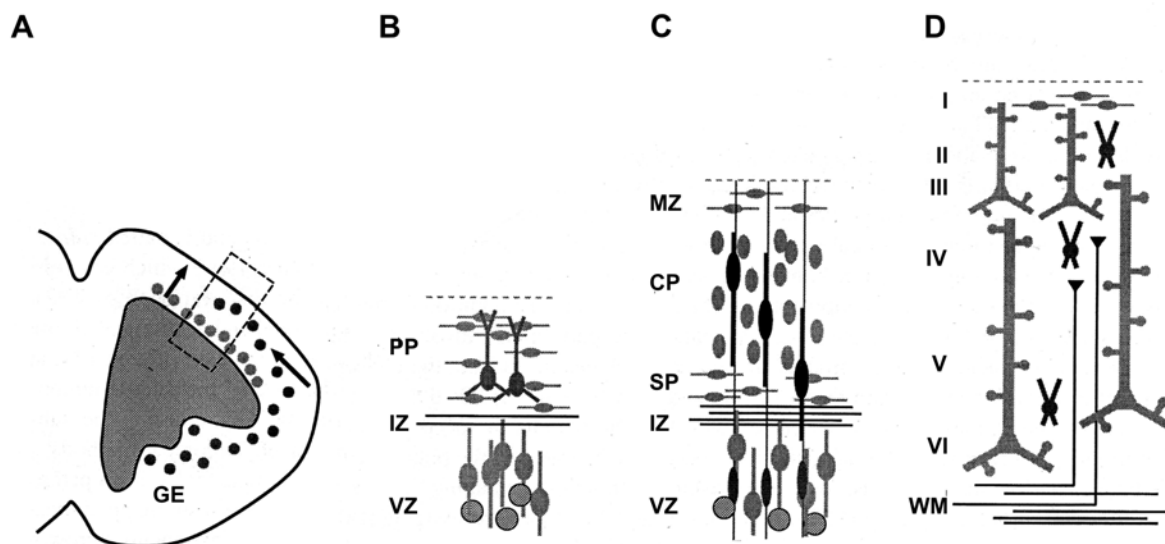


Fig. 1.1: Development of the cerebral cortex.

The sequence of increasing cortical organization in a typical region of the telencephalic wall (A, *dashed rectangle*) is shown for the early (B), middle (C) and late (D) phase of embryonic development. GE: ganglionic eminence; PP: preplate; IZ: intermediate zone; VZ; ventricular zone; MZ: marginal zone; CP: cortical plate; SP: subplate; roman numbers I to VI: cortical layer I to VI; WM: white matter (modified from Parnavelas, 2000). Arrows indicate cell migration.

1.2 Principles of synaptic transmission

The word "synapse" was coined by Sir Charles Scott Sherrington and his colleagues and derives from the Greek "syn-" ("together") and "haptain" ("to clasp"). Synapses can be either chemical or electrical, whereas in organisms, electrical synapse-based systems co-exist with chemical-based, but are limited to systems that require the fastest possible response. At the molecular level electrical synapses consist of two hexameres of connexin proteins, one contributed by each cell at the synapse (Kandel et al., 2000; Bennett and Zukin, 2004; Hormuzdi et al., 2004), which form a direct connection between cell lumina and in this way couple the neurons electrically. That kind of direct connection between neurons does not exist at chemical synapses. Here, the excitation of a presynaptic neuron is passed down to the postsynaptic neuron via chemical messengers, the neurotransmitters, and is afterwards transformed back to electrical excitation (Collingridge and Lester, 1989). Neurotransmitters are stored in vesicles and are released in case of excitation of the presynaptic cell (fig. 1.2). Hence, the synthesis is temporally separated from the release of neurotransmitters. Very high concentrations of transmitter are achieved in the synaptic vesicles (Schikorski and Stevens, 1997; Conti and Weinberg, 1999), which can be rapidly secreted into the synaptic cleft in relatively constant quantities. The secretion itself is coupled to a presynaptic depolarization by voltage-dependent Ca^{2+} -channels (Augustine et al., 1987; Fillenz, 1995; Schneggenburger and Neher, 2000). The increased Ca^{2+} -concentration leads to a conformation change of a protein complex between presynaptic membrane and vesicle membrane (Bajjalieh and Scheller, 1995; Benfenati et al., 1999), which in turn leads to fusion of the membranes and thereafter release of transmitter into the synaptic cleft. It has been proposed, that upon depolarization of the presynaptic terminal only a single vesicle is released. In the statistical sense, the release is not a confidential occurrence, but takes only place with a certain probability (Redman, 1990; Bolshakov and Siegelbaum, 1995; Auger and Marty, 2000). The absence of release despite a presynaptic depolarization is called "failure".

In principle the effect of neurotransmitters (exciting or inhibiting) is determined by specific receptors in the postsynaptic membrane. These receptors cause either directly, as ligand-gated ion channels, or indirectly, as G-protein coupled metabotropic receptors, a change of conductivity of the postsynaptic membrane (Wisden and Seeburg, 1993; Nakanishi et al., 1994; Hollmann and Heinemann, 1994). Depending on depolarization or hyperpolarization of the postsynaptic neuron, the transmitter will act in an exciting or inhibiting way. By spatial and temporal integration of inputs from a large number of synapses, an action potential can be

generated in the postsynaptic neuron, which thereupon can lead to release of transmitter at the downstream presynaptic terminals (Mainen and Sejnowski, 1996).

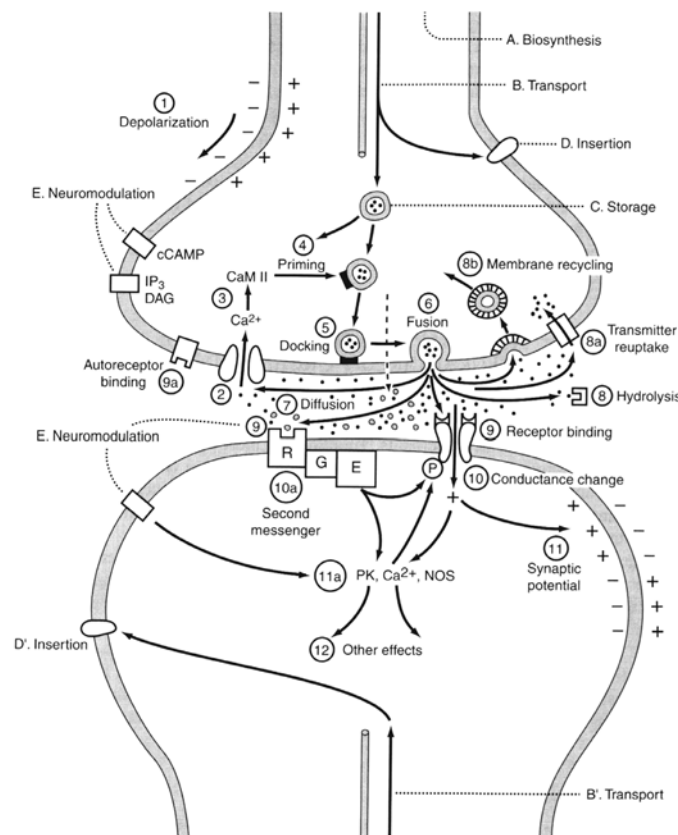


Fig. 1.2: Summary of some main mechanisms involved in immediate signaling at the synapse.

Steps 1 to 12 show some of the most important mechanisms that are involved in synaptic transmission at chemical synapses. IP₃: inositol triphosphate; AC: adenylate cyclase; CaM II: Ca/calmodulin-dependent protein kinase II; DAG: diacylglycerol; G: G-protein; PK: protein kinase; R: receptor (modified from Shepherd, 1994).

1.3 The glutamatergic synapse (Gray type I)

Synapses in the brain can be arranged in two groups: those with asymmetrical densification of their presynaptic and postsynaptic membranes and those with symmetrical densification, termed *Gray type I* and *Gray type II*, respectively (Gray et al., 1959). *Type I* usually is associated with small, round, clear synaptic vesicles, and has been implicated in excitatory actions, whereas *type II* is usually associated with small, clear, flattened or pleomorphic vesicles and is implicated in inhibitory synaptic actions. Glutamatergic synapses belong to the *Gray type I* and their transmitter L-glutamate is the most important excitatory one in the central nervous system (CNS) (Mayer and Westbrook, 1987; Collingridge and Lester, 1989). At glutamatergic synapses the receptors can be divided into two groups regarding their

electrophysiological and pharmacological properties: Ionotropic receptors and metabotropic receptors, which differ concerning their sequence homologies and their transduction mechanisms. Metabotropic glutamate receptors are supposed to mediate modulatory functions (Nakanishi, 1994; Pin and Duvoisin, 1995; Cheyne and Montgomery, 2007; Kulla and Manahan-Vaughan, 2008; Morishita and Malenka, 2008) and plasticity processes like long-term potentiation (LTP) and long-term depression (LTD) (Bortolotto et al., 1994; Manahan-Vaughan and Braunewell, 2005; Harney et al., 2006; Kullmann and Lamsa, 2008). These 7-transmembrane receptors activate their effectors via G-proteins and “second messenger”-cascades, whereupon this indirect actions lead to ion currents with an outstanding long latency (Gasic and Hollmann, 1992; Tanabe et al., 1992, Nakanishi, 1994; Pin and Duvoisin, 1995).

Ionotropic glutamate receptors display ligand-gated ion channels, which can be opened by binding of L-glutamate. These receptors are heteromeres, whose channel pore consists of 4 homologue subunits (Premkumar and Auerbach, 1997; Rosenmund et al., 1998). According to their specificity to selective agonists they are further subdivided into 3 groups (Lodge and Johnson, 1990; Watkins et al., 1990): (1) AMPA- (α -amino-3-hydroxy-5-methylisoxazol-4-propionacid)-receptors, (2) Kainat-receptors and NMDA- (*N*-methyl-D-aspartate)-receptors. Upon binding of the neurotransmitter L-glutamate they change their conformation and the ion channel is opened. Postsynaptic currents mediated by those channels are characterized electrophysiologically by a fast rise- and decay-time.

So far, four different AMPA-receptor subunits are described (GluR1-4), which can build AMPA-receptors in different compositions (Hollmann and Heinemann, 1994; Pandis et al., 2006; Gomes et al., 2007; Greger et al, 2007; Biou et al., 2008). Most AMPA-receptors have a very low conductivity for Ca^{2+} -ions that is caused by a post-transcriptional “editing” mechanism, which leads to an exchange of arginin to glutamine in the GluR2 subunit. The affinity of AMPA-receptors to L-glutamate is rather low (Patneau and Mayer, 1990; Hestrin, 1992).

Kainat-receptors consist of GluR5-7 and KA1-2 subunits and can be located at the presynaptic as well as at the postsynaptic membrane (Schmitz et al., 2000; Nicoll et al., 2000). Kainat-receptor mediated postsynaptic currents (PSCs) have a very small amplitude and are involved in presynaptic modulation of transmitter release (Li et al., 1999; Kidd and Isaac, 1999, Kullmann et al., 2001; Huettner et al., 2003; Braga et al., 2003; Pinheiro et al., 2005; Rodriguez-Moreno, 2006; Wu et al., 2007; Mathew et al., 2008).

NMDA-receptors are composed of at least one NR1 subunit and several NR2 (A-D) subunits (Hollmann and Heinemann, 1994), with the NR2 subunits having a high impact on the

biophysical properties of the receptors (Monyer et al., 1994; Erreger et al., 2007). In contrast to the fast PSCs mediated by AMPA- and Kainate-receptors, the action of glutamate through NMDA-receptors is more complicated (reviewed by Ascher and Nowak, 1988). The NMDA-receptor possesses some extraordinary properties that suggest an involvement in important physiological functions, for example in synaptic plasticity. Beside a very high affinity to glutamate, these receptors also have a high conductivity for Ca^{2+} ions (Ascher and Nowak, 1988; MacDermott et al., 1986; McBain and Mayer, 1994). Because of its important role (Ca^{2+} as intracellular “second messenger”), different signal cascades are triggered by an activation of synaptic NMDA-receptors. Moreover, the NMDA-receptor presents a molecular coincidence-detector, i.e. it can only be activated at simultaneous presynaptic and postsynaptic excitation. This is caused by a voltage-dependent Mg^{2+} -block, these ions lock up the channel pore at resting membrane potential (Mayer et al., 1984; Nowak et al., 1984; Monyer et al., 1994). Upon depolarization of the membrane to more than -40 mV the Mg^{2+} ions are crowded out of the pore and cations can pass the channel. NR2C subunit containing NMDA-receptors usually have a low Mg^{2+} sensitivity (Monyer et al., 1994; Fleidervish et al., 1998). Furthermore, for a full activation of the NMDA-receptor glycine or an endogenous glycine-like molecule has to be bound (Johnson and Ascher, 1987; Kleckner and Dingledine, 1988; Hollmann and Heinemann, 1994). Therefore, glycine is named the co-agonist of NMDA-receptors. Additionally, the receptor can be activated by polyamines (Nowak et al., 1984; McGurk et al., 1990; Monyer et al., 1994) and inhibited by Zn^{2+} ions (Christine and Choi, 1990; Legendre and Westbrook, 1990).

AMPA- and NMDA-receptors are most often co-localized at cortical synapses (Bekkers and Stevens, 1989; McBain and Dingledine, 1992; McBain and Mayer, 1994). Hence, the excitatory PSCs (EPSCs) at glutamatergic synapses consist of two different components: a fast AMPA-receptor mediated component (Edmonds et al., 1995) and a much slower NMDA-receptor mediated one (Bekkers and Stevens, 1989; Forsythe and Westbrook, 1988; Mayer and Westbrook, 1987; Sansom and Usherwood, 1990). NMDA-receptor mediated currents show a quite slow rise time (~20 ms) and last up to several hundred milliseconds (McBain and Mayer, 1994; Edmonds et al., 1995; Mori and Mishina, 1995). A developmental change of the decay kinetics has been described (Carmignoto and Vicini, 1992; Hestrin, 1992; Khazipov et al., 1995; Gottmann et al., 1997; Hoffmann et al., 2000), which presumably is caused by a change of NMDA-receptor subunit composition (Flint et al., 1997; Hoffmann et al., 2000).

With scaffolding proteins, glutamate-receptors are associated to the so-called “postsynaptic density”. So, AMPA-receptors are anchored via the proteins GRIP and PSD-95 (Dong et al., 1997; Braithwaite et al., 2000; Schnell et al., 2002; Dakoji et al., 2003; Elias et al., 2006), whereas NMDA-receptors are anchored via the protein PSD-95 (Kornau et al., 1995; Sheng, 1997; El-Husseini, 2000; Gardoni, 2001). Beside the anchoring proteins, this structure contains filamentous proteins like tubulins, actins and spectrins (Sedman et al., 1986; Adam and Matus, 1996; Kennedy, 1997; Sheng and Pak, 2000). The largest amount of postsynaptic associated protein is represented by Ca^{2+} -calmodulin dependent protein kinase II (CaMKII), which plays an important role in synaptic plasticity (Barria et al., 1997; Otmakhov et al., 1997; Giese et al., 1998; Elgersma and Silva, 1999; Skibinska-Kijek et al., 2007; Zhou et al., 2007).

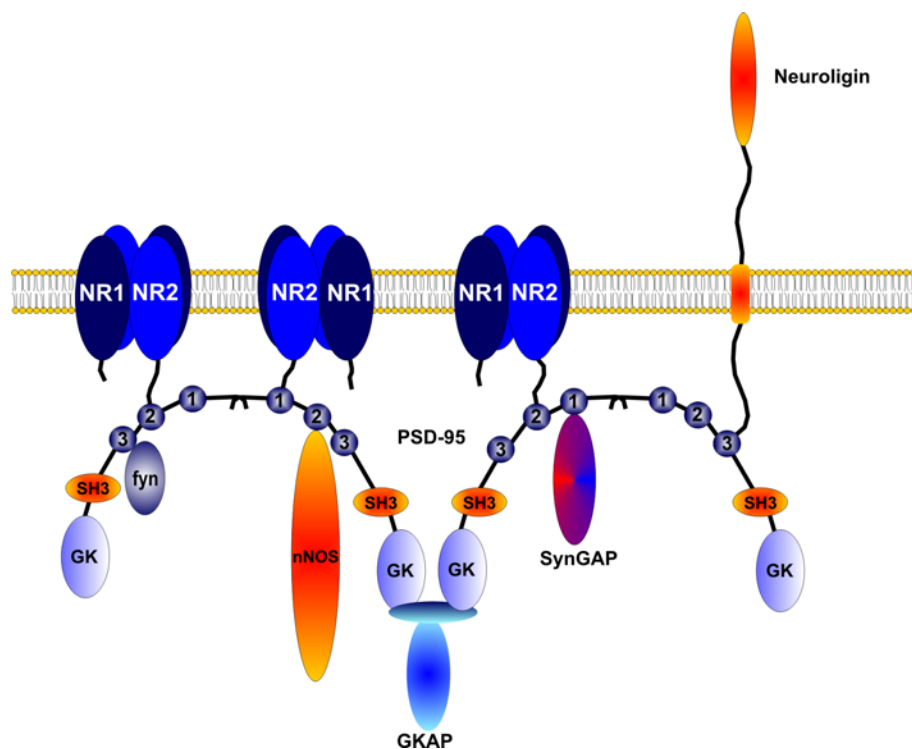


Fig. 1.3: Model of different intracellular interactions of the NMDA-receptor.

The NMDA-receptor interacts on the molecular level with different postsynaptic adapter- and effector-proteins. Domains in the PSD-95: “1”, “2” and “3”: PDZ-domains; SH3-domain; GK-domain (modified from Sheng and Pak, 2000).

1.4 The GABAergic synapse (Gray type II)

GABAergic synapses belong to the *Gray type II* and their transmitter γ -aminobutyric acid (GABA) is the most important inhibitory one in the CNS (Krnjevic, 1974; Fagg and Foster,

1983; Sivilotti and Nistri, 1991). In the cerebral cortex and thalamus GABA releasing cells account for approximately 20% to 30% of all neurons. The group of neurons that uses GABA as a neurotransmitter are instrumental in defining and confining the response properties not only of single neurons, but also of large neuronal circuits. In early postnatal development GABA is able to mediate excitation, because the Cl⁻ ion transporters (KCC-1, -2 and -3), which establish the chloride gradient between extracellular and intracellular space, are not functionally expressed yet (Cherubini et al., 1991; Rivera et al., 1999; Demarque et al., 2004). Generally, the release of GABA leads to generation of inhibitory postsynaptic potentials (IPSPs). There exist three major types of GABA-receptors, which are referred to as (1) GABA_A, (2) GABA_B and (3) GABA_C (Sivilotti and Nistri, 1991; Bormann, 2000; Bowery et al., 2002; Jentsch et al., 2002). GABA_A-receptors are ionotropic receptors, permeable for Cl⁻ ions and located mainly at the postsynaptic side (Bormann, 1988; Kaila, 1994; McDonald and Olson, 1994), where their anchorage is mediated by the cytoskeleton-binding protein gephyrin (Essrich et al., 1998; Kneussel et al., 1999; Ramming et al., 2000; Kneussel and Betz, 2000). Furthermore GABARAP („GABA_A-receptor associated protein“) may play a role in anchoring, because it can bind both at the γ 2-subunit of GABA_A-receptors and N-terminal microtubules (Wang et al., 1999; Wang and Olsen, 2000).

GABA_B-receptors belong to the metabotropic receptors, whose transduction is mediated via “second messenger” cascades (Bowery, 1989; Sivilotti and Nistri, 1991; Marshall et al., 1999).

The last type, GABA_C-receptors, is in turn an ionotropic receptor, which conducts Cl⁻ ions and is most pronounced in the retina (Feigenspan and Bormann, 1994; Bormann, 2000), but it can be detected also in the colliculus superior (Pasternack et al., 1999; Schmidt et al., 2001; Boller et al., 2001). An interaction with the microtubule associated protein MAP1B has been shown (Hanley et al., 1999).

The selectivity of GABA_A-receptors to Cl⁻ ions leads to a reversal potential of GABA_A-receptor mediated responses that is at the equilibrium potential for Cl⁻ (~ -75 mV). Fast GABA_A-receptor mediated IPSPs possess a rapid rising phase and a slower decay and have a duration of tens of milliseconds. The receptor is a hetero-oligomer (fig. 1.4) with modulatory binding sites for neurosteroids, benzodiazepines and barbiturates (Kaila, 1994; Bormann 2000). Bicucullinmethochloride as well as gabazine block GABA_A-receptor mediated responses in a competitive way, whereas picrotoxin blocks the receptors non-competitively. The receptor complex consists of 5 subunits, originated from different gene families (α 1-6, β 1-4, γ 1-4, δ , ϵ and π). Each subunit is composed of 4 transmembrane domains (TM1-TM4).

The grand intracellular loop between TM3 and TM4 contains protein kinase sensitive phosphorylation sites, the pore is formed by the TM2 domains.

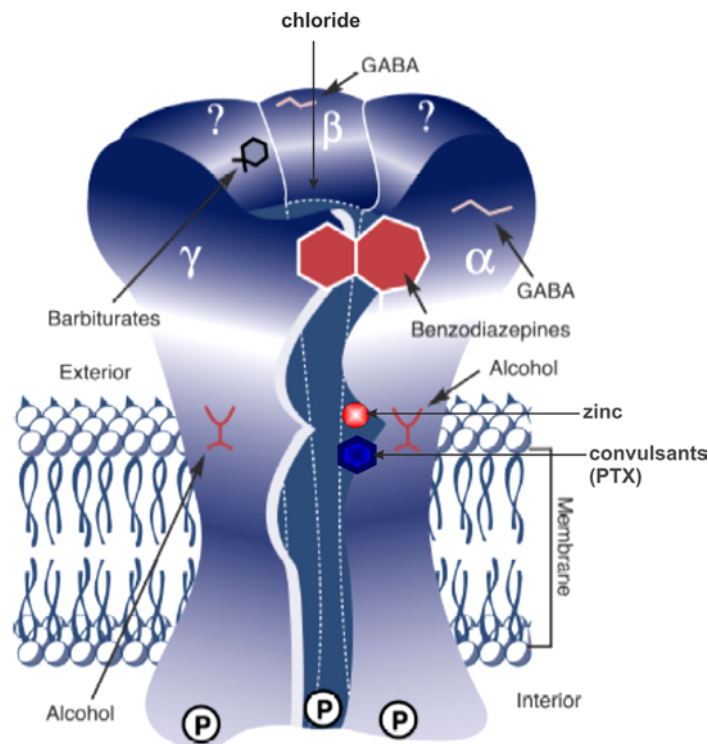


Fig. 1.4: Schematic illustration of the GABA_A-receptor and its binding sites.

The receptor consists of 5 subunits. The proposed binding sites for GABA, benzodiazepines, barbiturates and alcohol are indicated. Locations, affected by convulsants and zinc are given (modified after Mihic and Harris, 1997).

1.5 Long-term plasticity of glutamatergic synapses

The strength of a synapse is defined by the change in transmembrane potential resulting from activation of the postsynaptic neurotransmitter receptors. This change in voltage is known as a postsynaptic potential, and is a direct result of ionic currents flowing through the postsynaptic ion channels. Changes in synaptic strength can be short-term and without permanent structural changes in the neurons themselves, lasting seconds to minutes — or long-term (e.g. long-term potentiation, LTP), in which repeated or continuous synaptic activation can result in the generation of second messenger molecules initiating protein synthesis, ultimately resulting in alteration of the structure of the synapse itself. Learning and memory are believed to result from such long-term changes in synaptic strength, known as synaptic plasticity. There are several underlying mechanisms that cooperate to achieve synaptic plasticity, including changes in the quantity of neurotransmitter released and changes in how effectively

cells respond to those neurotransmitters (Gaiarsa et al., 2002). There are in principle two molecular mechanisms for synaptic plasticity, the first one involves modification of existing synaptic proteins (typically protein kinases) resulting in altered synaptic function (Shi et al., 1999). The second mechanism depends on second messengers regulating gene transcription and changes in the levels of key proteins at synapses. This second mechanism can be triggered by protein phosphorylation but takes longer and lasts longer, providing the mechanism for long-lasting memory storage. Long-lasting changes in the efficacy of synaptic connections between two neurons can involve the making and breaking of synaptic contacts. A synapse's strength also depends on the number of ion channels it has (Debanne et al., 2003). Several facts suggest that neurons change the density of receptors on their postsynaptic membranes as a mechanism for changing their own excitability in response to stimuli. In a dynamic process that is maintained in equilibrium, NMDA and AMPA receptors are added to the membrane by exocytosis and in turn removed by endocytosis (Shi et al., 1999; Song and Huganir, 2002; Pérez-Otaño and Ehlers, 2005). These processes, and by extension the number of receptors on the membrane, can be altered by synaptic activity (Shi et al., 1999; Pérez-Otaño and Ehlers, 2005). Experiments have shown that AMPA receptors are delivered to the membrane due to repetitive NMDAR activation (Shi et al., 1999; Song and Huganir, 2002). If the strength of a synapse is only reinforced by stimulation or weakened by its lack, a positive feedback loop will develop, leading some cells never to fire and some to fire too much. But two regulatory forms of plasticity, called scaling and metaplasticity, also exist to provide negative feedback (Pérez-Otaño and Ehlers, 2005). Synaptic scaling serves to maintain the strengths of synapses relative to each other, lowering amplitudes of small excitatory postsynaptic potentials in response to continual excitation and raising them after prolonged blockage or inhibition. This effect occurs gradually over hours or days, by changing the number of AMPA receptors at the synapse. Metaplasticity, another form of negative feedback, reduces the effects of plasticity over time. Thus, if a cell has been affected by a lot of plasticity in the past, metaplasticity makes future plasticity less effective. Since LTP and LTD rely on the influx of Ca^{2+} through NMDA channels, metaplasticity may be due to changes in NMDA receptors, for example changes in their subunits to allow the concentration of Ca^{2+} in the cell to be lowered more quickly (Pérez-Otaño and Ehlers, 2005).

It is still discussed contradictory, if synaptic potentiation is maintained at the presynaptic or the postsynaptic side (Malenka and Nicoll, 1993; Malinow, 1994; Kullmann and Siegelbaum, 1995; Feldman et al., 1999).

1.5.1 Plasticity at presynapses

Experiments using the minimal stimulation method showed a reduced occurrence of „failures“ (see chapter 1.5.3), but no increase of the response at transmitter release after induction of LTP (Stevens and Wang, 1994). A possible explanation for this phenomenon would be a retrograde messenger that causes from the postsynaptic site a presynaptic modification, which then leads to an increased release probability (Bliss, 1990). In this context arachidonic acid, neurotrophins (see chapter 1.6) and diffusing gases like NO and CO are discussed (Korte et al., 1995; Lessmann, 1998; Volgushev et al., 2000; Lu and Gottschalk, 2000). But still there is no accepted model that could explain presynaptic LTP mechanistically (Malenka and Nicoll, 1999; Huang et al., 2005).

1.5.2 Plasticity at postsynapses

Various experiments are interpreted in a way that LTP is caused by postsynaptic modifications. After induction of LTP a selective potentiation of AMPA-receptor mediated responses was observed (Kauer et al., 1988). Use of the NMDA-receptor specific, irreversible “open-channel” blocker MK-801, in order to see a change in release probability, showed no modification of this parameter after LTP (Manabe and Nicoll, 1994). Therefore, a purely postsynaptic mechanism is discussed like an enzyme induced phosphorylation of AMPA-receptors (Barria et al., 1997; Lisman et al., 1999; Lee et al., 2000).

1.5.3 Plasticity at „silent“ synapses

Originally, for interpretation of LTP experiments a constant number of synapses during the experiment was assumed. However, a change of the mean response to a stimulation can not only be achieved by a change of the release probability (classical presynaptic mechanism) or a change of the size of the response after release (classical postsynaptic mechanism), but also by a change of the number of functional release sites (synapses). A long lasting potentiation of synaptic connections would require a fast conversion of previously inactive synapses (so-called “silent synapses”) into functional ones (Faber et al., 1991; Malenka and Nicoll, 1997; Atwood and Wojtowicz, 1999; Zhuo, 2000). An activity dependent activation of synapses has already been shown in the cortex of rats (Liao et al., 1995; Isaac et al., 1995; Durand et al., 1996; Isaac et al., 1997; Rumpel et al., 1998; Atwood and Wojtowicz, 1999). Also during

development synapses are formed quite early, but not all of them are necessarily functional. Some may remain silent. There exist two different types of “silent synapses”, presynaptically silent synapses and (the classical) postsynaptically silent synapses (fig. 1.5). Postsynaptically silent synapses are well known as NMDA-receptor only synapses. They are lacking AMPA-receptors, but express functional NMDA-receptors. Functional AMPARs are delivered to the subsynaptic membrane after LTP induction. This long lasting effect has been shown so far only in early postnatal development (P1 to P12). It seems to be characteristic for this early developmental phase in the brain, where a quite intensive synaptogenesis takes place (Malenka and Nicoll, 1997; Feldman and Knudsen, 1998; Feldman et al., 1999; Atwood and Wojtowicz, 1999).

In contrast to this, in a presynaptically silent synapse, both –AMPA- and NMDA- are present, but they are activated only extremely rarely. This is due to a very low release probability, because no docked vesicles are present. Such a synapse would not respond at all if no vesicle release occurs during the experiment and therefore would show a failure rate up to 100%. LTP then would increase the release probability and the synapse would respond after LTP induction (Gasparini et al., 2000; Voronin et al., 2004; Walz et al., 2006).

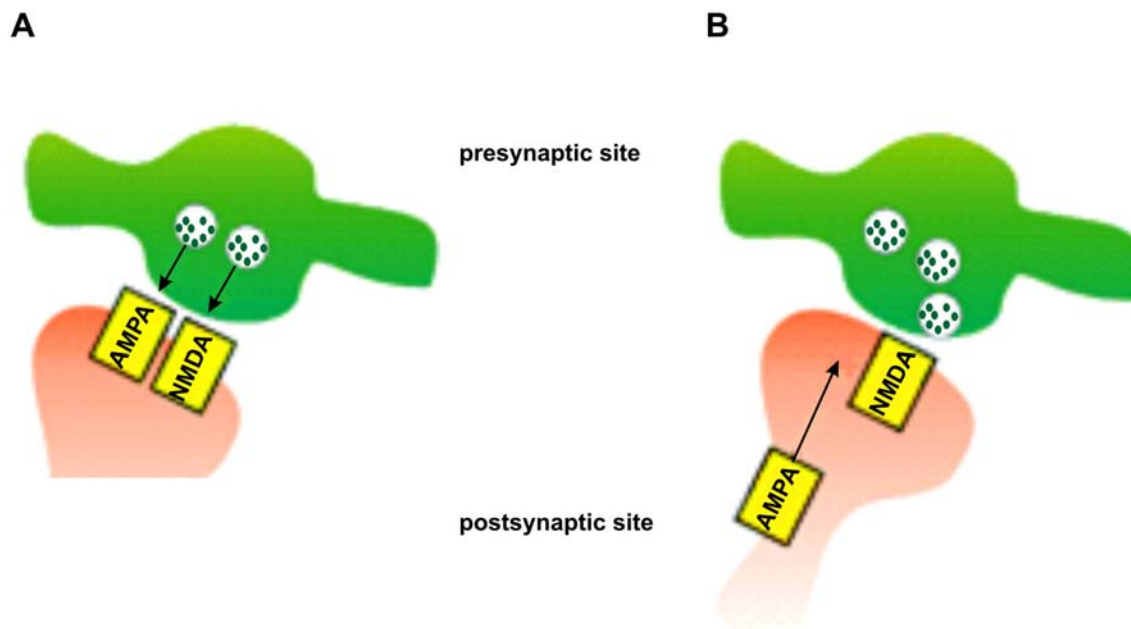


Fig. 1.5: Models of silent synapses

In the presynaptically silent synapse (A) both AMPA- and NMDA-receptors (*yellow boxes*) are present in the subsynaptic membrane, but they are activated only extremely rarely because of their low release probability (no docked vesicles). LTP would reduce the initially high failure rate and increase the release probability (*black arrows*). Postsynaptically silent synapses (B) lack AMPA-receptors, but express functional NMDA-receptors (*yellow box*). AMPA-receptors are delivered to the subsynaptic membrane (*black arrow*) after LTP induction (modified from Voronin et al., 2004).

1.6 Neurotrophins

During development neurons require so-called neurotrophic factors, which play a crucial role in survival, differentiation, dendritic growth and synaptic plasticity (McAllister et al., 1999). During adulthood these factors are needed for maintenance of functionality as well as for functional and morphological adaptation to environmental changes. Depending on their structure the neurotrophic factors can be grouped into several families. The family of neurotrophins contains NGF („nerve growth factor“), BDNF („brain-derived neurotrophic factor“) and the neurotrophins NT-3 and NT-4/5. The later and only in fish described neurotrophins NT-6 and NT-7 will not be considered in this work. The specific receptors for neurotrophins are the Trk-receptors (fig. 1.6), which have an intracellular tyrosine kinase activity and a high affinity to their ligands. NGF binds specifically to TrkA-receptors, BDNF and NT-4/5 to TrkB-receptors and NT-3 to TrkC-receptors. Beside these Trk-receptors exists the neurotrophin-receptor p75, to which all of the neurotrophins bind with a low affinity (for review see: Barbacid, 1994; Heumann, 1994; Lewin and Barde, 1996).

The signal transduction is very similar at all Trk-receptors, though there are differences concerning cell-type, age, state of differentiation and other modulators. In general, binding of neurotrophin dimers to the corresponding receptor induces the dimerization of two tyrosine kinase molecules. The intracellular domain of the receptor shows, as already mentioned, tyrosine kinase activity and possesses a couple of tyrosines. These are autophosphorylated at ligand binding in such a way as to enable the attachment of several small adapter proteins. These proteins are the origin of diverse signal transduction cascades (for review see: Kaplan and Miller, 2000; Patapoutian and Reichardt, 2001). The neurotrophin BDNF was described for the first time in 1982 (Barde et al., 1982) and is exclusively expressed by neurons. Its cloning and heterologous expression succeeded for the first time in 1989 (Leibrock et al., 1989).

The BDNF-mRNA can be detected in all brain regions of the adult CNS of rats, and the expression is most prominent in the hippocampus and the cerebral cortex (Hofer et al., 1990). The maximal expression level during development is reached in the first place in mature tissue (Maisonpierre et al., 1990). Increasingly, BDNF is not only mentioned in developmental processes, but is also associated with synaptic plasticity processes. In homozygous BDNF-knockout mice it has been shown that a lack of this neurotrophin has serious consequences. These animals are quite small, their coordination of movement and balance is strongly impaired and in many cases they are either hyperactive or completely amotile. Usually these mice die at an age of three weeks. The brains show a relatively normal

anatomy, as also shown in TrkB-knockout mice, but the brains of BDNF-knockout mice are overall smaller in size than those of controls.

The first investigated function of the neurotrophin BDNF was rescue of neurons from apoptosis (for review see: Lewin und Barde, 1996). Likewise, the effects of BDNF on neurite growth and differentiation of neurons were discovered (Lindsay et al., 1985; Cohen-Cory and Fraser, 1995). More recent experiments proposed a crucial role of BDNF in synaptic plasticity processes and that BDNF – like neurotransmitters – is able to initiate action potentials in CNS neurons (Kafitz et al., 1999).

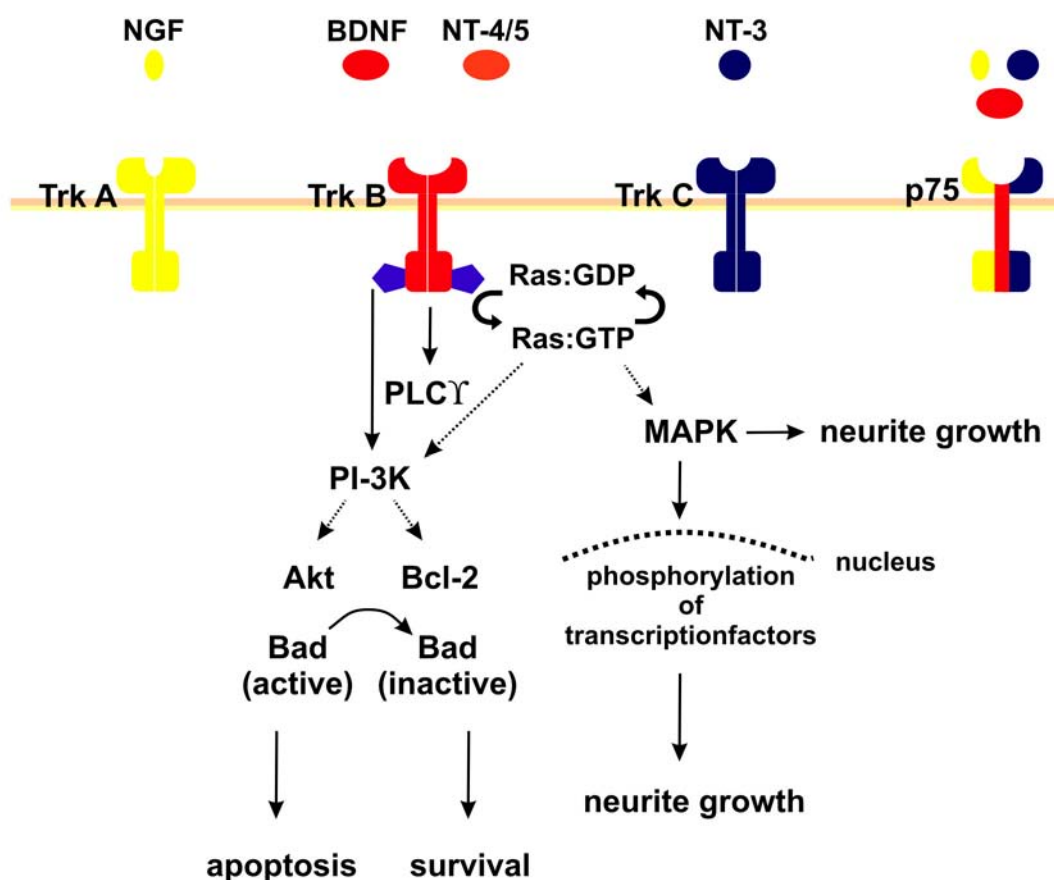


Fig. 1.6: Simplified model of the signal transduction of neurotrophins.

NGF binds specifically to TrkA-receptors, BDNF and NT-4/5 to TrkB-receptors and NT-3 to TrkC-receptors. To the neurotrophin-receptor p75 all of the neurotrophins bind with a low affinity. Akt: also PKB: protein kinase B; Bad: proapoptotic Bcl-2 homolog; Bcl-2: B-cell-lymphoma-gene 2; MAPK: mitogen-activated protein kinase; PI-3K: phosphoinositol-3-kinase; PLC γ : phospholipase C γ ; GDP (GTP): guanosindiphosphate (guanosintriphosphate).

Several findings argue for an important role of BDNF in synaptic long-term plasticity (LTP), for example as a retrograde messenger. On the one hand, endogenous BDNF can be released with the same electrical stimulation parameters with which LTP can be induced (Balkowiec

and Katz, 2000; Hartmann et al., 2001). Furthermore, the neurotrophin expression can be regulated both by electrical activity (Zafra et al., 1990; Ernfors et al., 1991) and by neurotrophins themselves (Canossa et al., 1997). Even a direct increase of expression by induction of LTP could be observed (Patterson et al., 1992; Dragunow et al., 1993). The role of BDNF in synaptic long-term plasticity in the hippocampus has been intensively investigated (for review see: Thoenen, 1995; Korte, 1995; Leßmann, 1998; McAllister et al., 1999; Schuman, 1999; Schinder and Poo, 2000). An acute application of BDNF as well as NT-4/5 to cultured hippocampal neurons produced a potentiation of synapses (Leßmann et al., 1994), similar to experiments in hippocampal slices (Kang and Schuman, 1995). An increased probability of neurotransmitter release has been confirmed by several groups (Kang und Schuman, 1995; Leßmann et al., 1998; Berninger et al., 1999). However, to what extent BDNF is exactly involved in the mechanisms of LTP still remains unclear.

In addition, it has been shown that BDNF produced in the retina influences and modulates ocular dominance plasticity (Mandolesi et al., 2005) and furthermore that BDNF mRNA levels can provide an accurate "molecular readout" of the activity levels of cortical neurons and are consistent with a highly local action of BDNF in strengthening and maintaining active synapses during ocular dominance column formation. (Lein and Shatz, 2000)

1.7 Aims of the study

The fundamental subject of this study was the developmental plasticity at glutamatergic synapses. Therefore, the main goal was to describe functional changes of glutamatergic synapses during the development of mouse somatosensory cortex. This so-called barrel cortex is very suitable as a model system for the investigation of functional connectivity of specific neuron classes because of its very clear structural and functional organization (Agmon and Connors, 1991; Welker, 1971; Woolsey and Van der Loos, 1970). On the other hand only little is known about the molecular and cellular mechanisms underlying the formation of these cortical networks. The experiments were either carried out in acute slices of different developmental stages using the "patch clamp"-technique or in the second part of this study in organotypic cultures of mouse somatosensory cortex.

In the first part of this study, glutamatergic synapses on layer Vb pyramidal neurons were characterized concerning their presynaptic and postsynaptic properties. In addition, their plasticity-dependent changes were analysed. A defined local stimulation and the application of specific drugs in P7 and P14 mice brain slices was used to address, whether there might be 4

different developmental states present *simultaneously* at P7: (1) a mature state with a high release probability and the presence of postsynaptic AMPA- and NMDA-receptors, (2) an immature state with a high release probability exhibiting postsynaptically only NMDA-receptors, (3) an immature state with a low release probability and postsynaptic AMPA- and NMDA-receptors and finally, (4) an immature state with a low release probability and only NMDA-receptors.

The age range of P7 to P14 was chosen for the experiments, because the anatomical development of the layers of the somatosensory cortex is almost finished, but developmental maturation like the conversion of “silent synapses” into functional might be detected as shown in visual cortex (Rumpel et al., 1998). Another aim of the study was to figure out, if there might exist a coupling between presynaptic (low release probability) and postsynaptic (AMPA- and/or NMDA-receptors) developmental maturation. A functionally important indicator for postsynaptic maturation is a change in NMDA-receptor subunit composition (Flint et al., 1997), therefore a further goal was to investigate NMDA-receptor mediated currents during different maturational stages of glutamatergic synapses.

In the second part of this study the main goal was to examine the role of neurotrophins in developmental plasticity of cortical synapses. The neurotrophin BDNF is associated with Parkinsons disease and drug addiction as well as with schizophrenia. BDNF is not only linked to diseases, but has a crucial role during cortical development (Lindsay et al., 1985; Cohen-Cory and Fraser, 1995, McAllister et al., 1999). Furthermore, several findings argue for an important role of BDNF in synaptic long-term plasticity (LTP), in particular as a retrograde messenger. At the presynaptic site of glutamatergic synapses an increased probability of neurotransmitter release upon BDNF application has been confirmed by several groups (Kang und Schuman, 1995; Leßmann et al., 1998; Berninger et al., 1999). However, to what extent BDNF is exactly involved in developmental processes in the neocortex still remains unclear. To investigate a possible role of BDNF, especially as a retrograde messenger, synaptic inputs onto transplanted BDNF-deficient neurons in a wildtype organotypic slice were analyzed using the “patch clamp”-technique in combination with photolysis of *caged* glutamate. Additionally, the connectivity of integrated BDNF-deficient neurons was investigated concerning competition for synaptic inputs with surrounding wildtype neurons.

2. Materials and Methods

2.1 Chemicals

All chemicals were obtained from Tocris (TTX, D-AP5, DNQX, Bicucullinmethochloride), Sigma (Picrotoxin, TEA, MK-801, Ro 25-6981, ARA-C, EGTA, DNase, biocytin), Invitrogen (BME basal medium eagle, FCS, L-glutamine, horse serum, MEM minimum essential Medium, PBS phosphate-buffered saline, trypsin, Taq polymerase, dNTP mix, ethidiumbromide), MWG BioTech (primer), Molecular Probes (L-glutamic acid, γ -[α -carboxy-2-nitrobenzyl]ester = (γ -CNB)-Caged L-glutamic acid), Merck (cresyl-violet) and Qiagen (DNeasy tissue kit). Stock solutions were prepared as recommended by the manufacturer and added to the ACSF.

2.2 Media and Solution

a) Preparation-medium for preparation of organotypic slice cultures (100 ml)

Substances	Amount (ml)
Minimum Essential Medium (MEM), sterile	99
Glutamine (200 mM), sterile	1
pH 7,35 (adjusted with NaOH)	

b) Incubation-medium for cultivation of organotypic slice cultures (100 ml)

Substances	Amount (ml)
Minimum Essential Medium (MEM), sterile	45,875
Basal Medium Eagle (BME), sterile	25
Horse Serum, heatinactivated, sterile	25
Fetal Calf Serum (FCS), sterile	1
Glutamine (200 mM), sterile	1
Glucose, 40%, sterile	1,563
Penicillin	25 U/ml
Streptomycin	25 μ g/ml
pH 7,35 (adjusted with NaOH)	

c) Artificial cerebrospinal fluid for acute brain slices

Substances	Concentration (mM)
NaCl	119
KCl	2,5
CaCl ₂	2,5
MgCl ₂	1,5
NaHCO ₃	26,2
Na ₂ HPO ₄	1
Glucose	10
Glutamine	1

pH 7,3 (adjusted with carbogen)

d) Artificial cerebrospinal fluid for mPSCs in organotypic slice cultures

Substances	Concentration (mM)
NaCl	119
KCl	5
CaCl ₂	2,5
MgCl ₂	1,5
NaHCO ₃	26,2
Na ₂ HPO ₄	1
Glucose	10
Glutamine	1

pH 7,3 (adjusted with carbogen)

e) Artificial cerebrospinal fluid for *caged*-glutamate experiments in organotypic slice cultures

Substances	Concentration (mM)
NaCl	124
KCl	3
CaCl ₂	1,6
MgCl ₂	1,8
NaHCO ₃	26
Na ₂ HPO ₄	1,25
Glucose	10

pH 7,3 (adjusted with carbogen)

f) Intracellular Solution I

Substances	Concentration (mM)
K-gluconate	100
KCl	10
CaCl ₂	0,25
EGTA	10
HEPES	20
Biocytine	1%

pH 7,3 (adjusted with NaOH)

g) Intracellular Solution II

Substances	Concentration (mM)
Cs-methansulfonate	110
CaCl ₂	0,25
TEA	20
EGTA	10
HEPES	20
Biocytine	1%

pH 7,3 (adjusted with CsOH)

h) Intracellular Solution III

Substances	Concentration (mM)
KCl	155
NaCl	5
MgCl ₂	1,2
CaCl ₂	2,4
EGTA	5
HEPES	10
Biocytine	1%

pH 7,3 (adjusted with KOH)

i) Intracellular Solution IV

Substances	Concentration (mM)
K-gluconate	117
KCl	13
MgCl ₂	2
CaCl ₂	1
Na ₂ ATP	2
NaGTP	0,5
EGTA	11
HEPES	10
Biocytine	1%

pH 7,3 (adjusted with KOH)

j) BDNF-WT-PCR (master-mix for 1 probe)

Substances	Portion (µl)
taq polymerase	0,2
10x buffer	2,5
dNTPs (1,25 mM)	2,5
BKO-1-primer (50 µM)	1,0
BD2A-primer (50 µM)	1,0
MgCl ₂ (50 mM)	1,0
A. bidest	7,8
DNA (1:50 diluted)	10

k) BDNF-KO-PCR (master-mix for 1 probe)

Substances	Portion (µl)
taq polymerase	0,2
10x buffer	2,5
dNTPs (1,25 mM)	2,5
NEO-primer (50 µM)	1,0
BD2A-primer (50 µM)	1,0
MgCl ₂ (50 mM)	1,0
A. bidest	7,8
DNA (1:50 diluted)	10

l) Cresyl violet stock solution

Substances	Portion
A. dest.	1000 ml
Cresyl violet	1,0 g
Acetic acid (99%)	3,1 ml
Na-acetate	0,235 g

2.3 Creation and genotyping of genetically modified mice

To create a genetically modified BDNF-„knock-out“ (KO) mouse, a neomycin-cassette (neomycin-resistance gene) was cloned between two Xba I-sites in the coding region of the BDNF-gene (Korte et al., 1995). 75% of the BDNF protein coding exon was thus deleted in the BDNF-KO mouse and replaced by the neomycin-cassette. The remaining 25% do not appear as a protein, because this sequence is located at the C-terminal site of the polyA-tail of the neomycin-cassette. The mRNA of the 75% of the deleted DNA is definitely not detectable (Korte et al., 1995).

In this way generated BDNF-KO-animals were crossed with a wildtype-line to get a heterozygous BDNF-KO mouse. Animals used in our experiments were obtained by breeding of these heterozygous BDNF-KO-mice. According to Mendel the probability to obtain a „wildtype“ (WT)- or KO-mouse was at 25 % per litter.

Neocortical dissociated cells of these genetically modified mice were obtained as described in chapter 2.4.3 and transplanted to cortical slices obtained from a wildtype-line (C57/BL6). The preparation of the single-cell-suspension was carried out separately for each individual. The respective genotype was determined using a „polymerase chain reaction“ (PCR)-analysis. For genotyping the DNeasy-Kit by Qiagen was used. Lysis of the biopsies was reached by addition of 180 µl ATL-buffer and 20 µl proteinase K. After incubation at 37°C overnight

biopsies were completely lysed. To precipitate the DNA 200 µl AL-buffer were added to the lysate and afterwards thoroughly mixed with 200 µl ethanol (96–100%). The homogeneous solution was pipetted onto the adequate column (DNeasy Mini spin column) placed in a collection tube (2 ml) and centrifuged at 8000 rounds per minute (rpm) for one minute. The flow-through and the collection tube were discarded and the column was placed in a new 2 ml collection tube. After addition of 500 µl buffer AW1 and centrifugation at 8000 rpm for one minute the flow-through and the collection tube again were discarded. Upon placing the column in a new 2 ml collection tube, 500 µl AW2 buffer were added, followed by centrifugation at 14000 rpm for three minutes to dry the DNeasy membrane, since residual ethanol may interfere with subsequent reactions. Once again the flow-through and the collection tube were discarded. The DNA containing column was placed carefully in a 1,5 ml microcentrifuge tube and 200 µl AE buffer were pipetted directly onto the membrane. Incubation at room temperature (RT) for one minute was followed by centrifugation at 8000 rpm for one minute to elute the DNA. The characteristic genomic sequences of the respective genotypes were amplified from the isolated DNA by using specific primers in a PCR.

For genotyping of the BDNF-KO mice the previously described primers (Korte et al., 1995) were used:

BD-2A: 5' - GTG TCT ATC CTT ATG AAT CGC – 3'

BKO-1: 5' - ATA AGG ACG CGG ACT TGT ACA – 3'

3' NEO: 5' - GAT TCG CAG CGC ATC GCC TT – 3'

With the 3'NEO and BD-2A primers the neomycin-cassette of the knockout-alleles was amplified, with the BKO-1 and BD-2A primers the wildtype-allele was amplified. Solutions used for the fragment-amplification are listed in 2.2 (j, k). To avoid unspecific interactions with genomic DNA the „annealing“-temperature (AT) was chosen as follows:

1. 94°C 5 min.
2. 58°C 45 sec.
3. 72°C 90 sec.
4. 94°C 45 sec.
5. go to 2. 40 cycles
6. 72°C 10 min.

After application onto a 2% agarose gel the genotype of the animals was determined from the samples of the amplified fragments.

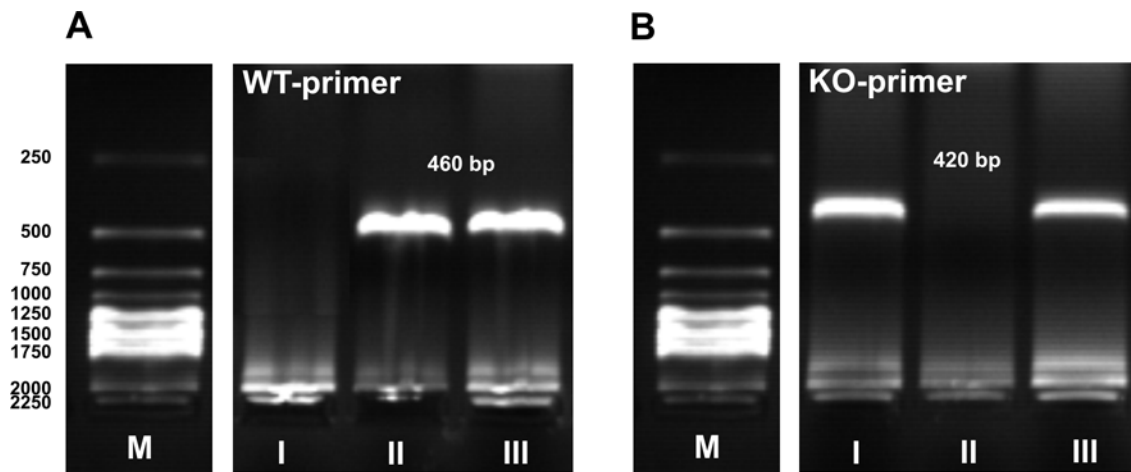


Fig. 2.1: Genotyping of genetically modified mice using PCR.

Shown are an amplification with WT-primers (A) and an amplification with BDNF-KO-primers (B), each with samples of a homozygous BDNF-KO animal (I), a WT animal (II) and a heterozygous animal (III). KO fragments (420 bp) move faster than WT fragments (460 bp). M = marker with bands at 250, 500, 750, 1000, 1250, 1500, 1750, 2000, 2250, 2500, 2750, 3000, 4000, 5000, 6000 and 8000 bp.

2.4 Slices of the mouse neocortex

2.4.1 Preparation of acute slices

For slice preparation we used both male and female mice (C57/BL6, postnatal day 7 or 14). After decapitation the skull was placed immediately in ice cold artificial cerebrospinal fluid (ACSF) to avoid hypoxic damages. Upon exposure of the brain and two coronal incisions a 30 mm thick tissue block was extracted, which contained the primary somatosensory cortex (fig. 2.2).

The tissue was glued (Permapond C2, Eastleigh, UK) to the platform of a vibratome (Serie 1000, tpi, St. Louis, MO, USA; settings: speed 4 to 5, vibration 70 to 80 Hz, Auto Strop Blades “VALET”) and the cooled cutting chamber was filled with ice cold ACSF. Overall 2 to 3 slices with a nominal thickness of 400 μ m were obtained from each preparation.

The hemispheres of the slices were separated with a scalpel and slices were stored in a special chamber at RT for at least one hour to equilibrate. Slices were transferred to the recording chamber and fixed with a grid consisting of nylon threads glued to an U-shaped platinum wire. A constant perfusion with 34°C warm ACSF at a rate of about 5 ml/min. guaranteed an optimal supply of the acute slices.

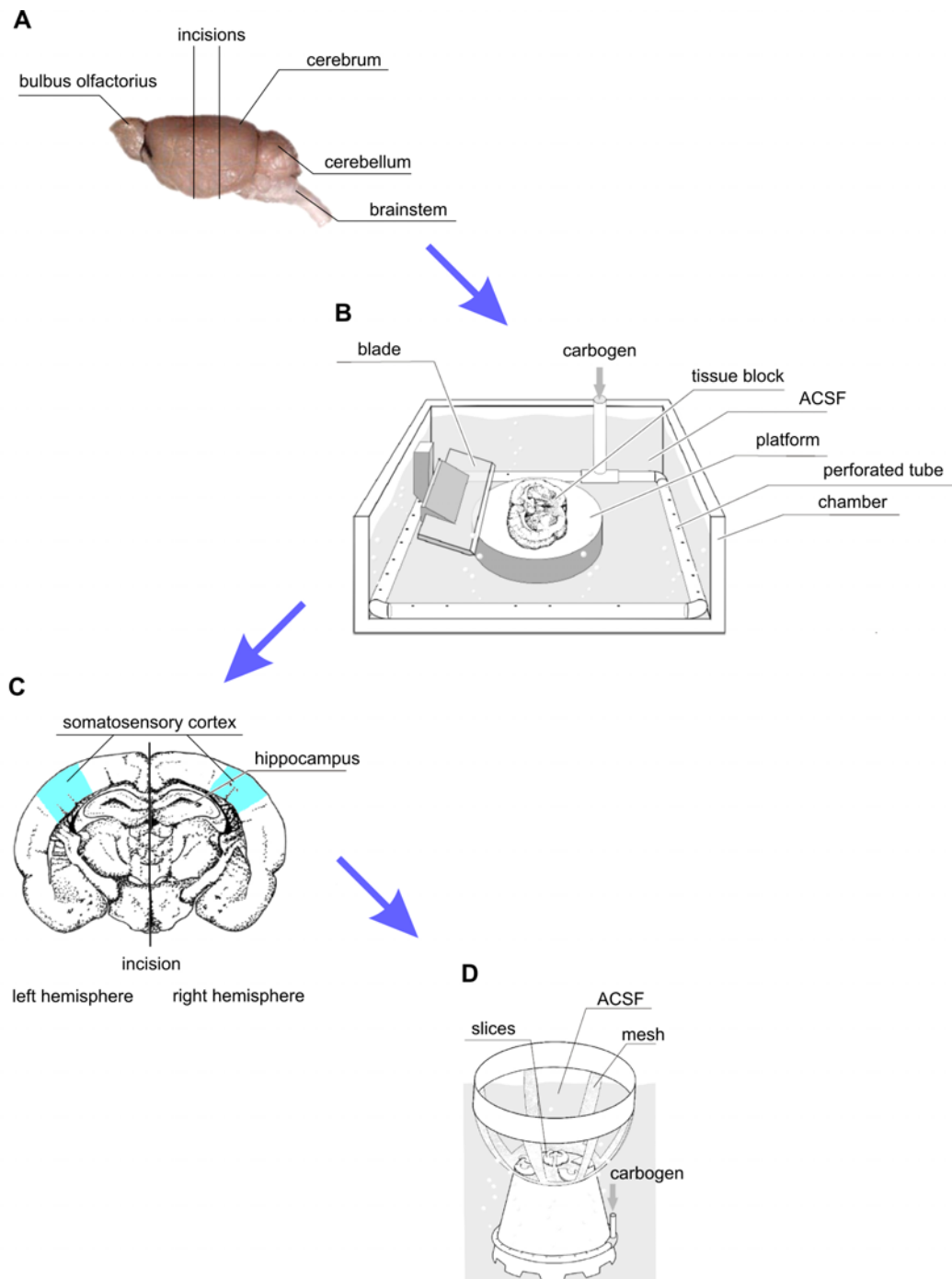


Fig. 2.2: Preparation and storage of in vitro slice preparations.

(A) After decapitation a somatosensory cortex containing tissue block is removed from the skull. (B) After cooling the tissue block is glued to the platform of a vibratome. 400 μm thick coronal slices are cut (C) and the hemispheres are separated. (D) Until start of experiments (at least for one hour) the slices are stored at RT in a special chamber (modified after Schubert et al., 2003).

2.4.2 Preparation of neocortical slice cultures

For preparation of neocortical slice cultures male and female mice (C57/BL6) a few hours after birth (P0) were used. To avoid contaminations the whole preparation was carried out under a sterile bench. Animals were sacrificed by decapitation and the skull was opened using two forceps. The brain was transferred to ice cold preparation medium and cooled down for 1 to 2 minutes. The hemispheres were separated from the rest of the brain and put onto the platform of a tissue-chopper (H. Saur) with a small spoon. After cutting in 300 µm thick coronal slices the hemispheres were stored in the preparation medium. By using a binocular neocortical slices were cut with a scalpel.

The slices were cultivated on Millicell-CM membranes (Millipore) with a diameter of 30 mm and a pore size of 0,4 µm placed in sterile 6-well-plates (Falcon). 1,2 ml of the incubation medium was pipetted directly under the membrane (Stoppini et al., 1991).

The neocortical slices were placed upon the membrane by using a sterile pipette tip and a drop of preparation medium. Afterwards the medium was evacuated. The cultivation of the slices took place at 37°C, 95% humidity and 5% CO₂ in an incubator (Heraeus Instruments, Germany). Every 2 to 3 days the incubation medium was exchanged completely and once in a week 5 µM of the proliferation blocker Cytosine-β-D-Arabinofuranosidhydrochloride (ARA-C) was added. Slices were cultivated for at least 28 days, but no longer than 33 days in vitro (DIV).

2.4.3 Coculture of neocortical slices and EGFP-expressing neurons

To obtain EGFP-expressing BDNF-KO neurons an EGFP-expressing mouse strain (Hadjantonakis et al., 1998; Unit for Embryology and Genetics, Clinical Research Center, Huddinge University Hospital, S-14186 Huddinge, Sweden) was crossed with the heterozygous BDNF-KO mouse line (2.3). Under UV light non fluorescent mice were sorted out in every litter until a stable EGFP-expressing heterozygous BDNF-KO mouse line was established, which were further bred with each other (inbred line). EGFP-expressing neocortical neurons were obtained from individual transgene postnatal mice (P0 to P1) to separate the different genotypes. After decapitation the heads were washed thoroughly in ice cold phosphate-buffer (PBS) to eliminate contaminations. Then the brain was exposed by removal of sculp, muscles and skull and afterwards put in ice cold PBS to avoid degenerative effects caused by oxygen deficiency. Under a binocular neocortical tissue blocks (Ø 500-800

µm) were cut from the postnatal brain with a scalpel. About ten blocks were incubated for dissociation in PBS and 0,1 % Trypsin at 37°C for 5 min. By washing the tissue in serum containing medium the proteolytic effects of trypsin were stopped immediately. Afterwards the incoherent tissue was dissociated mechanically with a 1000 µl pipette. The resulting suspension was centrifuged at 2000 rpm for 1 min. (Labofuge II, Heräus Christ) and the supernatant was discarded. The pellet was dissolved in 2 ml incubation medium and the cell density was determined using a Neubauer cell counting chamber. After dilution to a cell density of 600 to 800 per µl with incubation medium 3 to 5 µl of the suspension were pipetted onto the recently prepared neocortical slice cultures (2.4.2). The cocultures were cultivated at 37°C, 95% humidity and 5% CO₂ in an incubator for 25 to 33 DIV.

2.5 Principles of the patch clamp technique

The patch clamp technique is an electrophysiological technique that allows the study of individual ion channels in cells. This technique is a refinement of the classical voltage clamp technique and was developed by Erwin Neher and Bert Sakmann in the late 1970s and early 1980s, for which they received the Nobel Prize in Physiology or Medicine in 1991. In contrast to traditional voltage clamp recordings, the patch clamp technique uses a single electrode to voltage clamp a cell. This allows to keep the voltage constant while observing changes in current. Alternately, the cell can be current clamped, keeping current constant while observing changes in membrane voltage.

Therefore a glass pipette with an open tip diameter of about 1 µm and filled with electrolyte is positioned near a cell of interest by using micromanipulators. Then the pipette is attached to the cell membrane and suction is applied to the inside of the electrode. The suction causes the cell to form a tight seal with the electrode (a so-called "gigaohm seal", since the electrical resistance of that seal is in excess of a gigaohm). Based on this "cell attached"-configuration several variations of the basic technique can be applied, depending on the aim of the study. The inside-out and outside-out techniques are called "excised patch" techniques, because the patch is removed (excised) from the main body of the cell. Cell-attached and both excised patch techniques are used to study the behavior of ion channels on the section of membrane attached to the electrode, while whole-cell patch and perforated patch allow to study the electrical behavior of the entire cell (fig. 2.3):

1. The electrode is left in place and more suction is applied to rupture the portion of the cell's membrane that is inside the electrode, thus providing access to the intracellular space of the cell. Under this condition so-called “whole-cell recordings” can be performed, where currents through multiple channels at once can be recorded.
2. After the whole cell configuration is formed, the electrode can be slowly withdrawn from the cell, allowing a bulb of membrane to bleb out from the cell. When the electrode is pulled far enough away, this bleb will detach from the cell and reform as a ball of membrane on the end of the electrode, with the outside of the membrane being the surface of the ball. This “outside-out patch” gives the opportunity to examine the properties of one or more ion channels.
3. The electrode is quickly withdrawn from the cell after reaching the “cell attached” configuration, thus ripping the patch of membrane off the cell, but leaving the patch of membrane attached to the electrode exposing the intracellular surface of the membrane to the external media. This “inside-out” configuration is used to manipulate the environment affecting the inside of ion channels.

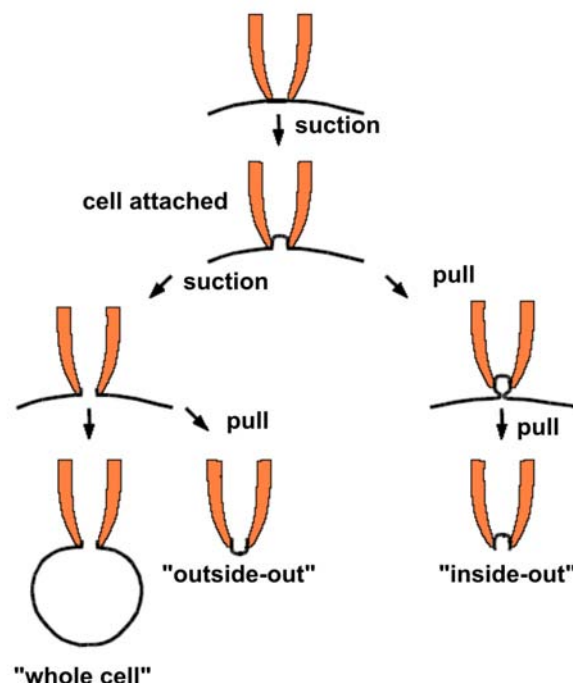


Fig. 2.3: Different configurations of the patch clamp technique.

The tip of the pipette and a part of the cell membrane is shown. Attachment of the pipette to the membrane and suction leads to a “cell attached” configuration. Withdrawal of the pipette results in an „inside-out“ configuration. Enhancement of the suction leads to a rupture of the membrane and therefore to a “whole-cell” or “outside-out” configuration (modified after Hamill et al., 1981).

By presynaptic transmitter release induced activation of postsynaptic receptor channels during synaptic transmission leads to ion currents, which cause a change of the potential of the postsynaptic cell. These changes activate voltage dependent ion channels, so that beside a transmitter induced postsynaptic current also a voltage dependent component occurs, which may elicit an action potential. Therefore a selective recording of transmitter induced ion currents is only possible under potentiostatic conditions. This is enabled by the voltage clamp circuit used in patch clamp technique. The operational amplifier (OPA) represents the central element that consists of several transistors and is wired as current-to-voltage-converter (fig. 2.4). The cell potential is impressed at the “-“input of the OPA, whereas the command voltage (V_{comm}) is impressed between “+”- and “-“input, to which the membrane potential should be clamped. The OPA is an active element that compensates the potential difference between “+”- and “-“input. Hence, in an equilibrium condition the command voltage is impressed on the “-“input. At negligence of the pipette resistance also the command voltage is impressed over the membrane. The output of the OPA is connected with the “-“input by a so-called feedback-resistance (R_f). At the membrane occurring currents then can flow to the OPA through the patch pipette. Because of the extremely high input-resistance of the OPA (ideal: endless magnitude; real: $10^{12} \Omega$) the current flows over the feedback resistance (0,5 G Ω). Since in a balanced state the command voltage is impressed on the “+”-input, for the voltage gripped at the output of the OPA is true (if a current I_m is flowing over the membrane): $V_{\text{out}} = V_{\text{comm}} + I_m * R_f$. Thus, current flow over the membrane leads concerning the output voltage of the OPA to a change of V_{out} that is proportional to the strength of the current. Therefore, V_{out} can be used for the recording of ion currents that flow over the membrane. To separate the fraction of the command potential and receive a voltage signal that is direct proportional to the current flow, a differential amplifier is installed downstream to the patch clamp circuit. The adjustment of the membrane potential to the value of the command potential occurs only with a finite velocity (in contrast to the ideal system), because the dynamic properties of the voltage clamp are affected by the slow reloading speed of the cell membrane. Hence, the membrane potential follows the given command potential with a certain delay. Therefore, most amplifiers give the opportunity to compensate the cell- and pipette-capacitance. For the efficacy of the voltage clamp exclusively the disk tension over the membrane is important. The membrane resistance is series connected with the input resistance. Thus, the disk tension is partially released at the input resistance and consequently, the relation of these two resistances determines the efficacy of the voltage clamp. If the

membrane resistance is at about 50 to 100 fold higher than the input resistance, the failure constitutes accordingly 1 to 2 % and can be neglected. Because the input resistance, respectively the series resistance depends on the pipette resistance, pipettes with a resistance as small as possible are used. The influence of the series resistance on the properties of the voltage clamp can be compensated with most amplifiers using a special circuit (Hamill et al., 1981).

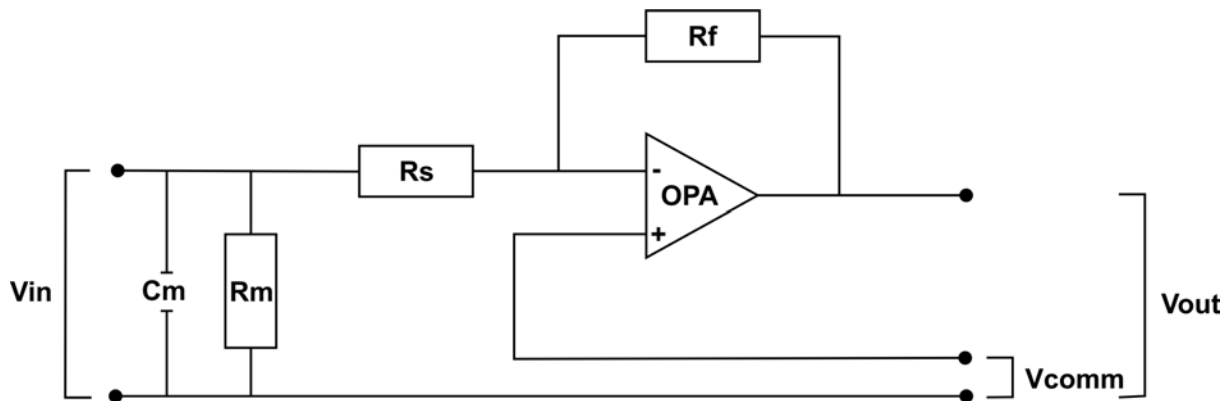


Fig. 2.4: Simplified circuit diagram of patch clamp recording.

Rf: feedback resistance; **Ri**: input resistance; **Rm**: membrane resistance; **Cm**: membrane capacitance; **Vin**: Potential difference between cell interior and reference electrode; **Vcomm**: command potential; **Vout**: output potential, measured variable.

2.6 Experimental setup for patch clamp experiments in acute slices

The experimental setup consisted of an upright microscope (Zeiss Axioskop 2 FS) with a recording chamber mounted at the front side. The setup was additionally upgraded by various specific components such as the Dodt Gradient Contrast (DGC, Luigs & Neumann, Ratingen, Germany). This contrast system was developed by H.-U. Dodt (MPI Munich, Germany). It enables to visualize the structures in sliced tissue. Specific adjusting of the contrast enables various structures to be highlighted. The DGC was mounted between the microscope stand and the lamp housing. In the same way it is also possible to obtain fluorescence and infra-red pictures simultaneously without any great effort. Furthermore the standard objective was replaced with a 40x water immersion objective (40x/0,75 W; Olympus, Hamburg, Germany) with a higher working distance (> 2,2 mm). The cells could be observed via oculars (10x) or an infrared sensitive CCD camera (C5405, Hamamatsu; control unit C2400, Hamamatsu; video monitor WV-BM1410, Panasonic). The microscope could be moved independently from the manipulators (LN Mini 25 Units, Luigs & Neumann) by using a shifting table (Luigs & Neumann). It was mounted on a vibration damping table (Microplan) and protected against electromagnetic interspersions by a surrounding faraday cage. Solutions were stored outside

the faraday cage in a water bath and kept at 37°C. Slices were perfused with 34°C warm solution by using a flexible-tube pump (Minipuls 3, Fa. Gilson) at a rate of about 5 ml per min (fig. 2.5).

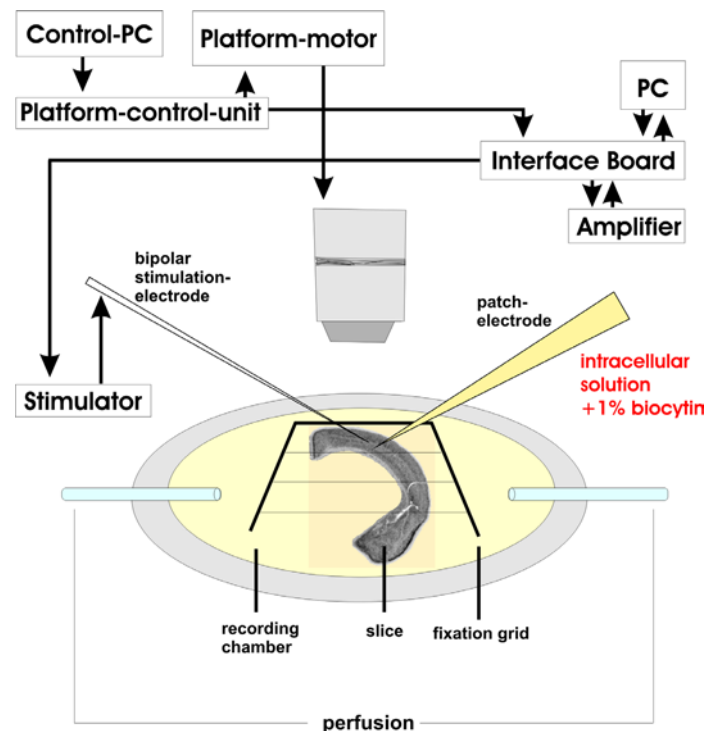


Fig. 2.5: Diagram of the experimental setup.

Shown is the recording chamber (**middle**) with slice, patch- and stimulation electrode, perfusion, and the PC platform (**top**) with stimulator, amplifier, oscilloscope and interface.

Approaching the cell of interest was carried out under visual control by using the DGC. At contact with the soma the applied pressure was withdrawn. By a repetitive voltage jump of 3 mV applied to the pipette it was possible to monitor pipette resistance and to apply suction at increasing pipette resistance to reach the “cell attached” configuration. Subsequent repeated suction led to the ripping of the membrane and establishment of the “whole cell” configuration. Recording of ion currents was performed using the Axopatch 200B amplifier (Molecular Devices, Sunnyvale, CA, USA). After digitalization of the amplified and filtered (low pass filter 3 kHz) signals by an A/D D/A converter (Digidata 1322A interface, Molecular Devices) the recordings were saved to a personal computer with the software pClamp 9.0 (Molecular Devices). As a control the signals were additionally monitored on an oscilloscope (HM 305, Hameg, Mainhausen, Germany). For extracellular stimulation a stimulator (SD 9, Grass Technologies, West Warwick, RI, USA) with adjustable stimulation strength was triggered by the A/D D/A converter. Pulses with duration of 100 μ s were applied by bipolar

tungsten electrodes. The distance to the soma of the recorded cell was between 50 and 150 μm .

2.7 Production of glass pipettes

To produce patch clamp micropipettes fine borosilicate glass pipettes (GC150TL-10, Clark Electrochemical Instruments) with a length of 10 cm, an outer diameter of 1,5 mm and an inner diameter of 1,17 mm were used. At the inner surface a filament was attached to ease the filling of the pipettes. Pipettes were pulled by an electronically controlled horizontal electrode puller (DMZ Universalpuller, Zeitz Instruments, Martinsried, Germany). The electrode resistance was at about 6-8 $\text{M}\Omega$ after filling with intracellular solution.

2.8 Electrophysiological experiments

2.8.1 Recordings of postsynaptic currents evoked by extracellular stimulation

Bipolar tungsten electrodes ($5\text{M}\Omega$; #5755, Science products, Hofheim, Germany) were placed under visual control in the same layer of the somatosensory cortex as the recorded cell in a distance of about 50 to 150 μm to the patch electrode (fig. 2.6). Pulses with a duration of 100 μs were applied every 10 s.

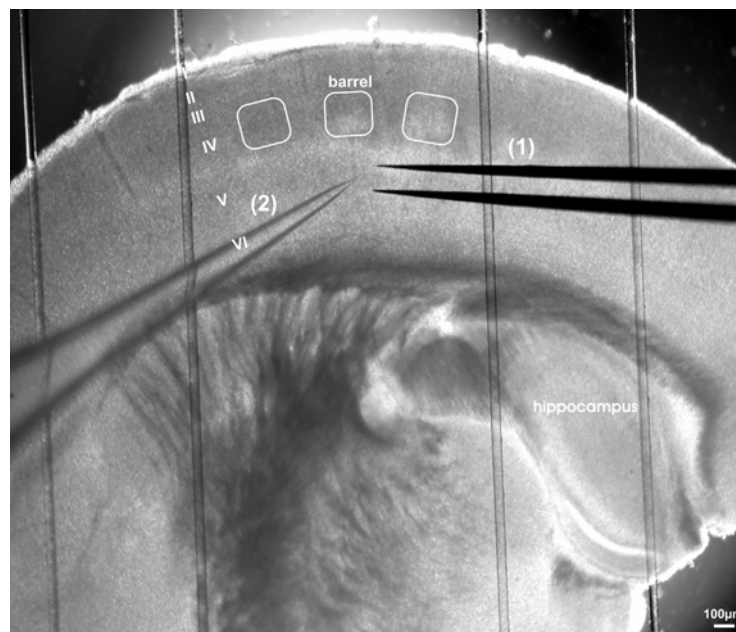


Fig. 2.6: Electrophysiological recordings of evoked PSCs in mouse somatosensory cortex. Image of a coronal slice of mouse somatosensory cortex with positioned stimulation (1) and patch (2) electrodes. Cortical layers I to VI are indicated by roman numbers.

For the minimal stimulation protocol (Sokolov et al., 2002) paired pulses were applied with an interval of 50 ms. The stimulus strength was adjusted manually at about 1 V to evoke minimal responses with failures in response to the first pulse.

2.8.2 Recordings of spontaneous miniature postsynaptic currents

Recordings of spontaneous miniature postsynaptic currents (mPSCs) were carried out in the „whole cell“ configuration of the patch clamp technique. mPSCs were recorded at a holding potential of -70 mV. To exclude action potential induced transmission 1 μ M TTX was added to the ACSF. To isolate GABA_A receptor mediated mPSCs the non-NMDA receptor antagonist DNQX was added to the ACSF in a concentration of 10 μ M. mPSCs were recorded over a period of 3 min.

2.8.3 Recordings of synaptic activity in single EGFP-expressing neurons

To identify single EGFP-expressing neurons transplanted to neocortical slice cultures, the fluorescence signal of these cells was detected under UV-light (HBO 100, Carl Zeiss MicroImaging GmbH, Göttingen, Germany) with a GFP filter set (Zeiss). The patch pipette then was moved to the soma under visual control in the infrared contrast. After establishment of the “cell attached” configuration the fluorescence signal was controlled again under UV-light. After establishing the “whole cell” configuration the exchange of the intracellular milieu with pipette solution led to a rapid decrease of the fluorescence signal.

To perform recordings in the current clamp mode a SEC-05LX amplifier (npi-electronics, Tamm, Germany) was used to measure the cell membrane potential. In this configuration spontaneous postsynaptic potentials (PSPs) were recorded. Furthermore the passive and active membrane properties were investigated. Therefore the potential was – if necessary - hold at -60 mV by a continuous hyperpolarizing current. Every 10 seconds hyperpolarizing and depolarizing pulses with different amplitudes were applied.

2.9 Analysis of electrophysiological recordings

2.9.1 Analysis of postsynaptic currents evoked by extracellular stimulation

During the time period immediately before the stimulation pulse was applied, the standard deviation (SD) of the recording noise was calculated. To decide whether a signal was rated as “success” or as “failure”, the amplitude was compared to the 2x SD value. If the signal amplitude was higher than 2x SD, the signal was rated as success. This is statistically consistent with an alpha error of $\alpha \leq 0,027$.

To ensure, that the signal was a monosynaptic response to the applied stimulation, only signals with latencies below 5 ms were analysed. Amplitudes, rise times of successes and the time constant of decay were analysed using Clampfit 9.0 software. The rise time was calculated as the interval between 10% and 90% of the maximal amplitude. To analyse the time constant of decay of the evoked PSCs, a monoexponential function was fitted to the response decay between the maximal amplitude of the synaptic response and the point of return to the baseline. The function used reads as follows: $I(t) = A \cdot e^{-t/\tau} + C$. The parameters were modified by the Chebychev algorithm (Clampfit). Isolated AMPA or NMDA receptor mediated responses were analysed in this way. In cases where AMPA receptor mediated PSCs were not blocked before recording NMDA receptor mediated PSC components, the rise time was not determined and the amplitude was calculated 30 ms after onset of the synaptic response to exclude effects of the AMPA receptor mediated PSC component.

2.9.2 Analysis of spontaneous miniature postsynaptic currents

To analyse spontaneous miniature PSCs the software Clampfit 9.0 was used. To use the „template search“ function, a template file suitable for detecting GABA_A receptor mediated miniature PSCs was created. This template defines the shape that is searched for in the recordings. In this process the signal amplitude is not relevant to the finding of matches, but the temporal signal parameters are included. For analysis of each recording event the boundaries for event duration, baselines and the calculation of signal statistics were defined in the template. After running the template search data were written to an “event sheet” in a

result window and could afterwards be exported to SigmaPlot 9.0 for further analysis (see 2.14).

2.9.3 Analysis of synaptic activity in single EGFP-expressing neurons

The EGFP-expressing neurons were characterized concerning their passive and active membrane properties. The shown values of membrane potentials were not corrected for liquid junction potentials. The liquid junction potentials had values of about 10 mV according to the experimental conditions and the used solutions and were calculated using the software JPCalc (Barry et al., 1994). As passive intrinsic membrane properties the resting membrane potential (V_{rmp}), the membrane time constant (τ_m) and the membrane resistance (R_m) were analysed. For calculation of τ_m and R_m the membrane potential was analysed during application of subthreshold depolarizing and hyperpolarizing current pulses with a duration of 200 ms. As active intrinsic membrane properties the action potential firing pattern and the interval between first and second action potential (*1st Interspike Interval* = 1.ISI) as well as the second and the third action potential (*2nd Interspike Interval* = 2.ISI) were analysed.

2.10 Principles of „caged glutamate“ photolysis

For a subsequent analysis of the morphology of the recorded neurons the intracellular solution contained 1% biocytine (Sigma-Aldrich Chemie, Steinheim, Germany) in all experiments. To stimulate neurons via focal photolysis-induced glutamate release, 1 mM esterified (=caged) glutamate (L-glutamic acid, γ -[α -carboxy-2-nitrobenzyl]) ester = (γ -CNB)-caged L-glutamic acid; Molecular Probes, Eugene, USA) was added to the ACSF (fig. 2.7). Caged-glutamate has a wide absorption spectrum (280-380 nm) with the maximum at about 360 nm. The stimulation via UV-flashes would in theory - at a quantum yield of 0,1 and with full flash intensity - release a maximal concentration of 100 μ M of active glutamate (Katz and Dalva, 1994). To determine the specificity and reproducibility of the activation of synaptic inputs via local photolysis of caged-glutamate, several controls were carried out previously (Schubert et al., 2001). By these controls unwanted, unspecific effects of stimulation conditions and solutions were examined. Furthermore the spatial resolution of photolysis-induced activity was calculated and the stimulation intensity was calibrated. An influence of caged-glutamate

on membrane properties or a desensitization of glutamate receptors have previously been excluded for the experimental conditions used (Schubert, 2003).

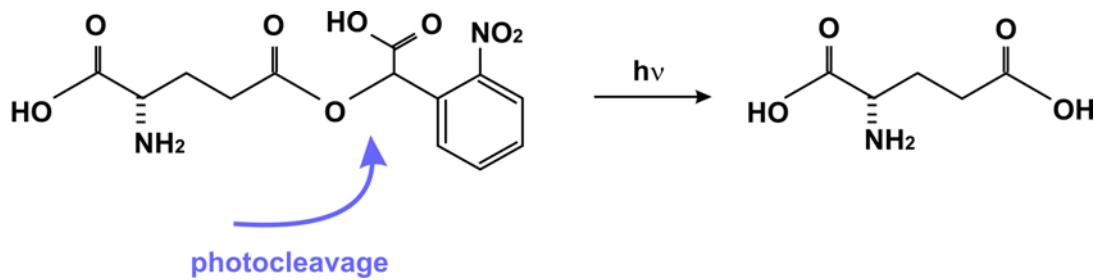


Fig. 2.7: Photolysis of caged-glutamate.

Caged-glutamate (L-glutamic acid, α -[γ -carboxy-2-nitrobenzyl] ester) is bound to a side group via a photoreactive ester bond. This side group forms a molecular cage for the glutamate. The ester bond can be disrupted photolytically by a UV-flash (~ 360 nm) in the range of μ s. Active glutamate is then released.

2.11. Experimental setup for photolysis induced activity in cocultures

The experimental setup consisted of an upright microscope (Axioskop FS, Carl Zeiss, Göttingen, Germany) with a fixed recording chamber (Kötter et al., 1998; fig. 2.8) on a shifting table (Infrapatch, Luigs & Neumann, Ratingen, Germany). Other components like the DGC and objectives with a higher working distance were mounted as described in chapter 2.6. The image of the slice was transferred via a digital camera (CoolPix 950, Nikon, Düsseldorf, Germany) or an infrared sensitive CCD-camera (C5405-01; Hamamatsu Photonics, Herrsching, Germany). UV flashes ($\lambda = 340$ - 390 nm, 0,5 ms duration) from a pulsed Xenon arc lamp (TILL Photonics, Planegg) were conducted via glass fibers through a continuously adjustable grey filter ($D_r = 0,0$ - $2,0$; Melles Griot, Irvine, USA). By this filter an exact adjustment of the flash intensity was possible allowing for a selective suprathreshold stimulation of somata, but not dendrites. The flash was limited by a square aperture to a field of $50 \mu\text{m} \times 50 \mu\text{m}$ after passing a 390 nm short pass filter. A dichroic mirror (405 nm) was then reflecting the UV flash through the objective onto the slice. Each field of interest could be accessed computer-controlled as well as manually.

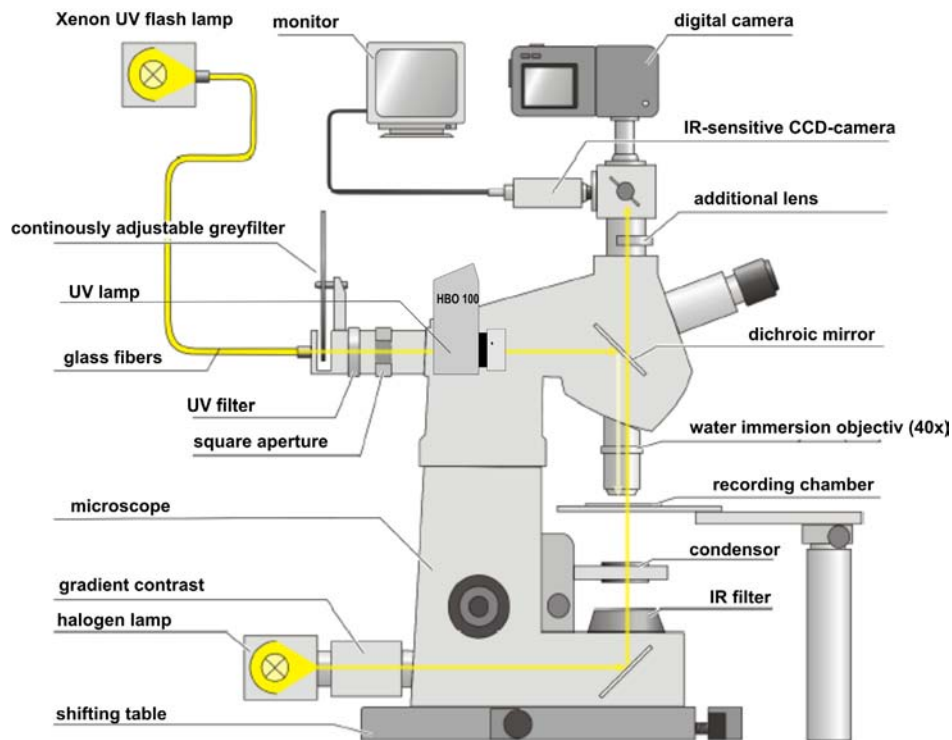


Fig. 2.8: Diagram of the optic components.

Illustration of the combination of infrared-video-microscopy and UV-flash-photolysis of *caged*-glutamate with automated position-control. Yellow: optical path of IR- and UV-light. *UV*: Ultraviolet; *IR*: Infrared; *CCD*: Charged-Coupled-Device (modified after Schubert 2003).

For patch-clamp recordings the current clamp mode was used with a discontinuous single-electrode amplifier system (SEC-05L, npi-electronics, Tamm). Signals were pre-amplified (DPA 2F, npi-electronics, Tamm), filtered at 3 kHz and digitized by an ITC-16 Interface (Instrutech, Great Neck, NY, USA). Recording and analysis of the signals was performed using the software TIDA5 (Heka Elektronik, Lambrecht, Germany). At the same time this PC-platform controlled the current injection protocols for the amplifier and triggered the isolated stimulation unit (BioLogic, Claix, France).

2.12 Mapping of photolysis induced activity

Before each mapping the focus was adjusted under visual control to the location of the patched cell soma in the slice (40 to 80 μm depth). With every UV-flash the membrane potential of the cell was recorded simultaneously. For a topographic acquisition of photolysis induced activity the field of interest (50 μm x 50 μm) was shifted by 50 μm every 10 s. In this way up to 250 fields (one flash/field) around the patched cell were consistently examined.

Synaptic inputs onto the patched cell were recorded in normal ACSF. To better uncover hyperpolarizing inhibitory inputs, the neuron was in alteration clamped in the *slow voltage-clamp controlled current-clamp mode* to a membrane potential of -60 mV and -40 mV, respectively. Double flashes with an interval of 5 s allowed the mapping of one field at the two different holding potentials. The intrinsic membrane properties of the neuron were controlled before and after each mapping.

2.13 Analysis of photolysis induced activity

The relatively high spontaneous activity in slice cultures requires criteria to clearly identify photolysis induced neuronal activity. To avoid a misinterpretation of spontaneous activity as photolysis induced activity, an individual threshold was calculated for each cell. This threshold reflected the maximal spontaneous activity in a given time interval (fig. 2.9). Therefore control traces were recorded without any photostimulation and the integral of all spontaneous depolarizing events in a period of 150 ms was calculated. The period of 150 ms corresponds to the period of 150 ms *post stimulus*, which was used for all following analysis of photolysis induced activity. For each cell the maximal integral obtained during 20 control recordings was determined and defined as threshold for photolysis induced activity. Experimental conditions in control recordings were similar to those during the mapping, i.e. membrane potential (-60 mV) and ACSF with *caged*-glutamate were identical. Inhibitory spontaneous activity was very uncommon, therefore only excitatory events were considered in the controls.

To investigate the photolysis induced activity, at every field a period of 150 ms *post stimulus* was analyzed. Hereby photolysis induced direct activity (depolarizations, which are caused by activation of synaptic and extrasynaptic glutamate receptors in the membrane of the patched neuron) was distinguished from photolysis induced synaptic activity. This distinction was possible because of the relatively long latency between stimulus and onset of synaptic activity. The photolysis induced synaptic activity was analysed concerning (a) the latency between stimulus and onset of activity, (b) the maximal amplitude of excitatory postsynaptic potentials (EPSPs), (c) the integral of EPSPs during the period of 150 ms after stimulation and (d) the occurrence of inhibitory postsynaptic potentials (IPSPs). The calculation of integrals (c) included all depolarizing events during the 150 ms *post stimulus* time interval and provides information about the strength of the elicited excitatory activity. All integrals were corrected by subtracting spontaneous activity using the calculated threshold for photolysis-

induced activity. In case of interference of direct and synaptic activity, the direct activity was excluded from calculation of the integral of the synaptic activity. After analysis the activity parameters were transformed to pseudocolor values by the software Origin 7G (Microcal Software Inc, Northampton, USA). The resulting maps were overlaid to the native image of the slice.

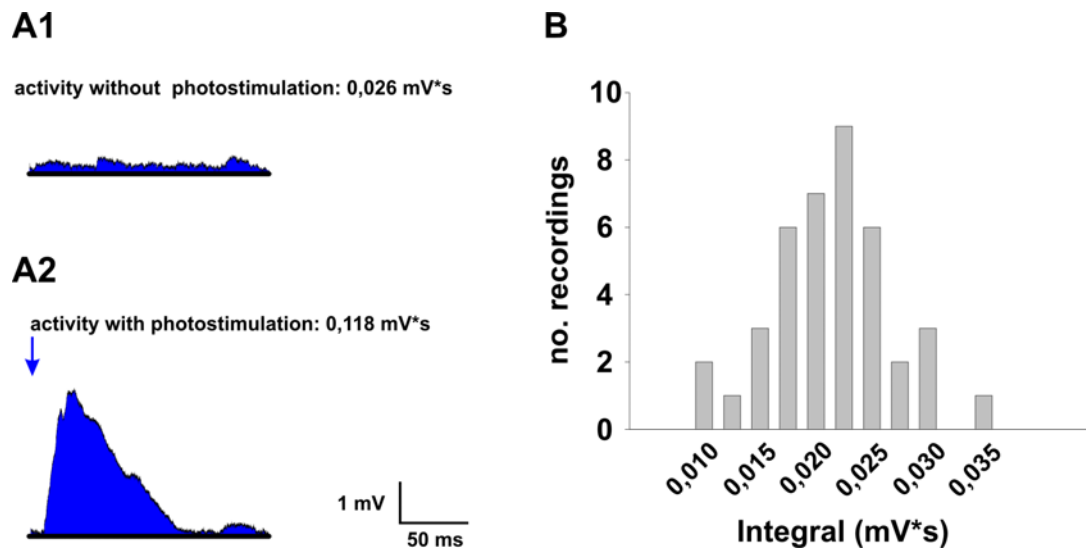


Fig. 2.9: Differentiation between spontaneous activity and photolysis induced activity.

Calculation of the cell-specific threshold for photolysis induced activity. (A) Recording examples and calculation of integrals (*blue area*) of a control neuron in organotypic slice culture without photostimulation (A1) and with (*blue arrow*) photostimulation (A2) during a period of 150 ms. (B) Histogram used for determining the cell-specific threshold shows the distribution of integrals of spontaneous activity, analysed in 40 recordings for a period of 150 ms.

To quantify the spatial distribution of synaptic inputs (i.e. presynaptic somata) onto the patched neuron for different distances to the soma, the mean percentage of fields was calculated, in which the photostimulation caused excitatory or inhibitory inputs irrespective of their strength. All recordings without detectable photolysis induced activity were excluded from the analysis. Furthermore fields were excluded, in which EPSPs were so intensively overlaid by strong direct activity or action potentials that a calculation of integrals was impossible. This happened only in one or two fields in the perisomatic region in a few mappings.

2.14 Data analysis and statistics

For calculations and statistical analysis data were imported to the software “Excel” (Windows) or „SigmaPlot 9.0“ (Jandel Scientific). All data are given as mean \pm standard deviation (SD). Statistical analysis was carried out with the “Student’s t-test“ or “Kolmogorov-Smirnov test” (“Prism” and “InStat” by GraphPad Software, San Diego, CA, USA). Illustration of recordings, images and figures was performed using the software “CorelDraw 12.0” (Corel, Unterschleißheim, Germany).

2.15 Histology

2.15.1 Histological staining of cortical slices

Nissl-staining:

Slices (400 μ m) were fixed overnight in paraformaldehyde (4 % in 0,1 M phosphate buffer (PB)) and afterwards stored in saccharose-solution (20 % in 0,1 M PB) for 12 hours. Slices were cut down to 30 μ m with a cryo-microtome. After washing first in 0,1 M PB and then in 0,05 M PB slices were brought onto a gelatine-coated object holder and dried overnight. Further washing and staining was carried out as followed:

Solution:	Time:
- Cresyl violet solution	10 min.
- A.dest.	30 sec.
- Ethanol (70%)	1 min.
- Ethanol (95%)	1 min.
- Ethanol (100%)	2 min.
- 2 Xylol (100%)	5 min.
- Covering with DePeX	

Staining of single neurons with biocytine:

For visualization of single neurons in a slice and subsequent morphological reconstruction all patched neurons were filled with biocytine. Biocytine was brought into the cell via the patch pipette using an intracellular solution containing 1% biocytine. Neurons were patched for at

least 15 min to guarantee a complete filling of the cell with biocytine. After the end of experiments the slices were photographed at smaller magnification with still positioned electrodes to document the location and the surrounding of the recorded neuron. Then slices were fixed in 4% paraformaldehyde in 0,1 M PB at 4°C for at least 24 hours and then transferred into PB. The processing and visualization of biocytine-filled neurons was performed according to a standard protocol (Angulo et al., 1999). Slices were washed in PB after blocking of endogenous peroxidases (1% H₂O₂ in PB). This was followed by incubation in 30% saccharose in PB (as an antifreezing compound) and a triple cycle of freezing in liquid nitrogen and unfreezing. After several washing steps in PB slices were incubated overnight at 4°C in peroxidase coupled with streptavidine (ABC reagent, 1:200, Vector Laboratories, Burlingame, USA). The peroxidase-reaction was started with 0,01% H₂O₂ after a preincubation of 10 min in 1 mg/ml 3,3'-diaminobenzidine (Sigma-Aldrich Chemie, Steinheim, Germany). The reaction was stopped by washing in PB and slices were cut down to 100 µm thickness with a vibratome. The cutting step was left out in organotypic slice cultures, because these slices, adhered to a membrane, are already flattened to 100 to 150 µm after 28 to 32 DIV. The staining was intensified with 1% OsO₄ in PB for one hour and slices were dehydrated in increasing ethanol concentrations including a contrast enhancement step (45 min. in 1% uranyl acetate in 70% ethanol). After immersion in propylene oxide the slices were embedded in Durcupan ACM (Fluka, Buchs, Switzerland) for further analysis.

2.15.2 Visualization and reconstruction of single neurons

The histologically processed slices (2.13.1) were photographed under a microscope (Nikon Eclipse 800 Nikon, Ratingen, Germany) and the biocytine-filled neurons were further analysed using a computer-system (“Neurolucida”, Microbrightfield Europe, Magdeburg, Germany), which was coupled to the microscope. Neurons could be three-dimensionally reconstructed and their morphology (soma, dendrites, axon) could be analysed. By comparing landmarks in the histologically processed slice with those in the slice during physiological experiments, both images could be overlaid in a topographical correct manner. In the same way the image of the reconstructed neuron could be placed at the correct location. All illustrations and final revision of the images was preformed using “CorelDraw 12” (Corel, Unterschleißheim, Germany).

3. Results

3.1 Characterization of AMPA receptor-mediated EPSCs in layer Vb pyramidal neurons

The experiments of this study were carried out to describe developmental changes of glutamatergic synapses during the development of the mouse somatosensory cortex. In this first part immature glutamatergic synapses on layer Vb pyramidal neurons were analyzed concerning their presynaptic and postsynaptic properties. The two different types of immature “silent synapses”, presynaptically silent synapses and (the classical) postsynaptically silent synapses were investigated. Initially, the presynaptically silent synapses were examined using the patch-clamp technique.

3.1.1 Morphology and basic electrophysiology of layer Vb pyramidal neurons at P7

The cerebral cortex develops from the cortical plate, which differentiates into cortical layers II to VI (Supér and Uylings, 2001; Kageyama and Robertson, 1993) that are characterized by the appearance of different cell types (Peters and Kara, 1985; Sur and Cowey, 1995). At postnatal day 7 (P7) all layers can be distinguished, as well as the cortical columns, which have been proposed to be the basic functional units of cortex (Mountcastle, 1997). The Nissl-staining (fig. 3.1 A) shows clearly the different laminae in the somatosensory cortex of a P7 mouse. Below the broad appearing layer IV the large pyramidal neurons of layer Vb are found. These neurons can be subdivided into “*Intrinsically Bursting*” (IB) and “*Regular Spiking*” (RS) pyramidal neurons, depending on their firing pattern (Amitai, 1994; Chagnac-Amitai et al., 1990; Connors et al., 1982; Hefti and Smith, 2000; Larkman and Mason, 1990; Mason and Larkman, 1990; Williams and Stuart, 1999). In the present study only RS-cells were included for analysis of developmental changes, because in young animals (below P14) only RS-cells were found. From P14 onwards additionally IB-cells can be detected. Overall 147 RS-pyramidal neurons from P7 mice and 112 RS-pyramidal neurons from P14 mice were studied. At P7 the dendritic tree already was rather complex and the apical dendrite reached layer I (fig. 3.1 B). In some cases the apical dendrite left out of the slice before attaining the pial surface caused by variations of the cutting plane. This did not influence the basic

electrophysiological properties of these cells (see methodological discussion). The apical dendrite had only few collateral branches and a small terminal dendrite tuft.

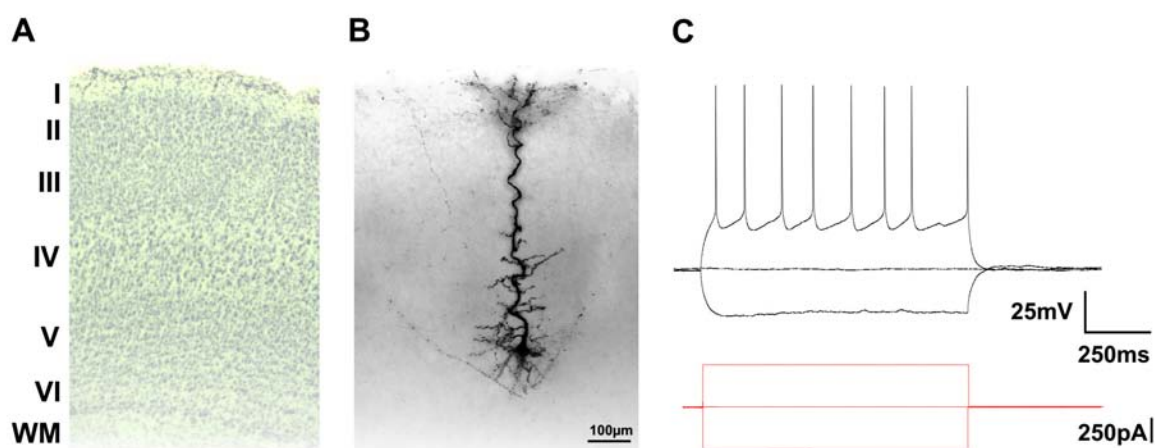


Fig. 3.1: Morphology and electrophysiology of immature layer Vb pyramidal neurons.

(A) The Nissl-staining of an acute slice at P7 revealed the laminar organization of mouse somatosensory cortex. Roman numbers (*I – VI*) indicate the cortical layers, also the white matter (*WM*) is shown. (B) The morphology of a typical immature layer Vb pyramidal neuron (biocytine filled) included the apical dendrite reaching layer I and a couple of collateral branches and a small terminal dendrite tuft. (C) The current-clamp recording exhibited a RS firing pattern of this pyramidal neuron.

For a basic electrophysiological characterization the active and passive membrane properties were analyzed. For this purpose, patch-clamp whole-cell recordings were performed in acute slices of P7 mice using the regular ACSF for acute slices (see 2.2 c) and intracellular solution I (see 2.2 f). Experiments were carried out in the current clamp-mode. Directly after reaching the whole-cell configuration the membrane potential was recorded. Afterwards hyperpolarizing and depolarizing rectangular current pulses were applied every 10 seconds and the changing membrane potentials were recorded (fig. 3.1 C). At small charges the course of potentials was determined by the passive membrane properties, at higher depolarizations action potentials (AP) were elicited. On the basis of these recordings the characteristic parameters were analyzed as follows (table 1):

Passive intrinsic properties	
Resting membrane potential V_{rmp} (mV)	$-58,6 \pm 1,4$
Membrane resistance R_m ($M\Omega$)	$876,5 \pm 37,2$
Membrane time constant τ_m (ms)	$87,1 \pm 2,9$
Capacitance (pF)	$65,8 \pm 7,8$

Active intrinsic properties	
Maximum AP-frequency (s ⁻¹)	25,9 ± 1,3
AP-threshold (mV)	33,3 ± 1,6
Amplitude (mV)	68,3 ± 1,6
Half width of 1 st AP (ms)	2,2 ± 0,1

Table 1: Basic electrophysiological properties of immature layer Vb pyramidal neurons.

3.1.2 Presynaptic properties of immature glutamatergic synapses on layer Vb pyramidal neurons

As already mentioned, in a presynaptically silent synapse, both AMPA- and NMDA-receptors are present, but they are activated only rarely. This is due to a very low release probability (Pr), because no docked vesicles are present. Such a synapse without releasable vesicles would not respond at all during the experiment and therefore show a failure rate of up to 100%. LTP would increase the release probability and the synapse would respond after induction of LTP (Gasparini et al., 2000; Voronin et al., 2004; Walz et al., 2006). The low Pr also increases in “paired trials” due to presynaptic paired-pulse facilitation, i.e. if an additional pulse is delivered not more than 50 ms after the first, the synapse will respond occasionally to the second pulse, indicating the presence of AMPA-receptors (Voronin et al., 2004).

To investigate the presence of these presynaptically silent synapses with such a low Pr, layer 5B pyramidal neurons in mouse somatosensory cortex were studied using whole-cell patch-clamp-recordings. For extracellular paired-pulse stimulation a bipolar tungsten electrode was placed in the same layer in a distance of between 50 to 150 µm from the cell soma of interest (fig. 2A). For the minimal stimulation protocol (Sokolov et al., 2002) the stimulus strength was adjusted manually at about 1 V to evoke minimal responses with failures in response to the first pulse. The standard deviation (SD) of the recording noise was calculated during the period directly before the stimulation. If the signal amplitude upon stimulation was higher than 2x SD noise, the signal was rated as “success”, below 2x SD it was rated as “failure”. To ensure, that the signal is a direct, monosynaptic response to the given stimulation, only responses with latencies below 5 ms were analyzed. For analyzing the decay time constant of the evoked PSCs, a monoexponential function ($I(t) = A \cdot e^{-t/\tau} + C$) was fitted between the maximal amplitude of the synaptic response and the point of return to the baseline.

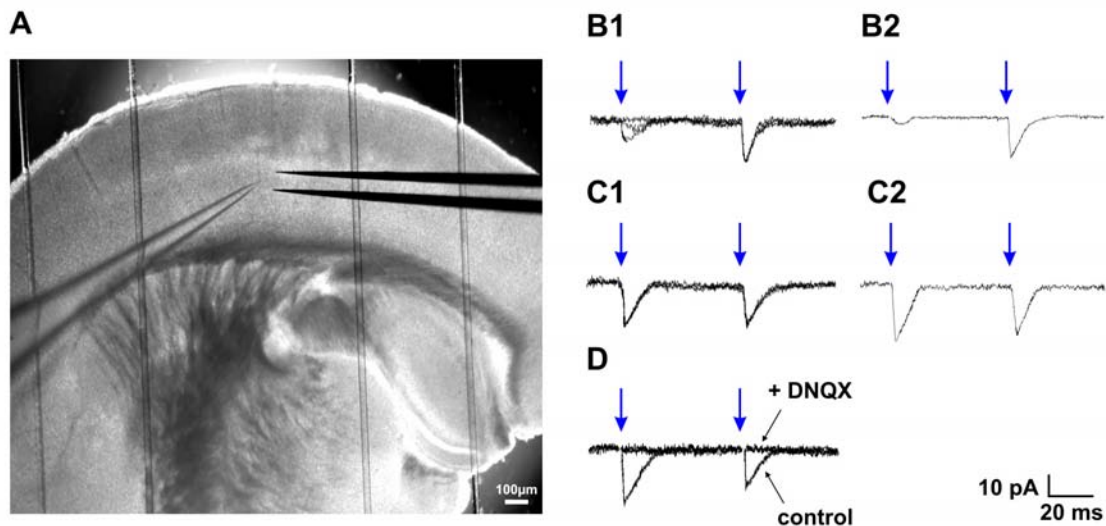


Fig. 3.2: Presynaptic properties of immature synapses on layer Vb pyramidal neurons.

(A) The transmitted light photograph of an acute slice at P7 shows the mouse somatosensory cortex with underlying structures and already positioned stimulation and patch electrodes. (B, C) Upon paired-pulse stimulation the EPSCs revealed either a high failure rate to the first pulse (B1, 3 single sweeps, B2, average of 5 sweeps) or EPSCs exhibited responses to both pulses with little failures (C1, three single sweeps, C2, average of 5 sweeps). (D) All EPSCs were reversibly blocked by 20 μ M DNQX (blue arrows indicate stimulation pulses).

Paired-pulse stimulation evoked AMPA-receptor mediated excitatory postsynaptic currents (EPSCs) were recorded at a holding potential of -60 mV (see table 2). In some recordings, the paired-pulse behavior of the synaptic responses revealed a strong facilitation and a reduced failure rate in response to the second pulse (see definition: presynaptically silent), indicating a very low Pr during the first pulse (fig. 2 B1 and B2). In addition, responses with a low failure rate to the first pulse, which showed a slight reduction in AMPA-receptor mediated EPSC amplitude and no change in failure rate to the second pulse (fig. 2 C1 and C2) could be obtained. All recorded AMPA-receptor mediated EPSCs were reversibly blocked by addition of 20 μ M DNQX (fig. 2D). Other properties of the AMPA-receptor mediated EPSCs are listed in table 2:

Amplitudes of evoked AMPA receptor mediated EPSCs (pA)	
Low Pr 1 st pulse	3,9 \pm 0,9
Low Pr 2 nd pulse	13,1 \pm 2,7
Low Pr 1 st pulse after pairing	7,9 \pm 1,2
Low Pr 2 nd pulse after pairing	8,9 \pm 2,2
High Pr 1 st pulse	12,4 \pm 2,9
High Pr 2 nd pulse	10,8 \pm 1,8

Properties of evoked AMPA receptor mediated EPSCs	
Rise time (ms)	$2,2 \pm 0,5$
Decay time (ms)	$15,6 \pm 5,9$
Latency (ms)	$3,7 \pm 0,8$

Table 2: Properties of AMPA-receptor mediated EPSCs at P7.

The quantitative analysis of these synaptic responses revealed an amount of about 25% of all synaptic responses tested, which showed an extremely high failure rate $> 30\%$ (and therefore a low Pr, [n = 33]) to the first pulse, whereas the remaining 75% showed only few failures in response to the first pulse and hence, a high Pr (fig. 3A, [n = 115]). Correspondingly, the coefficient of variance (CV) to the first pulse was initially high ($\geq 0,5$) in synapses with a low Pr and lower ($\leq 0,6$) in synapses with a high Pr (fig. 3B). In addition, a correlation between the CV and the corresponding mean amplitudes could be observed (fig. 3C).

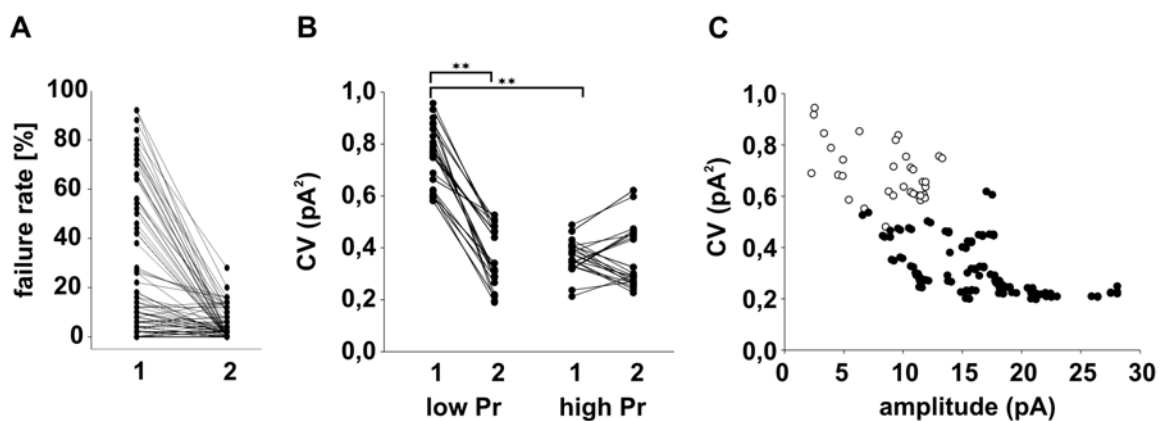


Fig. 3.3: Quantification of evoked AMPA-receptor mediated EPSCs of immature layer Vb pyramidal neurons.

(A) EPSCs with an extremely high failure rate to the first pulse as well as those with almost no failures were observed. Responses to the first and the second pulse from the same recording are connected by straight lines. (B) The CVs revealed correspondingly either a high (high failure rate and low Pr) or low value (low failure rate and high Pr) to the first pulse. (C) Likewise a correlation of CV and corresponding mean amplitudes was observed (*low Pr*: white circles, n = 33; *high Pr*: black circles, n = 115).

Furthermore, it has been reported that the amount of silent synapses found varies and depends on the experimental conditions such as the frequency of stimulation (Isaac et al., 1995; Liao et al., 1995; Durand et al., 1996; Gasparini et al., 2000; Montgomery et al., 2001). Therefore, as a standard characterization, different interpulse intervals from 25 up to 150 ms were tested

(fig. 4A, [n = 19]). Increasing the interstimulus interval (ISI) led, as expected, to a reduction of facilitation (paired-pulse ratio (PPR) > 1) reaching paired-pulse depression (PPR < 1) above 75ms ISI (fig. 4B and C).

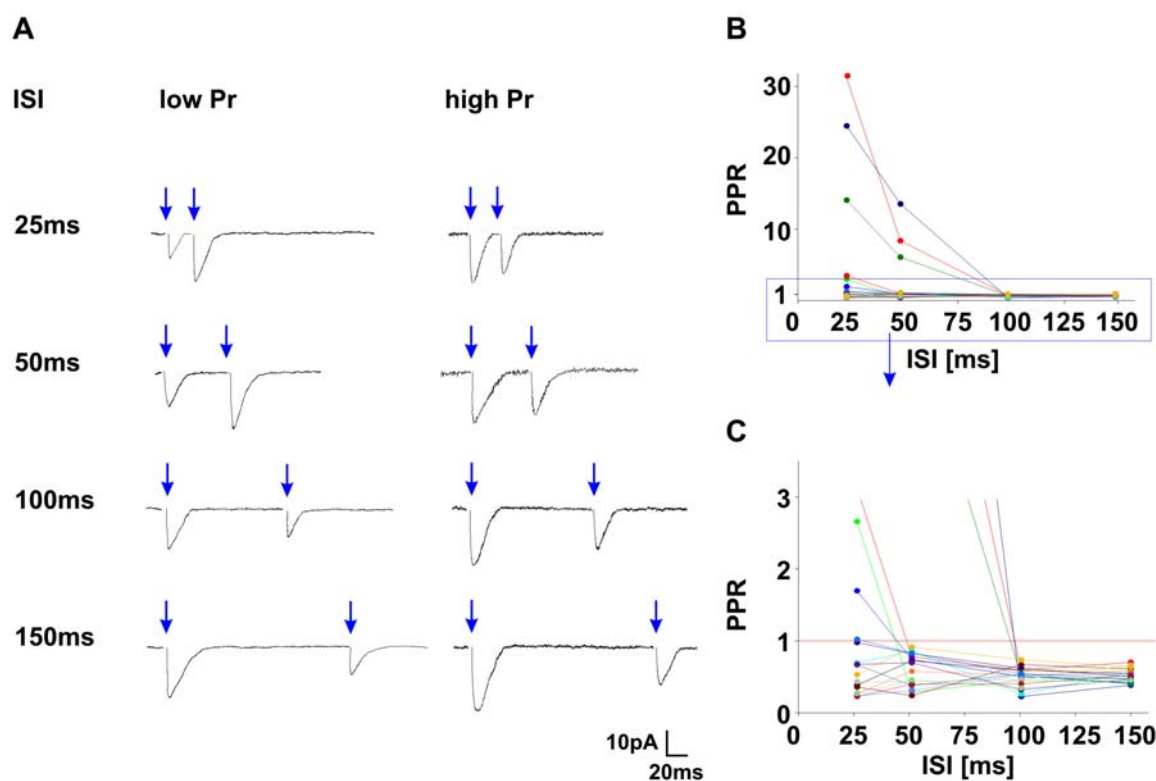


Fig. 3.4: Dependence of paired-pulse behavior on interstimulus interval.

(A) Examples of evoked AMPA-receptor mediated EPSCs (average of 10 sweeps in each case) with interstimulus intervals (ISI) from 25 to 150 ms showing a reduction in paired-pulse facilitation with increasing ISI (n = 19, blue arrows indicate stimulation pulses). (B) The paired-pulse ratio (PPR) decreased with increasing ISI. (C) Magnification (blue box in B) visualizes the changeover from facilitation (PPR > 1) to depression (PPR < 1) at 75 ms (different colours indicate different cells).

The continuum of different paired-pulse behaviors ranging from strong facilitation to depression can be divided into two arbitrary groups by analyzing the PPR versus the failure rate in response to the first pulse (fig. 5). The relation of PPR to failure rate to the first pulse showed two potential classes of glutamatergic synapses with a very low or a high Pr. Criteria for a very “low Pr synapse” were an initial failure rate of at least 30% and a PPR of more than 2 (n = 33). Synaptic responses that revealed a PPR of less than 2 and a failure rate below 30% were allocated to the “high Pr synapses” (n = 115). In this way 22,3 % of the synapses were categorized as low Pr and therefore immature synapses. The remaining 77,7 % of synapses tested were mature synapses with a high Pr.

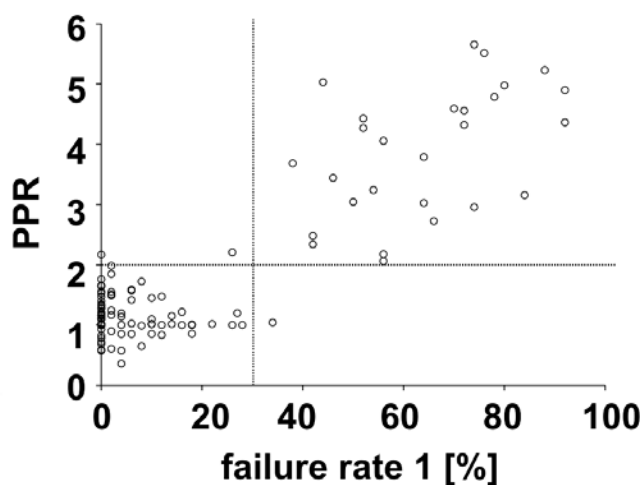


Fig. 3.5: Classification of AMPA-receptor mediated EPSCs of immature layer Vb pyramidal neurons.

Synapses can be divided into two classes with a low Pr or a high Pr by the criteria (1) PPR above 2 and failure rate above 30% (low Pr, immature, $n = 33$) as well as (2) PPR below 2 and failure rate below 30% (high Pr, mature, $n = 115$).

Interestingly, so far two of the above mentioned four different developmental states (see 1.7), which might be present simultaneously, could be detected at P7: (1) a mature state with a high release probability and postsynaptic AMPA- (and NMDA-) receptors and (2) an immature state with a low release probability and postsynaptic AMPA- (and NMDA-) receptors.

3.1.3 Developmental changes of presynaptic properties of glutamatergic synapses on layer Vb pyramidal neurons

The number of apparently silent synapses is large at birth and decreases during development as shown for postsynaptically silent synapses (Rumpel et al., 1998). Synaptic maturation has been proposed to be sequential in the sense that NMDAR-mediated signaling develops initially followed by AMPAR-mediated one. Insertion of AMPA-receptors due to a NMDA-receptor-dependent LTP-like process has been proposed as underlying mechanism. However, recent studies suggest additionally a strong involvement of presynaptic maturation of the release machinery. To study possible developmental changes on the presynaptic side, more mature pyramidal neurons from P14 mice were recorded.

The Nissl-staining (fig. 3.6 A) shows the abundantly clear laminae in the somatosensory cortex of a P14 mouse. At P14 the large pyramidal neurons of layer Vb can be subdivided into

“*Intrinsically Bursting*” (IB) and “*Regular Spiking*” (RS) pyramidal neurons, depending on their firing pattern (Amitai, 1994; Chagnac-Amitai et al., 1990; Connors et al., 1982; Hefti and Smith, 2000; Larkman and Mason, 1990; Mason and Larkman, 1990; Williams and Stuart, 1999). As already mentioned, only RS-cells were included for analysis of developmental changes, because in experiments at P7 only RS-cells could be found. Altogether 112 RS-pyramidal neurons from P14 mice were investigated. At P14 the dendritic tree appeared much more mature than at P7 and was rather complex. Usually the apical dendrite reached layer I (fig. 3.6 B), but again in some cases the apical dendrite left out of the slice before attaining the pial surface caused by variations of the cutting plane. Several collateral branches and a clear terminal dendrite tuft were observed. Just like at P7 for the basic electrophysiological characterization the active and passive membrane properties were analyzed. For patch-clamp whole-cell recordings again the regular ACSF for acute slices (see 2.2 c) and intracellular solution I (see 2.2 f) were used. Experiments were carried out in the current clamp-mode and the membrane potential was recorded. Hyperpolarizing and depolarizing rectangular current pulses were applied every 10 seconds and the changing membrane potentials were recorded (fig. 3.6 C). At small charges the course of potentials was strongly determined by the passive membrane properties, at higher depolarizations APs were elicited.

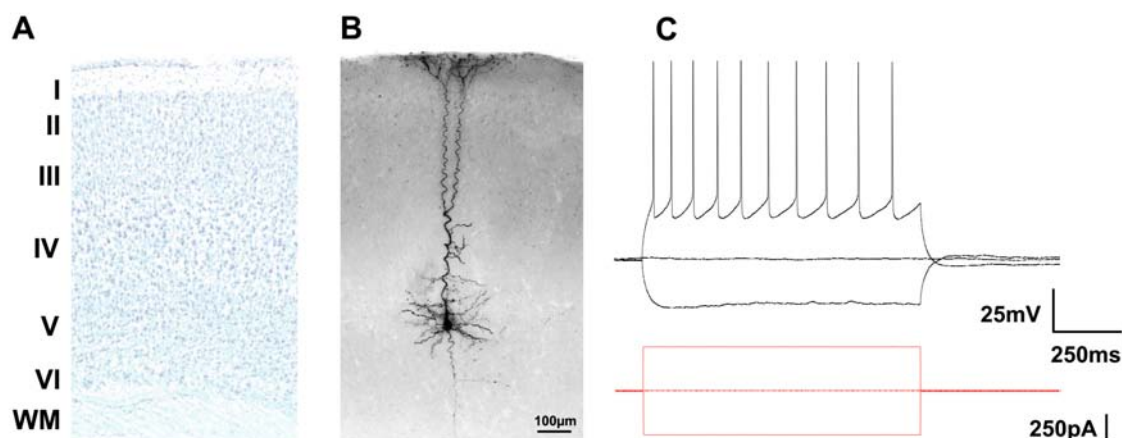


Fig. 3.6: Morphology and basic electrophysiology of mature layer Vb pyramidal neurons at P14. (A) The Nissl-staining of an acute slice at P14 revealed clearly the laminar organization of mouse somatosensory cortex. Roman numbers (*I – VI*) indicate the cortical layers, also the white matter (*WM*) is represented. (B) The morphology of a typical layer Vb pyramidal neuron at P14 shows the large apical dendrite reaching layer I and several collateral branches and a broad terminal dendrite tuft. (C) The *current-clamp* recording exhibits a RS firing pattern of this mature pyramidal neuron.

The basic electrophysiological parameters are listed in table 3:

Passive intrinsic properties	
Resting membrane potential V_{rmp} (mV)	$-63,6 \pm 1,4$
Membrane resistance R_m (M Ω)	$426,5 \pm 37,2$
Membrane time constant τ_m (ms)	$42,1 \pm 2,9$
Capacitance (pF)	$105,3 \pm 12,3$
Active intrinsic properties	
Maximum AP-frequency (s^{-1})	$35,4 \pm 1,5$
AP-threshold (mV)	$38,3 \pm 1,6$
Amplitude (mV)	$84,5 \pm 1,5$
Halfwidth of 1 st AP (ms)	$1,6 \pm 0,1$

Table 3: Basic electrophysiological parameters of layer Vb pyramidal neurons at P14.

In comparison to the active and passive intrinsic properties at P7, several developmental changes were observed. The resting membrane potential was enhanced significantly with increasing age ($p < 0,05$). The membrane resistance showed a highly significant developmental decrease ($p < 0,01$), whereas the capacitance clearly increased ($p < 0,01$). These changes should be essentially caused by the growth of the cells. The strong decrease of the membrane time constant ($p < 0,01$) during development might result in an elevated excitability of these neurons. The APs at P14 hardly adapted in their frequency, showing again the “regular spiking” firing pattern (Connors and Gutnick, 1990). The frequency ($p < 0,05$) as well as the amplitude ($p < 0,05$) was strongly increased at P14, whereas the half width was just about half as much as at P7 ($p < 0,01$). This might be caused by a higher density of voltage-dependent channels. These developmental changes correspond well with those described in the literature (Kasper et al., 1994; McCormick and Prince, 1997).

Evoked AMPA-receptor mediated excitatory postsynaptic currents (EPSCs) were recorded at P14 at a holding potential of -60 mV. With paired-pulse minimal stimulation exclusively responses with an initial failure rate at about zero were detected. These responses showed a clear paired-pulse depression in the AMPA-receptor mediated EPSC amplitude (see table 4, fig. 3.7 A, [n = 113]) and no change in CV (fig. 3.7 B), indicating a high Pr to the first pulse in these more mature neurons. A strong correlation between CVs and the corresponding amplitudes was observed (fig. 3.7 C). As already described for experiments at P7, all recorded AMPA-receptor mediated EPSCs were reversibly blocked by addition of 20 μ M DNQX.

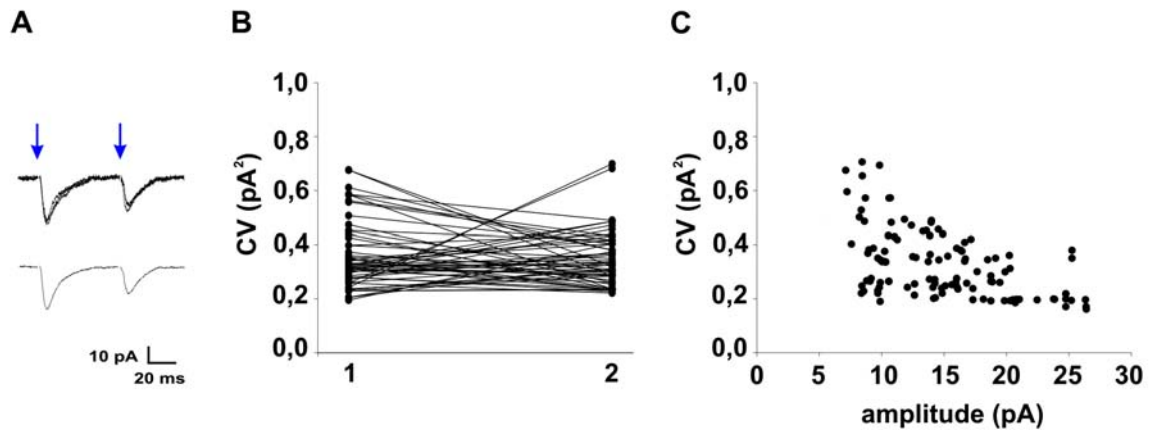


Fig. 3.7: Presynaptic properties of glutamatergic synapses on layer Vb pyramidal neurons at P14.

(A) Exclusively AMPA receptor-mediated EPSCs with a high Pr and no failures in response to the first pulse (top, 3e single sweeps, bottom, average of 5 sweeps) were observed ($n = 113$, *blue arrows indicate stimulation pulses*). (B) The CV correspondingly revealed rather low values (according to low failure rate and high Pr) to the first pulse. (C) Correlation of CVs and corresponding amplitudes.

Properties of the AMPA-receptor mediated EPSCs are listed in table 4:

Amplitudes of evoked AMPA receptor mediated PSCs (pA)	
Low Pr 1 st pulse	---
Low Pr 2 nd pulse	---
Low Pr 1 st pulse after pairing	---
Low Pr 2 nd pulse after pairing	---
High Pr 1 st pulse	$21,1 \pm 4,9$
High Pr 2 nd pulse	$13,8 \pm 3,4$
Properties of evoked AMPA receptor mediated PSCs	
Rise time (ms)	$3,5 \pm 0,5$
Decay time (ms)	$18,9 \pm 0,5$
Latency (ms)	$2,2 \pm 4,1$

Table 4: Properties of AMPA-receptor mediated EPSCs at P14.

In comparison with P7, the synaptic responses at P14 showed a clear reduction in CV (fig. 3.8 A, $p < 0,05$) and a highly significant decrease in PPR (fig. 3.8 B, $p < 0,01$). The developmental shift towards lower values is also quite apparent, if the CV is plotted against PPR (fig. 3.8 C). In summary, a presynaptic maturation was evident by more mature presynaptic properties like a higher Pr at P14.

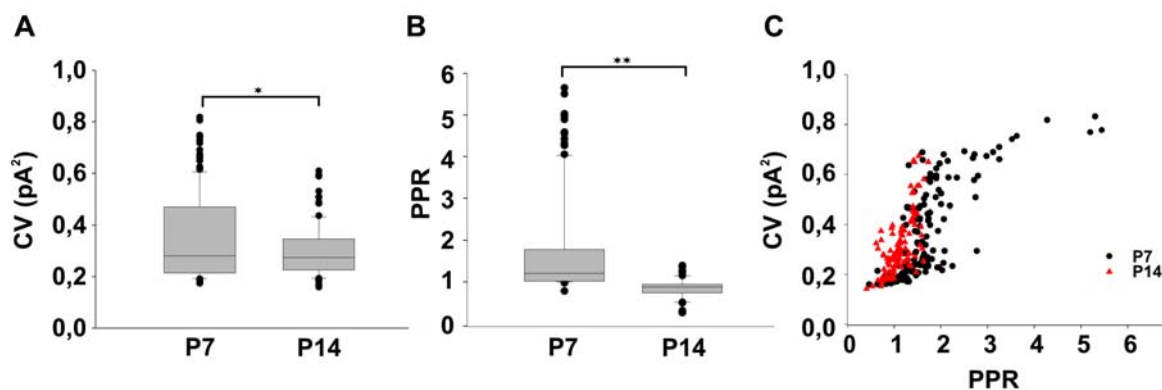


Fig. 3.8: Comparison of presynaptic properties of immature and mature layer Vb pyramidal neurons.

(A) The quantitative comparison of immature (P7, $n = 147$) and mature (P14, $n = 112$) layer Vb pyramidal neurons showed a pronounced reduction in the mean CV ($p < 0,05$). (B) Accordingly, the decrease in PPR was highly significant ($p < 0,01$). (C) Likewise the shift towards lower PPR and CV at P14 (red triangles) in contrast to P7 (black circles) is clearly visible.

3.2 Characterization of NMDA-receptors in immature layer Vb pyramidal neurons

After demonstration of the existence of presynaptically immature and mature developmental states in the somatosensory cortex at P7, the state of maturation at the postsynaptic site was analyzed at the same synapses. Therefore, corresponding NMDA-receptor mediated EPSCs were recorded using the whole-cell patch clamp-technique. Upon identification of the presynaptic properties of a given synapse via recording of AMPA-receptor mediated EPSCs at -70 mV holding potential, the minimal stimulation was repeated with identical strength at $+40$ mV holding potential after addition of $20 \mu\text{M}$ DNQX. A NMDA-receptor mediated response was observed in all cases independent from the presynaptic properties, i.e. a very low Pr (fig. 3.9 A1) or a high Pr (fig. 3.9 A2). All NMDA-receptor mediated EPSCs were blocked by addition of $50 \mu\text{M}$ of the specific NMDA-receptor antagonist D-AP5 (fig. 3.9 A1, A2). As unveiled by the quantitative analysis (fig. 3.9 B) the paired-pulse behavior of the NMDA-receptor mediated responses differed topmost significantly from that of the AMPA-receptor mediated ones ($p < 0,01$). NMDA-receptor mediated EPSCs at $+40$ mV showed always a low failure rate ($3,1 \pm 2,4$ at low Pr synapses and $2,5 \pm 2,4$ at high Pr synapses) despite the high failure rate in corresponding AMPA-receptor mediated responses at -70 mV ($60,0 \pm 16,7$ at low Pr synapses and $8,8 \pm 7,5$ at high Pr synapses). At synapses with a high Pr a similar low failure rate of NMDA-receptor mediated EPSCs was found. This lack of failures in response to the first pulse at NMDA-receptor mediated EPSCs suggests the presence of additional NMDA-receptor only synapses lacking AMPA receptors. Furthermore, qualitative differences were obtained concerning NMDA-receptor EPSC kinetics. At synapses with a

high Pr, indicating a presynaptically mature state, the kinetics were much faster than in synapses with a low Pr. This acceleration of kinetics from immature (low Pr) to mature (high Pr) synapses might be caused by a change in NMDA-receptor subunit composition during development (Flint et al., 1997). To unravel developmental changes in NMDA-receptor subunit composition, NMDA-receptors were investigated in detail in the following part of this study.

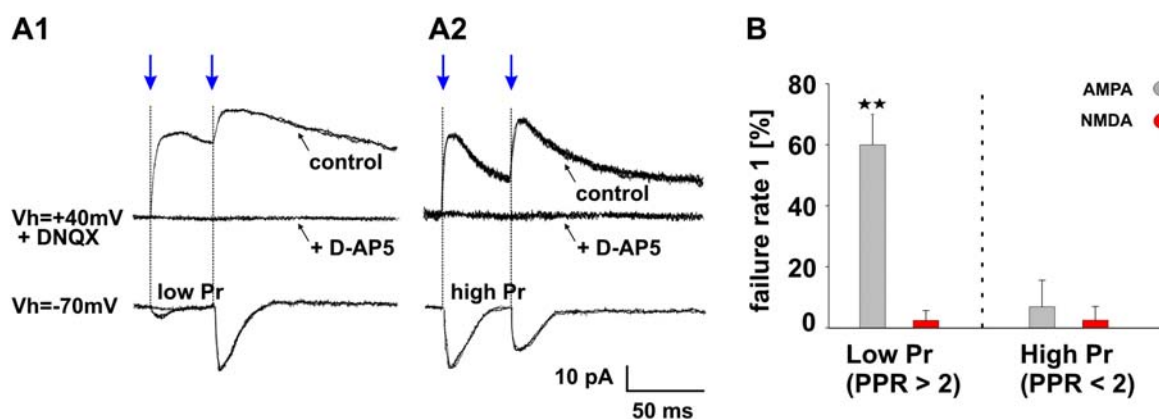


Fig. 3.9: Properties of NMDA-receptor mediated PSCs at P7.

(A) Examples of AMPA- and NMDA-receptor mediated responses in immature (A1, low Pr) and mature (A2, high Pr) synapses on layer Vb pyramidal neurons. NMDA-receptor mediated components were observed in all cases (*blue arrows indicate stimulation pulses*) and were blocked by D-AP5. (B) The quantitative analysis revealed a significantly ($p < 0,01$) different failure rate in AMPA- (*grey bars*) and NMDA-receptor (*red bars*) mediated EPSCs.

As already mentioned, there might be 4 different developmental states present *simultaneously* in mouse somatosensory cortex at P7: (1) a mature state with a high release probability and postsynaptic AMPA- and NMDA-receptors, which has already been found (see 3.2); (2) an immature state with a low release probability and postsynaptic AMPA- and NMDA-receptors that has been described likewise (see 3.2); (3) an immature state with a high release probability but postsynaptic only NMDA-receptors and finally, (4) an immature state with a low release probability and postsynaptic only NMDA-receptors that still remained to be analyzed. Pyramidal neurons at P7 were chosen for the further experiments, because the anatomical development of the somatosensory cortex is almost finished, but developmental maturation like the conversion of “silent synapses” into functional ones still can be detected (Rumpel et al., 1998). These postsynaptically silent synapses are well known as NMDA-receptor only synapses. They are lacking AMPA-receptors, but express functional NMDA-receptors. Functional AMPA-receptors are delivered to the subsynaptic membrane after LTP induction. It seems to be characteristic for this early developmental stage, where a quite intensive synaptogenesis takes place (Malenka and Nicoll, 1997; Feldman and Knudsen,

1998; Feldman et al., 1999; Atwood and Wojtowicz, 1999). Another well established indicator for postsynaptic maturation is a change of NMDA-receptor subunit composition (Flint et al., 1997) that fastens NMDA-receptor kinetics.

To analyze the postsynaptic development and to figure out, if there might exist a coupling between presynaptic (low Pr) and postsynaptic (AMPA- and/or NMDA-receptors) developmental maturation, NMDA-receptor mediated currents were investigated during different developmental conditions. The basic properties of the NMDA-receptor mediated EPSCs are listed in table 5:

Properties of evoked NMDA receptor mediated PSCs	
Rise time (ms)	14,1 ± 2,1
Amplitude (pA)	34,8 ± 14,7
Latency (ms)	3,8 ± 1,2

Table 5: Properties of NMDA-receptor mediated PSCs at P7.

3.2.1 NMDA-receptor only synapses on immature layer Vb pyramidal neurons

In immature cortex synapses with a purely NMDA-receptor mediated transmission have been described frequently. To analyze these so-called silent synapses in immature layer Vb pyramidal neurons, whole-cell patch clamp recordings were performed at P7. Glutamatergic EPSCs were isolated by addition of 100 μ M picrotoxin. By choice of different holding potentials AMPA- and NMDA-receptor mediated currents were separated, taking advantage of the voltage-dependent Mg^{2+} -block of NMDA-receptors. To improve the recording conditions at +40 mV holding potential, the intracellular solution II (see 2.2 g), containing TEA to block potassium currents, was used. Additionally, 100 μ M glycine was added to the ACSF as NMDA-receptor coagonist. Glutamatergic EPSCs were elicited by extracellular stimulation as previously described (see 3.1.2). The stimulation strength was adjusted according to the minimal stimulation protocol. At a holding potential of +40 mV a response was observed in all cases, whereas at -70 mV in some cases no response was detectable (fig. 3.10 A, [n = 5]). For further analysis of the NMDA-receptor mediated PSCs, SYM 2206 was added to the ACSF to eliminate any possibility of an influence of AMPA-receptor mediated currents. If these silent synapses are immature, they should contain only NMDA-receptors and further, only those with an immature subunit composition, i.e. NR2B subunits. This

hypothesis was corroborated by a complete block of the NMDA-receptor mediated response using the NR2B-specific blocker Ro 25-6981 (fig. 3.10 B, [n = 5]). Although NR2B-NMDA-receptors have been indicated to be essential for the expression of LTP in the somatosensory cortex during development (Lu et al., 2001), it could be observed that NR2B-containing NMDA-receptors are important for the conversion of silent synapses into functional ones in mature neuronal circuits. It has been shown that diminished activity-induced increase in the connectivity is accompanied by the surface delivery of NR2B-containing NMDA-receptors to form silent synapses. These synapses are subsequently converted to functional synapses by neuronal activation (Nakayama et al., 2005).

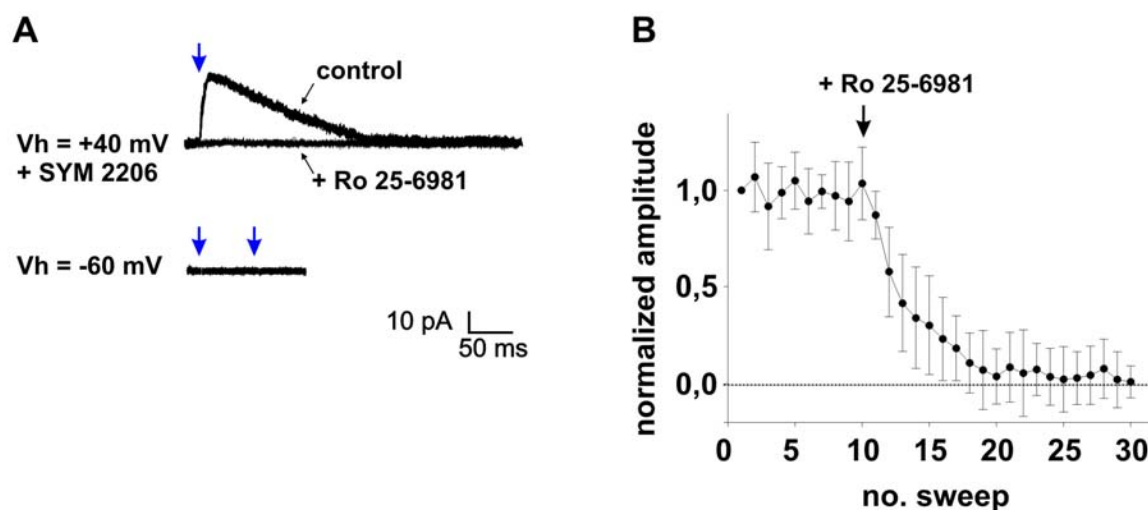


Fig. 3.10: Postsynaptically silent synapses on immature layer Vb pyramidal neurons.

(A) At +40 mV holding potential NMDA-receptor mediated PSCs were recorded, whereas at -60 mV only failures were detectable (n = 5, blue arrows indicate stimulation pulses, average of 5 sweeps in each case). (B) NMDA-receptor mediated PSCs were completely blocked by addition of the NR2B subunit specific antagonist Ro 25-6981.

3.2.2 NMDA-receptor subunit composition at immature and mature synapses on layer Vb pyramidal neurons at P7

To study coupling of pre- and postsynaptic maturation NMDA-receptor mediated PSCs were investigated. The duration of these PSCs is thought to be determined by intrinsic receptor properties (Lester et al., 1990; Lester and Jahr, 1992) rather than the persistence of glutamate in the synaptic cleft (Clements et al., 1992). Therefore, changes in NMDA-receptor mediated PSC duration are likely to result from alterations of the NMDA-receptor complex itself (Hestrin, 1992; Crair and Malenka, 1995). Several studies (*In situ* hybridization, Monyer et al., 1994; RNase protection assays, Zhong et al., 1995; immunoprecipitation experiments,

Sheng et al., 1994) have demonstrated that NR2 subunit expression is developmentally regulated. In the embryonic cortical plate, only NR2B is expressed at embryonic day 19 (E19), whereas NR2D begins to be expressed by postnatal day 0. By P7, all four NR2 subunits are expressed in cortex at different levels (Monyer et al., 1994). These data suggest that changes in subunit expression during cortical development might regulate the function of cortical NMDA-receptors. The proportion of cells expressing NR2A and displaying fast NMDA-receptor mediated PSCs increases during postnatal development, thus providing a molecular basis for the developmental changes in PSCs (Flint et al., 1997). Moreover, changes in NMDA-receptor efficacy have been proposed as a mechanism establishing critical periods for plasticity in neocortex (Fox et al., 1992; Crair and Malenka, 1995).

To provide evidence that differences in NMDA-receptor mediated PSC kinetics at different maturational stages of glutamatergic synapses at P7 might be caused by a change of NMDA-receptor subunit composition, whole-cell patch-clamp recordings were performed in acute slices at P7. Immature (low Pr, [n = 6]) and mature (high Pr, [n = 13]) synapses were detected at a holding potential of -60 mV. Subsequently, SYM 2206 was added to the ACSF to eliminate any possibility of an influence of AMPA-receptor mediated currents and NMDA-receptor mediated PSCs were recorded at a holding potential of +40 mV (fig. 3.11 A). In a first approach, the amount of NR2B-containing NMDA-receptors was evaluated. Therefore, the specific NR2B subunit antagonist Ro 25-6981 was added to the ACSF. This antagonist was used because it acts much more potent than ifenprodil (Fischer et al., 1997). In presynaptically immature (low Pr) synapses the NMDA-receptor EPSCs were significantly reduced to about 20% ($p < 0,01$), whereas mature (high Pr) synapses showed an insensitive component of about 80% of the NMDA-receptor PSC amplitude (fig. 3.11 B, C; $p < 0,01$). These findings indicate a large amount of NR2B subunit-containing NMDA-receptors in presynaptically immature synapses and a significantly smaller amount of these subunits in the more mature synapses ($p < 0,01$) (fig. 3.11 D).

In a second, complementary approach the NR2A subunit was selectively blocked using Zn^{2+} ions, because the voltage-independent inhibition occurs at much lower Zn^{2+} -concentrations in NR2A-containing NMDA-receptors, i.e. the IC_{50} is in the nanomolar range versus an IC_{50} in the micromolar range for receptors consisting of NR2B subunits (Paoletti et al., 1997).

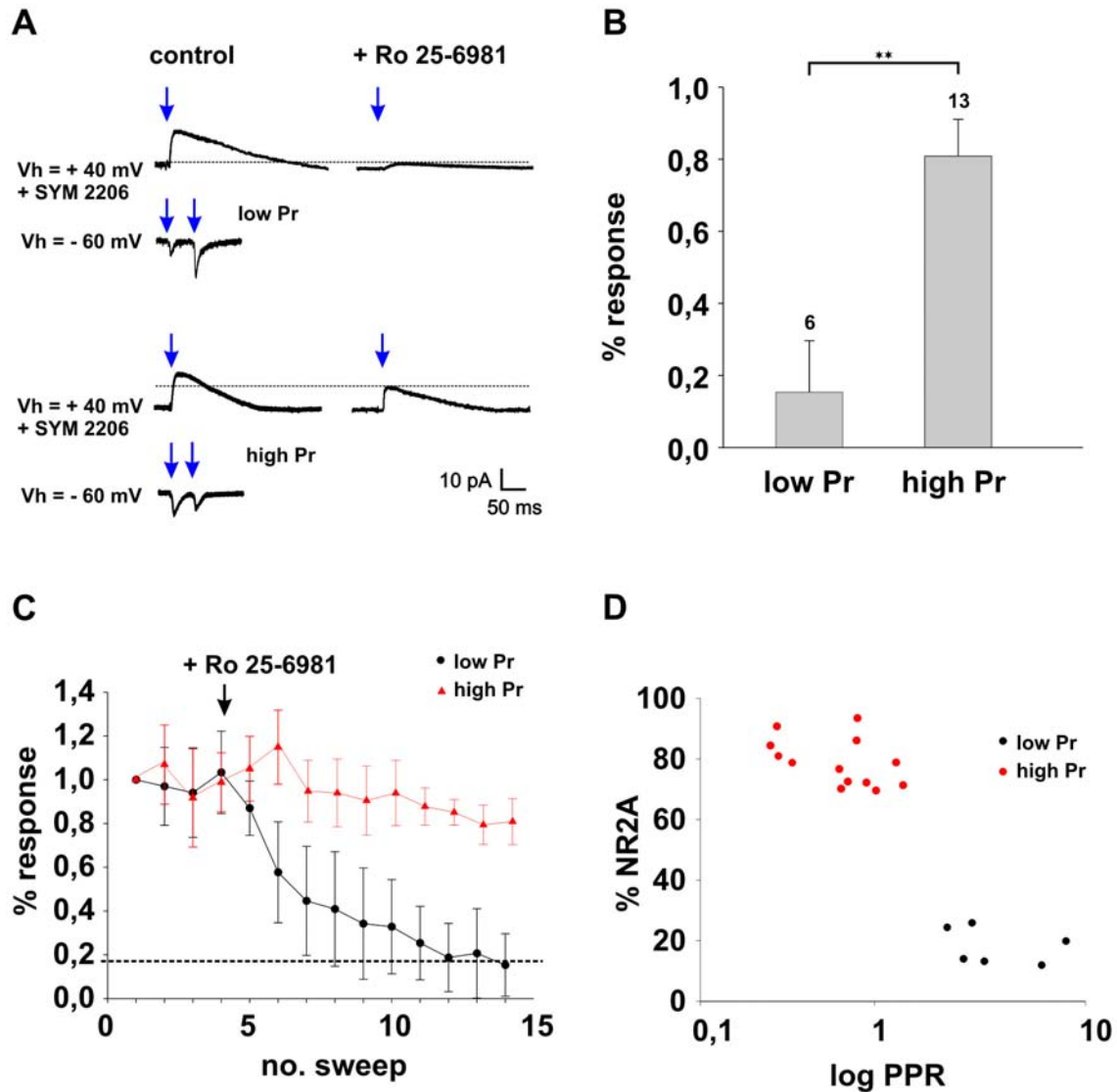


Fig. 3.11: Pharmacological analysis of NMDA-receptors using a NR2B subunit selective blocker. (A) Examples of AMPA- and NMDA-receptor mediated PSCs (average of 5 sweeps in each case, *blue arrows indicate stimulation pulses*) in immature (top, low Pr, $n = 6$) and mature (bottom, high Pr, $n = 13$) synapses including Ro 25-6981 application. (B) The quantification shows a significantly stronger reduction ($p < 0,01$) of NMDA-receptors PSCs after NR2B-block at immature (low Pr) synapses. (C) The progressive block of the NR2B subunit with Ro 25-6981 also reveals a stronger reduction of the NMDA-receptor PSCs in immature (low Pr, *black circles*) than in mature (high Pr, *red triangles*) synapses. (D) The different block indicates a small amount of NR2A subunits in immature (low Pr, *black circles*) and a high amount of NR2A subunits in mature (high Pr, *red circles*) synapses.

50 nM Zn^{2+} was added to the ACSF at P7 and the NMDA-receptor EPSCs were not reduced at all in immature (low Pr, [$n = 5$]) synapses, whereas mature (high Pr, [$n = 7$]) synapses showed a strongly reduced response of about 30% of the initial amplitude (fig. 3.12 A-C; $p < 0,01$). These results indicate a large amount of NR2A subunit-containing NMDA-receptors in the mature synapses and a lack of these subunits in the immature synapses (fig. 3.12 D; $p < 0,01$).

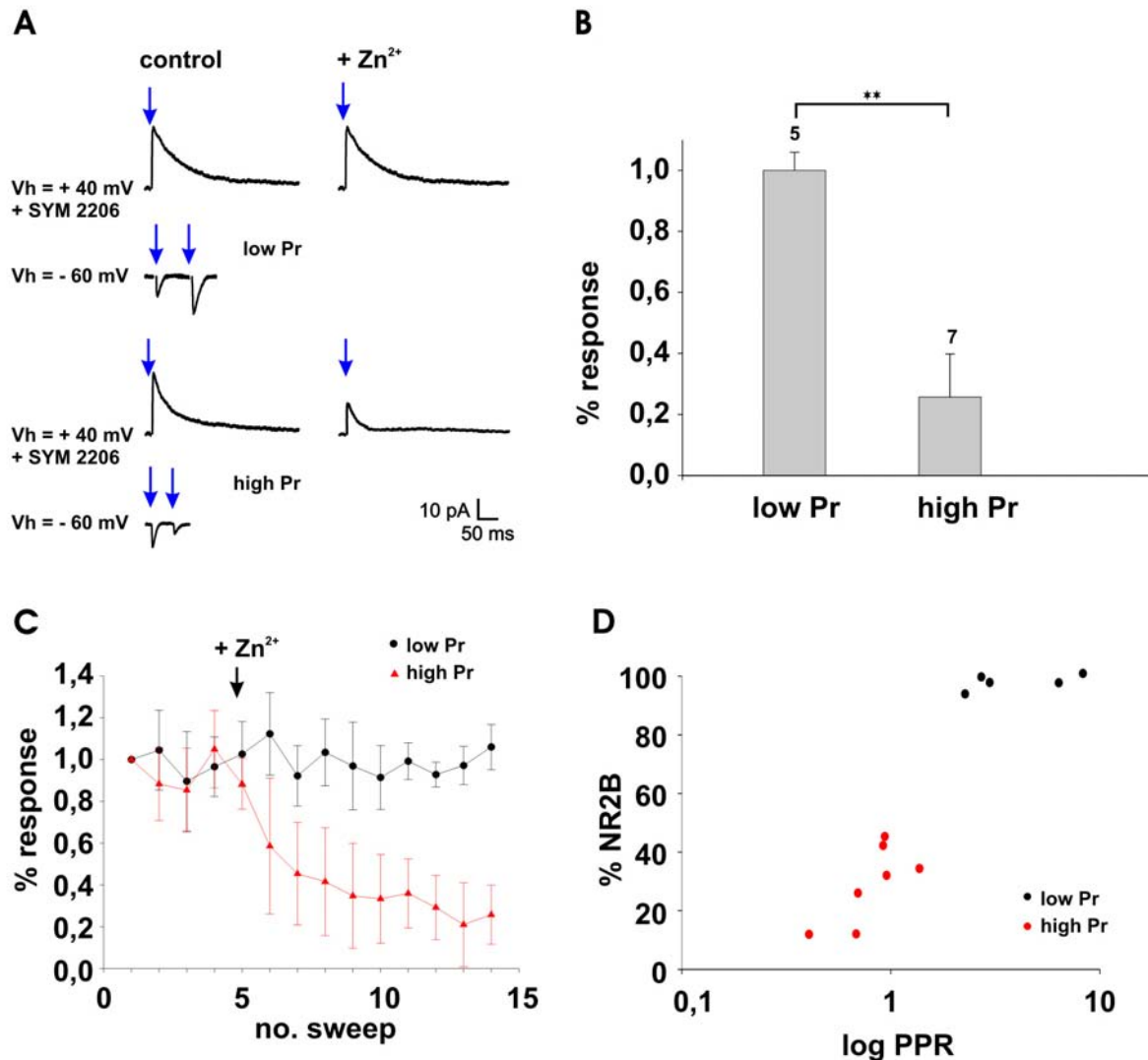


Fig. 3.12: Pharmacological analysis of NMDA-receptors using a NR2A subunit selective blocker. (A) Examples of AMPA- and NMDA-receptor mediated EPSCs (average of 5 sweeps in each case, *blue arrows indicate stimulation pulses*) in immature (top, low Pr, $n = 5$) and mature (bottom, high Pr, $n = 7$) synapses including 50 nM Zn²⁺ application. (B) The quantification showed a highly significant reduction ($p < 0,01$) in response after NR2A-block at mature (high Pr) synapses. (C) The progressive block of the NR2A subunit with Zn²⁺ also reveals a stronger reduction of the response in mature (high Pr, *red triangles*) than in immature (low Pr, *black circles*) synapses. (D) The different pharmacology indicates a high amount of NR2B subunits in immature (low Pr, *black circles*) and a smaller amount of NR2B subunits in mature (high Pr, *red circles*) synapses.

Additionally, to confirm the change in subunit composition at different maturational stages, NMDA-receptor decay kinetics were analyzed at P7. As mentioned previously (see 3.1.4), differences concerning NMDA-receptor decay kinetics were obtained at immature (low Pr) and more mature (high Pr) synapses. At mature synapses with a high Pr ($n = 20$) the kinetics (monoexponential fit) were significantly faster than in synapses with a low Pr ($n = 11$; $p < 0,05$). Although in immature synapses NMDA-receptor kinetics with a slow (above 400 ms) as well as a faster (about 150 ms) decay were found, the mature ones always revealed

NMDA-receptor mediated responses with a faster (below 300 ms) decay (fig. 3.13 A, B), indicating the presence of NR2A subunit containing NMDA-receptors. Altogether, we found evidence that the duration of NMDA-receptor mediated EPSCs is determined by intrinsic receptor properties, particularly, by the changing NMDA-receptor subunit composition (from purely NR2B to NR2A/NR2B) during development.

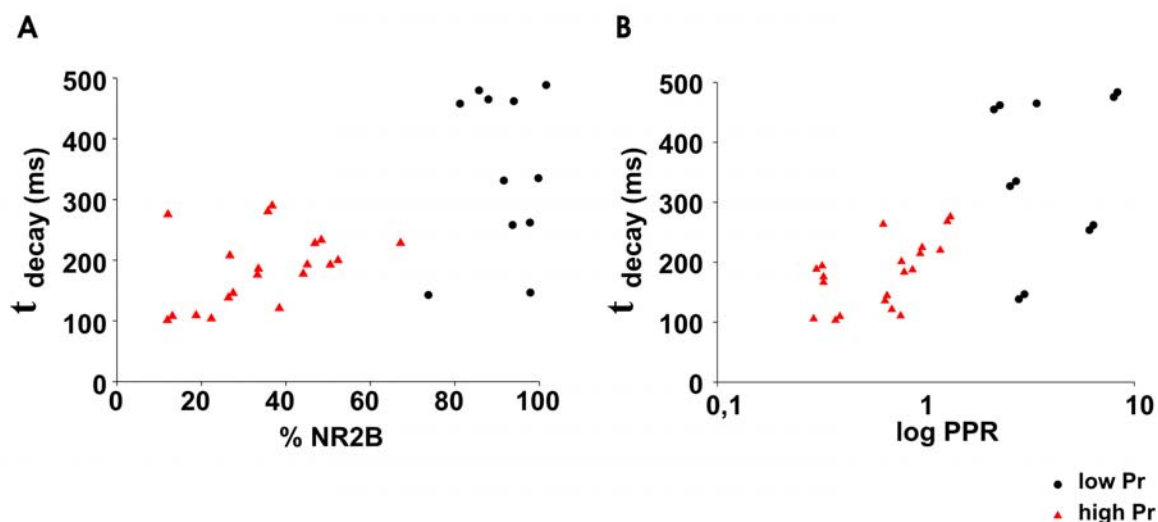


Fig. 3.13: Changes of NMDA-receptor kinetics at different maturational stages.

(A, B) Quantification of decay kinetics (monoexponential fit) revealed much slower kinetics above 400 ms in immature ($n = 11$, low Pr, *black circles*) than in mature ($n = 20$, high Pr, *red triangles*) synapses (below 300 ms). Although fast kinetics were also observed in immature (low Pr) synapses, slow kinetics (above 400 ms) were never detected in the mature (high Pr) ones.

3.2.3 Differences in release probability as indicated by MK801 block of NMDA receptors

The synaptic Pr plays a major role in determining the strength of a synapse, i.e. the average size of the postsynaptic response. Hence, the strength (efficacy) of a synapse can be modified by variation of its Pr (Bekkers and Stevens, 1990; Bolshakov and Siegelbaum, 1995; Magleby, 1982; Malinow and Tsien 1990; Manabe et al., 1993; Stevens and Wang 1994; Zucker, 1989). Because synaptic strength is that important for the function of neuronal circuits, a fundamental question is how Pr is distributed across a population of synapses. This question was already addressed in hippocampal synapses in culture and in slices (Hessler et al., 1993; Rosenmund et al., 1993). There, the progressive decrease of NMDA-receptor mediated PSCs was analyzed in the presence of the open-channel NMDA-receptor blocker MK-801. MK-801 blocks the receptor only in an open state, and because they are only opened

when transmitter is released, this progressive block of receptors provides an indirect measure of the Pr (Huang and Stevens, 1997).

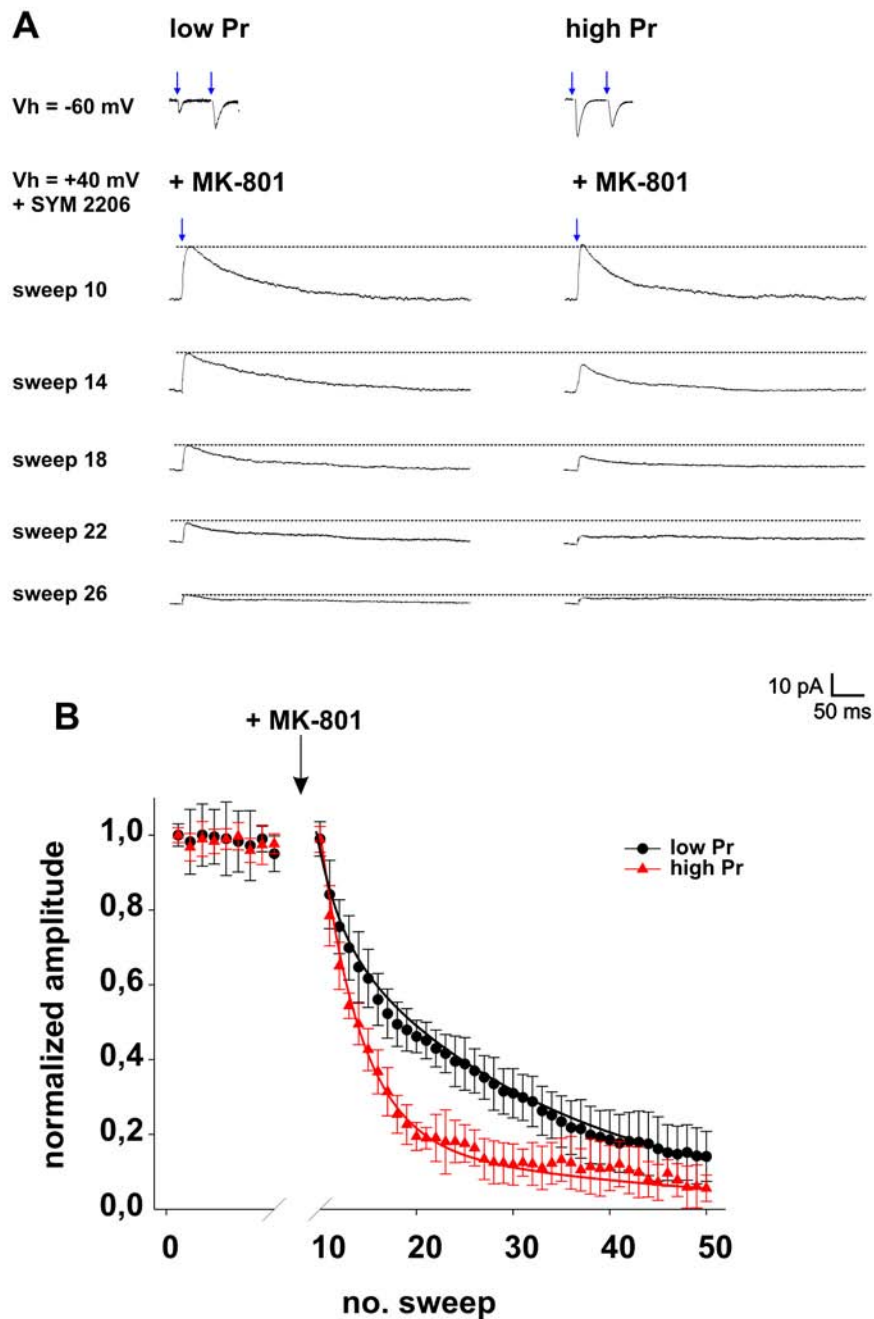


Fig. 3.14: Progressive block of NMDA-receptor mediated PSCs with MK-801.

(A) Examples of AMPA- and NMDA-receptor mediated EPSCs (*blue arrows indicate stimulation pulses*) in immature (left, low Pr, $n = 5$) and mature (right, high Pr, $n = 6$) synapses at different times of the progressive block with MK-801. (B) The summary of all experiments showed a significantly slower block ($p < 0,05$) at immature (low Pr, *black circles*) than in mature (high Pr, *red triangles*) synapses.

To confirm the differences in Pr at immature and mature synapses at P7, whole-cell patch-clamp recordings were obtained as described above (see 3.2.1). After characterizing immature and mature synapses at -60mV holding potential by extracellular minimal stimulation with a bipolar tungsten electrode, SYM 2206 was added to the ACSF to block AMPA-receptor mediated components. Single NMDA-receptor mediated PSCs were evoked at a holding potential of +40 mV with identical stimulation strength. The stimulus was repeated every 10 s and, after recording of 10 controls, 20 μ M MK-801 was washed into the slice. The progressive block was subsequently recorded for at least another 40 stimulations until a saturated block was reached (fig. 3.14 A). Immature synapses (n = 5) with a low Pr and NR2B subunit-containing NMDA-receptors showed a significantly slower block by MK-801 (Kolmogorov-Smirnov test, $P < 0,05$) than mature synapses (n = 6) with a high Pr and NR2A subunit-containing NMDA-receptors (fig. 3.14 B). Because the synaptic Pr plays a major role in determining the strength of a synapse and the strength (efficacy) of a synapse can be modified by variation of its Pr, our findings suggest that an increase in Pr occurs during early postnatal development and that this higher Pr leads to an improved efficacy (heightened strength) and therefore, a functional maturation of the synapse.

3.2.3 Pairing-induced potentiation of immature synapses in layer Vb pyramidal neurons

Conversion of a silent synapse into a functional one is one way to persistently increase synaptic efficacy (strength). In principle, synapses can be silent through postsynaptic as well as presynaptic mechanisms (see 1.5.3). Postsynaptically silent synapses are unable to detect glutamate release and do not conduct at rest due to the lack of AMPA-receptors in the subsynaptic membrane. By contrast, presynaptically silent synapses do not conduct, because their probability of glutamate release (Pr) is very close to zero (Voronin and Cherubini, 2004). The conversion of postsynaptically silent synapses into functional ones, due to insertion of AMPA-receptors, has been suggested to be particularly relevant during postnatal development, when a significant fraction of synapses contains only NMDA-receptors (Durand et al., 1996). The existence of presynaptically silent synapses (low Pr) has been suggested by experiments with minimal paired-pulse stimulation delivered to Schaffer collaterals or to mossy fibres in the hippocampus (Gasparini et al., 2000; Maggi et al., 2003). Neurones, which were exhibiting responses at +40 mV holding potential but only failures at -60 mV, occasionally responded to a second pulse delivered 50 ms after the first in a paired-pulse

paradigm. This kind of paired-pulse facilitation is thought to depend largely on an increase in Pr. Furthermore, a pairing of afferent stimulation with postsynaptic depolarization has been proposed to convert these presynaptically silent synapses into fully functional synapses and thus, to induce or to contribute to LTP.

To investigate a possible potentiation of the previously described presynaptically silent synapses (see 3.1.2), a pairing of extracellular stimulation with postsynaptic depolarization was carried out in immature layer Vb pyramidal neurons at P7. Therefore, extracellular stimulation was continuously delivered with a simultaneous postsynaptic depolarization to -10 mV for 10 min. Following this protocol, the immature synapses at P7 with a low Pr were potentiated and showed afterwards significantly increased EPSC amplitudes (fig. 3.15 A; $p < 0,01$; $[n = 9]$). A strongly reduced failure rate was observed in these synapses (fig. 3.15 B; $p < 0,01$) and the paired-pulse behavior revealed an evidentiary reduced facilitation after the pairing protocol (fig. 3.15 C; $p < 0,01$).

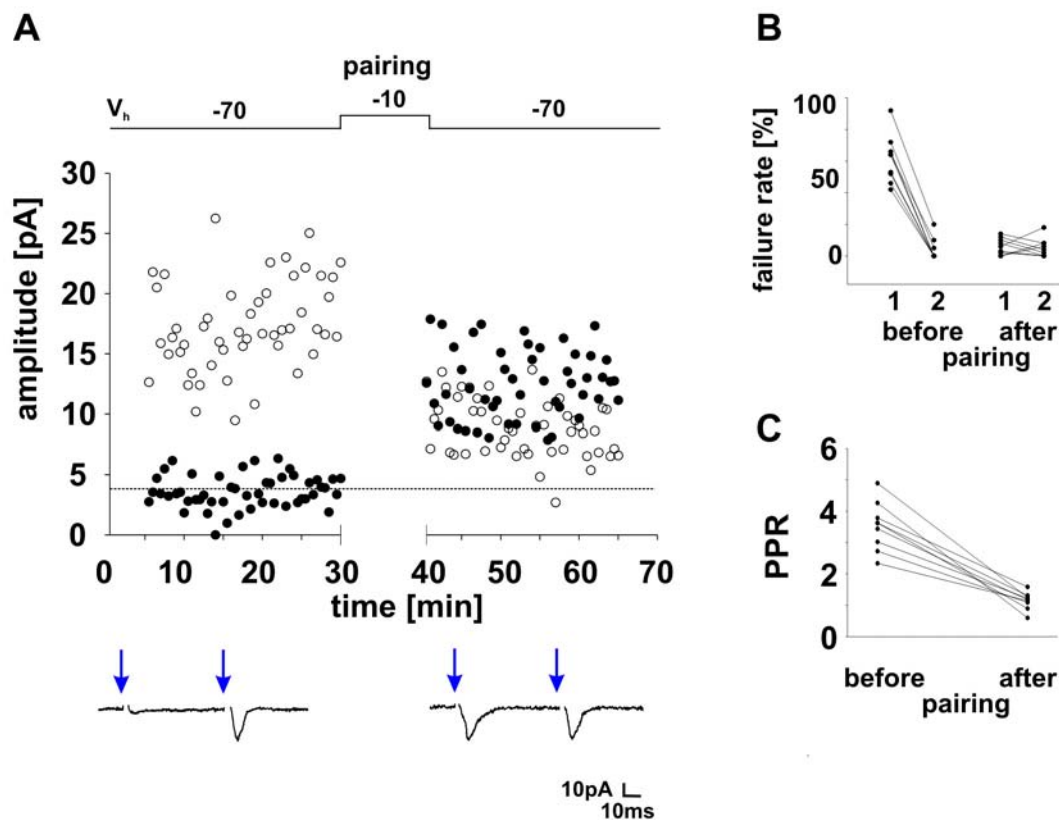


Fig. 3.15: Functional potentiation of presynaptically immature synapses.

(A) Example of AMPA-receptor mediated EPSC amplitudes in a presynaptically immature (low Pr) synapse ($n = 9$, blue arrows indicate stimulation pulses) with mostly failures to the first pulse (black circles) and responses to the second pulse (white circles). Pairing of presynaptic stimulation and postsynaptic depolarization led to a potentiation and increased amplitudes in response to the first pulse. (B) The failure rate was strongly reduced after pairing. (C) The paired-pulse ratio was shifted towards lower values after potentiation.

As mentioned previously, this kind of long-term potentiation should operate in an NMDA-receptor dependent manner. On that account, the pairing of extracellular stimulation combined with postsynaptic depolarization in immature layer Vb pyramidal neurons at P7 was repeated in the presence of 25 μM of the NMDA-receptor specific antagonist D-AP5. The performance of the pairing protocol did not induce any changes in EPSC amplitudes (fig. 3.16 A, [n = 7]). Accordingly, these synapses still revealed a high initial failure rate (fig. 3.16 B) and no change in the paired-pulse behavior occurred (fig. 3.16 C). Finally, we found evidence that immature (silent) synapses can be potentiated and converted into functional ones and furthermore, this kind of potentiation depended strongly on NMDA-receptor activation, as demonstrated by addition of the specific NMDA-receptor antagonist D-AP5.

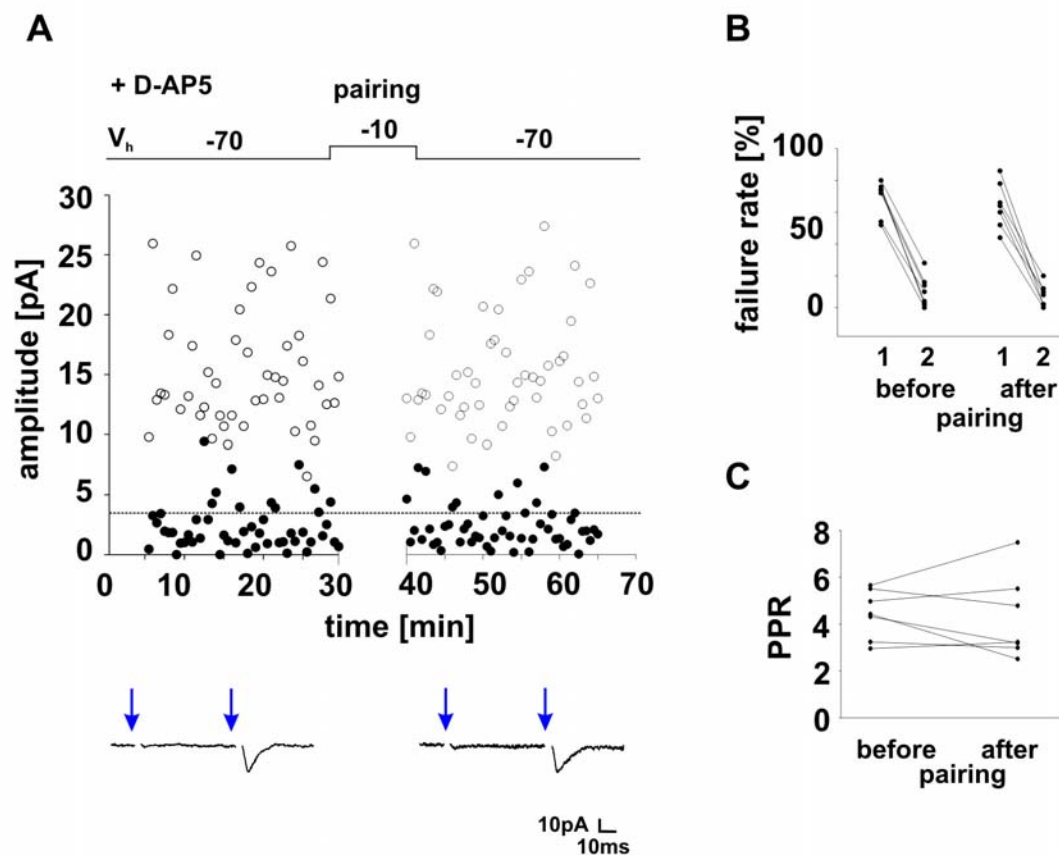


Fig. 3.16: Potentiation of immature synapses depends on NMDA-receptor activation.

(A) Example of AMPA-receptor mediated EPSC amplitudes in a presynaptically immature (low Pr) synapse (n = 7, blue arrows indicate stimulation pulses) with mostly failures to the first pulse (black circles) and responses to the second pulse (white circles). In the presence of D-AP5 pairing of presynaptic stimulation and postsynaptic depolarization induced no changes in EPSC amplitudes. (B) The failure rate remained high in response to the first pulse after pairing. (C) The paired-pulse behavior also remained constant after pairing.

3.3 Spatial mapping of synaptic inputs onto BDNF-deficient neurons transplanted to wildtype organotypic slice cultures

Neurotrophins, e.g. BDNF, have emerged as key signals that mediate activity-dependent functional and structural plasticity in both the embryonic and mature brain (Poo et al., 2001; Snider and Lichtman, 1996; Schuman, 1999; McAllister et al., 1999; Prakash et al., 1996; Katz and Shatz, 1996; Thoenen, 1995). They may act as retrograde signals influencing presynaptic neurons, as well as anterograde factors acting on postsynaptic cells. The existence and gradual conversion of silent synapses (NMDA-receptor only) in the developing brain is accepted as an important maturational step of glutamatergic synapses (Isaac et al., 1995; Liao et al., 1995; Montgomery et al., 2001). Recent studies have now shown that endogenous BDNF might be crucial for the maturation of AMPA-receptor mediated transmission in the developing mouse barrel cortex (Itami et al., 2003), because this kind of conversion of silent synapses is mostly blocked in BDNF knockout mice.

The effects of neurotrophins on synapse number, synaptic efficacy, and neuronal morphology therefore support their role as activity-dependent modulators of synaptic structures and circuits. Whether neurotrophins are indeed the object of competition during the activity-dependent refinement of neuronal maps as it was originally proposed (Katz and Shatz, 1996; Poo, 2001; Snider and Lichtman, 1996; Cabelli, 1997) remains an open question.

To investigate a potential role of BDNF, especially as a retrograde messenger, synaptic inputs on BDNF-deficient neurons and controls transplanted to a wildtype organotypic slice were compared and analyzed using the patch clamp-technique in combination with photolysis of *caged* glutamate.

3.3.1 Morphology and basic electrophysiology of transplanted BDNF-deficient neurons

In the majority of preparations that are made to examine the role of BDNF, all neurons in a given area of the cortex lack BDNF. Therefore, it is difficult to examine local actions of endogenous BDNF on synapses at particular neurons. To overcome these problems, we transplanted single BDNF knockout neurons in organotypic slice culture of somatosensory cortex. In these preparations endogenous BDNF is lacking in a single cell located in a defined area of the cortex. For the preparation of these cultures, a drop of a single cell suspension of either homozygous BDNF knockout or heterozygous BDNF knockout or BDNF wildtype cortical neurons (all expressing EGFP) was pipetted onto a previously prepared slice (see

2.4.3). After 28 DIV at 37°C, 95% humidity and 5% CO₂ the transplanted neurons were functionally integrated into the organotypic slice.

To identify these transplanted EGFP-expressing neurons, the fluorescence signal of the cell of interest was detected under UV-light with a GFP filter. The neuron then was patched under visual control using infrared contrast, the fluorescence signal was continuously controlled until reaching the “whole cell” configuration, which led to an exchange of pipette solution and intracellular space and therefore to a rapid decrease of the fluorescence (see 2.8.3). Overall, transplanted neurons in 30 slices were investigated. In most slices a transplanted and a endogenous neuron in the slice (as internal control) were recorded. More than 70% of the transplanted cells were located in the region of layer II/III (n = 22), a few cells were integrated in the region of layer IV to VI (n = 4).

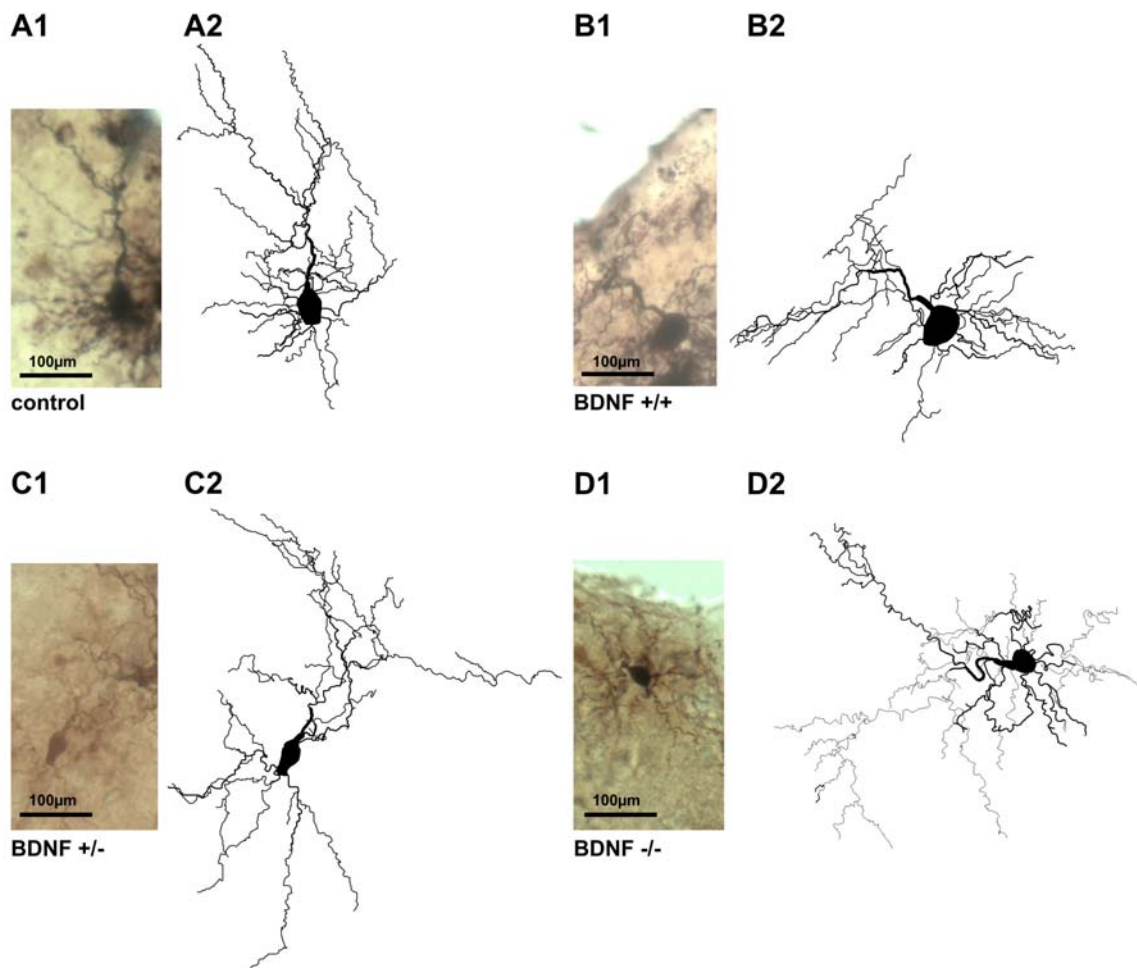


Fig. 3.17: Morphology of transplanted EGFP expressing neurons.

Examples of biocytin labelled neurons (A1 – D1) and the corresponding somatodendritic reconstructions (A2 – D2) of an endogenous control neuron (A) and transplanted BDNF wildtype (B) and heterozygous (C) as well as homozygous (D) BDNF knockout neurons are shown. No obvious differences in morphology of somata and dendrites were found.

The type of neuron was identified after filling with biocytin by subsequent analysis of morphology. 5 (multipolar) interneurons were recorded, but later excluded from further analysis, which focussed mainly on excitatory neurons. Furthermore, 3 spiny stellate-like cells were detected and the most prominent fraction were 28 pyramidal-like neurons. Finally, 5 of the recorded neurons could not be identified, because of lack of biocytin filling or destruction of the soma during the histological preparation of the slices. The latter were also excluded from further analysis. In general, no differences in morphology were observed between controls and transplanted neurons, as well as between homozygous BDNF knockout, heterozygous BDNF knockout and BDNF wildtype neurons (fig. 3.17).

For the electrophysiological characterization the active and passive membrane properties were analyzed (see table 6). Directly after reaching the “whole cell” configuration the membrane potential was recorded in the current clamp-mode. Afterwards hyperpolarizing and depolarizing rectangular current pulses were applied every 10 seconds and the changing membrane potentials were recorded. At small charges the course of potentials was determined strongly by the passive membrane properties, at higher depolarizations action potentials (APs) were elicited. According to their morphology, neurons with a regular spiking (RS) as well as a fast spiking (FS) firing pattern were detected (fig. 3.18 A1, A2). Characteristic parameters (fig. 3.18 B, C; 1. and 2 ISI: interval between first and second spike and interval between second and third spike, respectively), are listed for each cell in table 6:

Cell type	Pattern	1. ISI (ms)	2. ISI (ms)	amplitude (mV)	Rm (M Ω)	tm (ms)	Half width (ms)	Vrmp (mV)
Control	RS	41,1	50,7	75,2	873	86,2	3,1	-53
Control	RS	46,8	69,4	78,5	864	84,7	2,9	-71
Control	RS	45,1	57,4	65,3	867	84,3	2,7	-62
Control	RS	231,5	292,8	73,9	874	87,2	3,1	-65
Control	RS	93,8	106,2	57,8	892	89,1	3,0	-50
Control	RS	33,2	53,5	78,9	856	85,3	3,2	-56
BDNF +/+	RS	71,7	67,5	71,3	876	85,8	3,2	-59
BDNF +/+	RS	66,6	96,7	43,5	884	86,1	2,9	-60
BDNF +/+	RS	55,1	75,8	60,5	873	84,7	3,1	-58
BDNF +/-	RS	149,9	187,8	59,4	865	88,3	2,7	-73
BDNF +/-	RS	69,7	124,1	80,1	849	87,2	3,0	-66
BDNF +/-	FS	16,5	28,4	42,4	898	86,2	1,5	-46
BDNF +/-	FS	25,3	25,3	69,2	891	85,7	1,7	-63
BDNF -/-	RS	63,8	63,8	83,5	867	89,2	2,7	-54
BDNF -/-	FS	26,7	27,9	67,8	888	84,9	1,4	-46
BDNF -/-	RS	88,9	117,1	63,1	871	87,4	2,9	-45
BDNF -/-	RS	105,3	93,1	64	859	86,9	3,3	-67
BDNF -/-	RS	83,1	93,5	54,8	873	88,1	2,9	-65
BDNF -/-	FS	37,1	49,5	79,1	901	86,2	1,5	-68

Table 6: Basic electrophysiological properties of EGFP expressing neurons.

No significant differences in passive and active membrane properties were observed between controls and transplanted neurons, as well as between homozygous BDNF knockout, heterozygous BDNF knockout and BDNF wildtype neurons. Therefore, all recorded neurons seem to be integrated into the slice and hence, are comparable to endogenous cells of the organotypic slice.

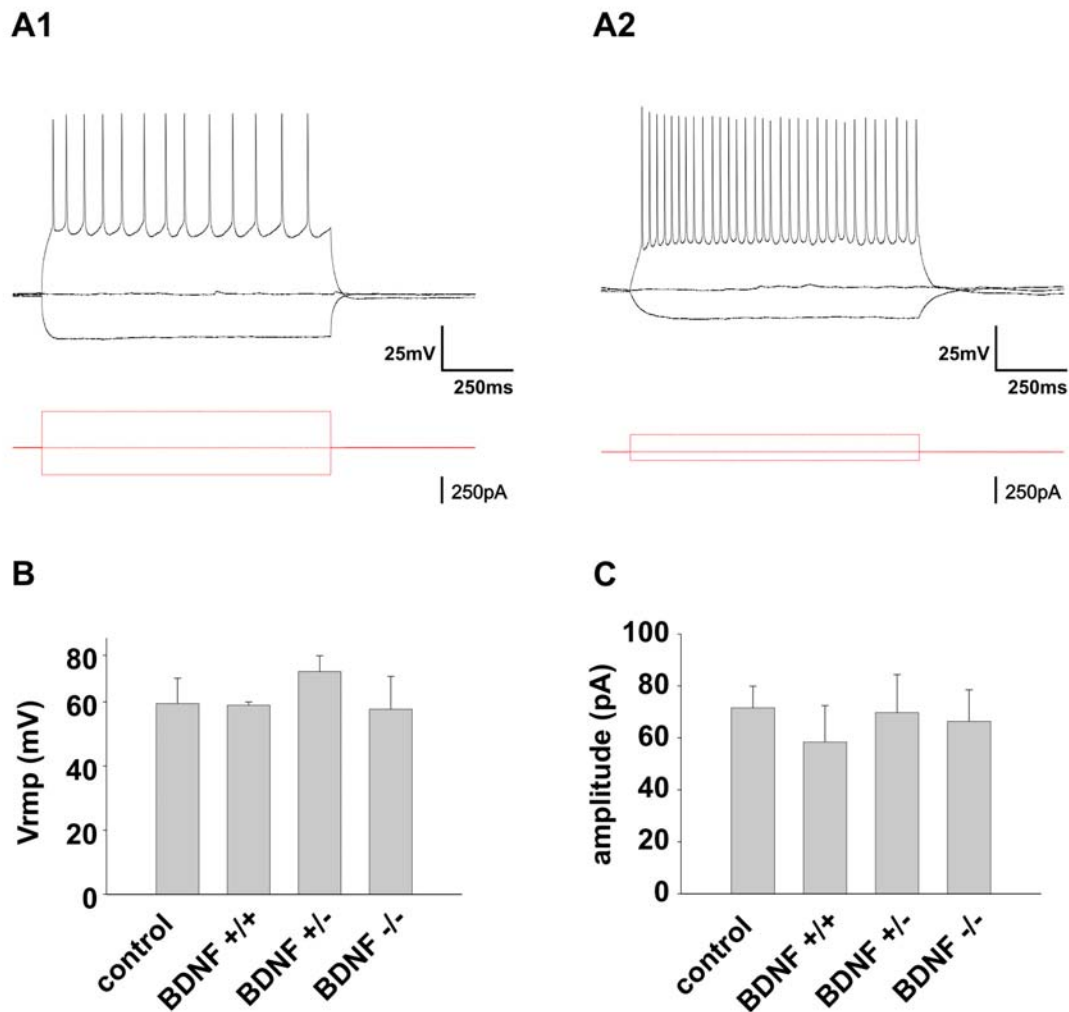


Fig. 3.18: Electrophysiological properties of transplanted EGFP expressing neurons. Representative example traces of current clamp recordings of a regular spiking (A1) and a fast spiking neuron (A2) are displayed. The mean resting membrane potentials of all tested genotypes did not differ significantly (B) as well as the mean AP amplitudes (C). Error bars indicate SDs.

3.3.2 Properties of photolysis-induced synaptic activity

To investigate the synaptic inputs onto transplanted BDNF knockout and BDNF wildtype neurons as well as onto endogenous controls, a spatial mapping using *caged* glutamate

photolysis was performed. For optimal maintenance of the neurons, ACSF for *caged* glutamate experiments in organotypic slices (see 2.2 e) and intracellular solution IV (see 2.2 i) were used during the mapping. Before each mapping the focus was adjusted under visual control to the depth of the patched neuron in the slice and with every UV-flash the membrane potential of the cell was recorded simultaneously. For a topographic acquisition of photolysis induced activity the field of interest (50 μm x 50 μm) was shifted by 50 μm every 10 s. In this way up to 250 fields around the patched cell were consistently examined. To better uncover hyperpolarizing inhibitory inputs, the neuron was clamped in the *slow voltage-clamp controlled current-clamp mode* to a membrane potential of -60 mV and -40 mV in change. Double flashes with an interval of 5 s allowed the mapping of one field at the two different holding potentials. The intrinsic membrane properties were controlled before and after each mapping (see 2.12). To study the photolysis induced activity, at every field a period of 150 ms *post stimulus* was analysed. Analysis was carried out concerning (a) the latency between stimulus and onset of activity, (b) the maximal amplitude of excitatory postsynaptic potentials (EPSPs), (c) the integral of EPSPs during the period of 150 ms after stimulation and (d) the occurrence of inhibitory postsynaptic potentials (IPSPs). The calculation of integrals included all depolarizing events during the 150 ms *post stimulus* and provided information about the strength of the elicited excitatory activity. All integrals were corrected for a threshold calculated from not photolysis induced, spontaneous activity. In case of interference of direct and synaptically mediated activity, the direct activity was excluded from calculation of the integral of the synaptic activity (see 2.13). Afterwards, activity parameters were transformed to pseudocolor values and the resulting maps were superimposed on the photomicrograph of the native slice and the somatodendritic reconstruction of the recorded neuron (fig. 3.19 A1-A4). The recorded cell could receive distinct excitatory and inhibitory synaptic inputs from presynaptically activated neurons. Previous experiments have shown that a repetitive stimulation of some fields reliably elicited IPSPs with stable rise-time and delay-to-onset time, but the amplitude of the IPSPs varied from trial to trial with a tendency to decrease (Schubert et al., 2001). Therefore, only the occurrence of IPSPs was analyzed, but not the strength of the synaptic input. EPSPs were elicited much more reliably and could be also analyzed concerning their strength.

The local photolysis of *caged* glutamate induced different types of activity in the recorded neuron. On the one hand, a so-called direct activity was induced, in which the photolysis-released glutamate binds directly to glutamate-receptors in the membrane of the recorded cell. At this, a photostimulation of the soma elicited action potentials (fig. 3.19 B), whereas a

photostimulation of the proximal dendrites induced reliably strong depolarizations of the membrane potential (fig. 3.19 C). The direct activity is characterized by a very short time-to-onset (< 4 ms).

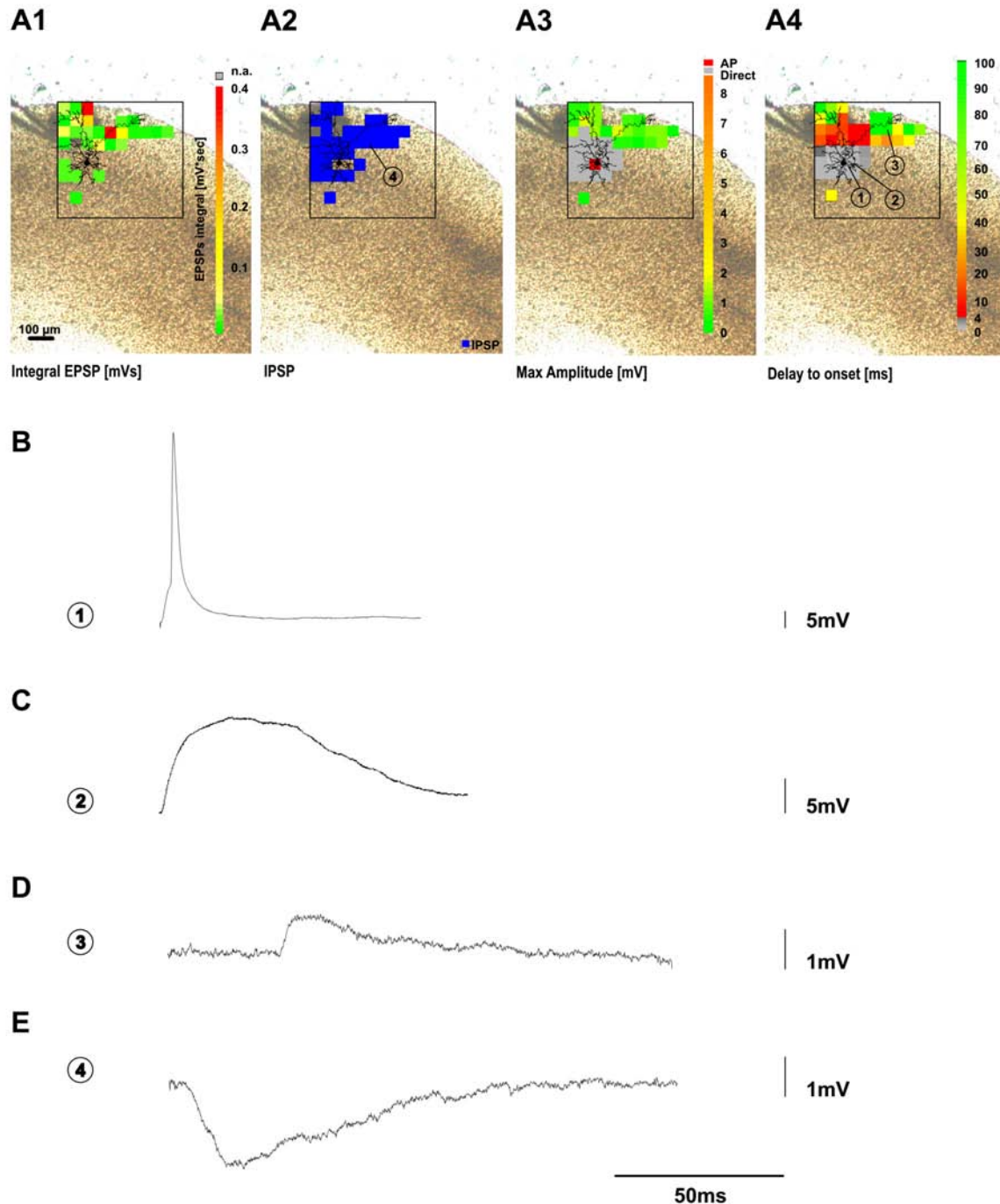


Fig. 3.19: Properties of photolysis induced direct and synaptic activity.

An example of the superimposed images of the activity map (EPSP integral, IPSPs, maximal EPSP amplitude, response latency), the photomicrograph of the native slice and the somatodendritic reconstruction of the recorded neuron (A1 – A4) is shown. The photostimulation of the soma elicited action potentials (B), stimulation of the proximal dendrites led to a strong depolarization of the membrane potential (C). Excitation of connected presynaptic neurons results in excitatory (D) or inhibitory postsynaptic (E) potentials.

On the other hand, the photolysis of *caged* glutamate can elicit synaptically mediated activity in the recorded neuron. This activity is based upon suprathreshold excitation of connected presynaptic neurons and results in postsynaptic potentials (PSPs) in the recorded cell. These PSPs were either excitatory (fig. 3.19 D) or inhibitory (fig. 3.19 E) ones, depending on the properties of the presynaptic neuron. The EPSPs and IPSPs usually showed much longer latencies (up to 50 ms) than the direct activity.

3.3.3 Synaptic inputs on transplanted BDNF-deficient neurons

For the topographic mapping of synaptic inputs onto transplanted neurons, at least 100 different fields of 50 x 50 μm in size were stimulated as described previously (see 2.12). The stimulated area comprised the region from the pial surface to the deeper cortical layers, although the laminar organization was not excessively distinctive after the long cultivation period of 28 to 32 DIV. Stimulation fields containing dendritic extensions of the recorded neuron often resulted in a mixture of direct activity and synaptic events. In accordance with the morphology of the cell, all responses with a very short delay-to-onset (< 4 ms) could be related to direct activation of the dendritic extensions.

To investigate the spatial distribution and strength of synaptic inputs onto transplanted as well as onto endogenous cells, mapping of the transplanted neurons with different genotypes (BDNF +/+, BDNF +/- and BDNF -/-) and of the endogenous neurons (control) was performed using *caged* glutamate photolysis. To allow for comparison across genotypes only pyramidal-like neurons with a RS firing pattern (see 3.3.1) were included in the analysis of the synaptic inputs. The resulting maps of a representative control (fig. 3.20) and a transplanted BDNF-wildtype neuron (fig. 3.21) as well as a heterozygous (fig. 3.22) and a homozygous (fig. 3.23) BDNF knockout neuron clearly indicated that all cells received widely distributed excitatory synaptic inputs. In all cases the inputs were located in all tested regions. Frequently, the stimulation of presynaptic fields elicited multiple EPSPs. To estimate the strength of an excitatory input the integral of all synaptically evoked excitatory events within a time window of 150 ms after stimulus was determined. To some extent, photostimulation elicited synaptically evoked events as well as a direct response. In these cases, the integral of the synaptically evoked events was calculated separately, if possible. All remaining traces were excluded from the further integral analysis. The integrals of EPSPs ranged in most cases from 0.01 to 0.03 mV*s. For all genotypes, integrals did not exceed these values.

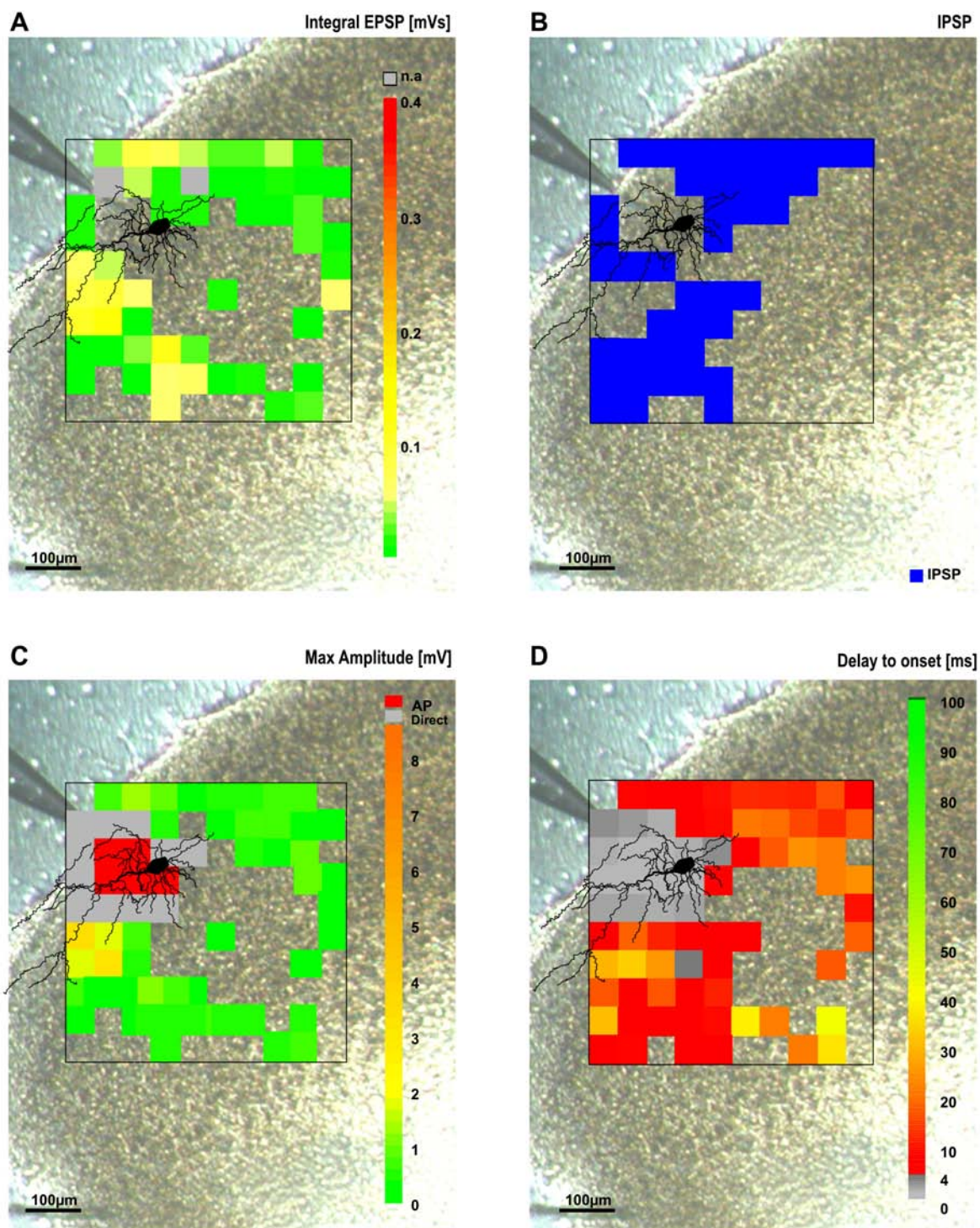


Fig. 3.20: Topographic map of synaptic inputs onto an endogenous neuron in an organotypic slice culture.

The somatodendritic reconstruction of the pyramidal-like neuron as well as the spatial map of the synaptic inputs was superimposed on the photomicrograph of the slice culture. The topographic maps illustrate integrals of the recorded EPSPs (A, *green to red*) and fields of origin for IPSPs (B, *blue*). Fields given in *grey* were excluded from analysis because of a strong temporal interaction among direct activation, action potentials and synaptic events. The maximal amplitude of synaptic events (C, *green to orange*) including direct responses (*grey*) and action potentials (*red*) is displayed as well as the delay-to-onset of the response (D, *red to green*). All stimulated fields that did not induce any response are transparent. The black frame indicates the extent of the investigated area (500 µm * 500 µm).

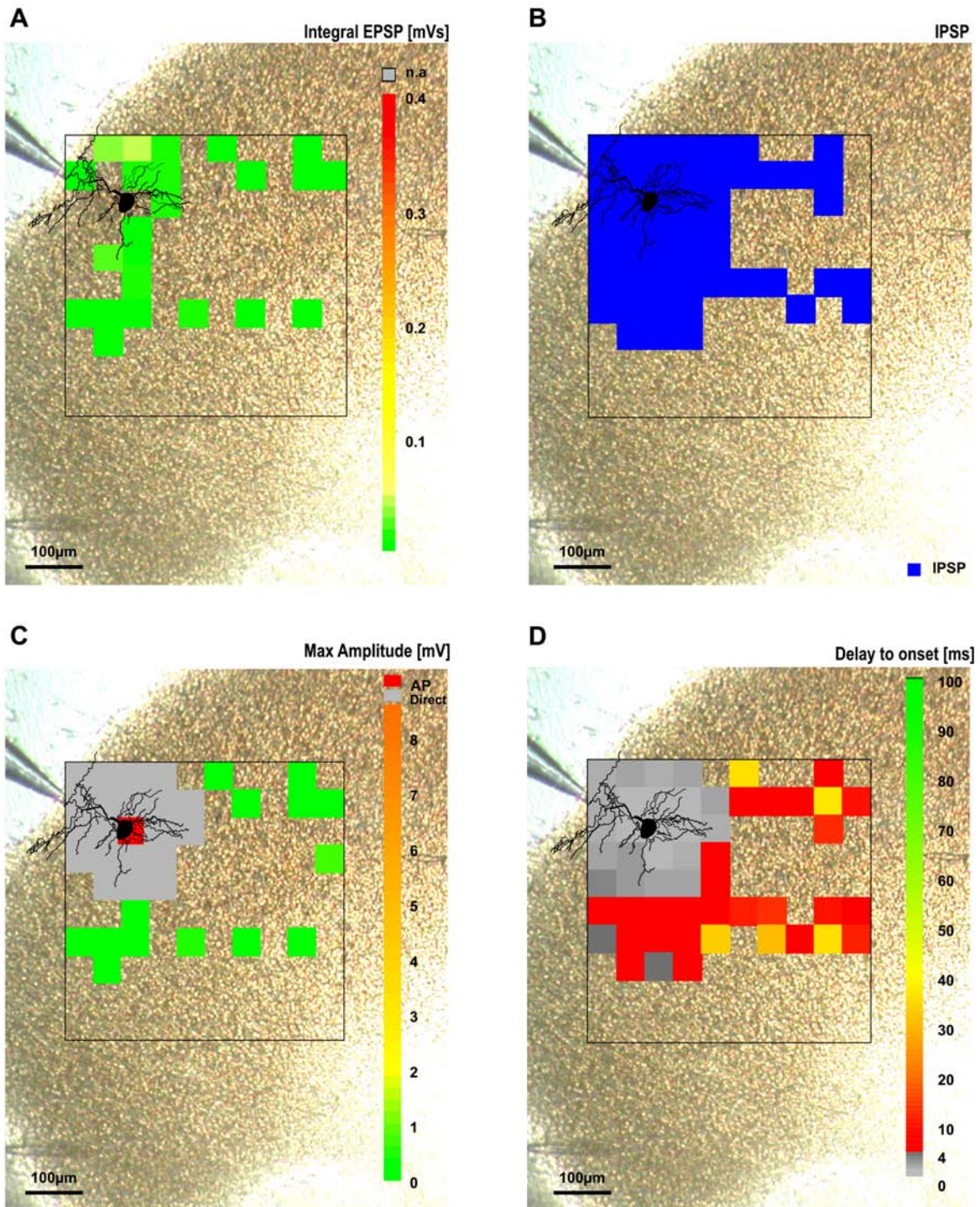


Fig. 3.21: Topographic map of synaptic inputs onto a transplanted wildtype neuron in an organotypic slice culture.

The somatodendritic reconstruction of the transplanted pyramidal-like neuron as well as the spatial map of the synaptic input was superimposed on the photomicrograph of the slice culture. The topographic maps illustrate integrals of the recorded EPSPs (A, green to red) and fields of origin for IPSPs (B, blue). The maximal amplitude of all events (C, green to orange) including direct responses (grey) and action potentials (red) is displayed as well as the delay-to-onset (D, red to green). All stimulated fields that did not induce any response are transparent. The black frame indicates the extent of the investigated area (500 µm * 500 µm).

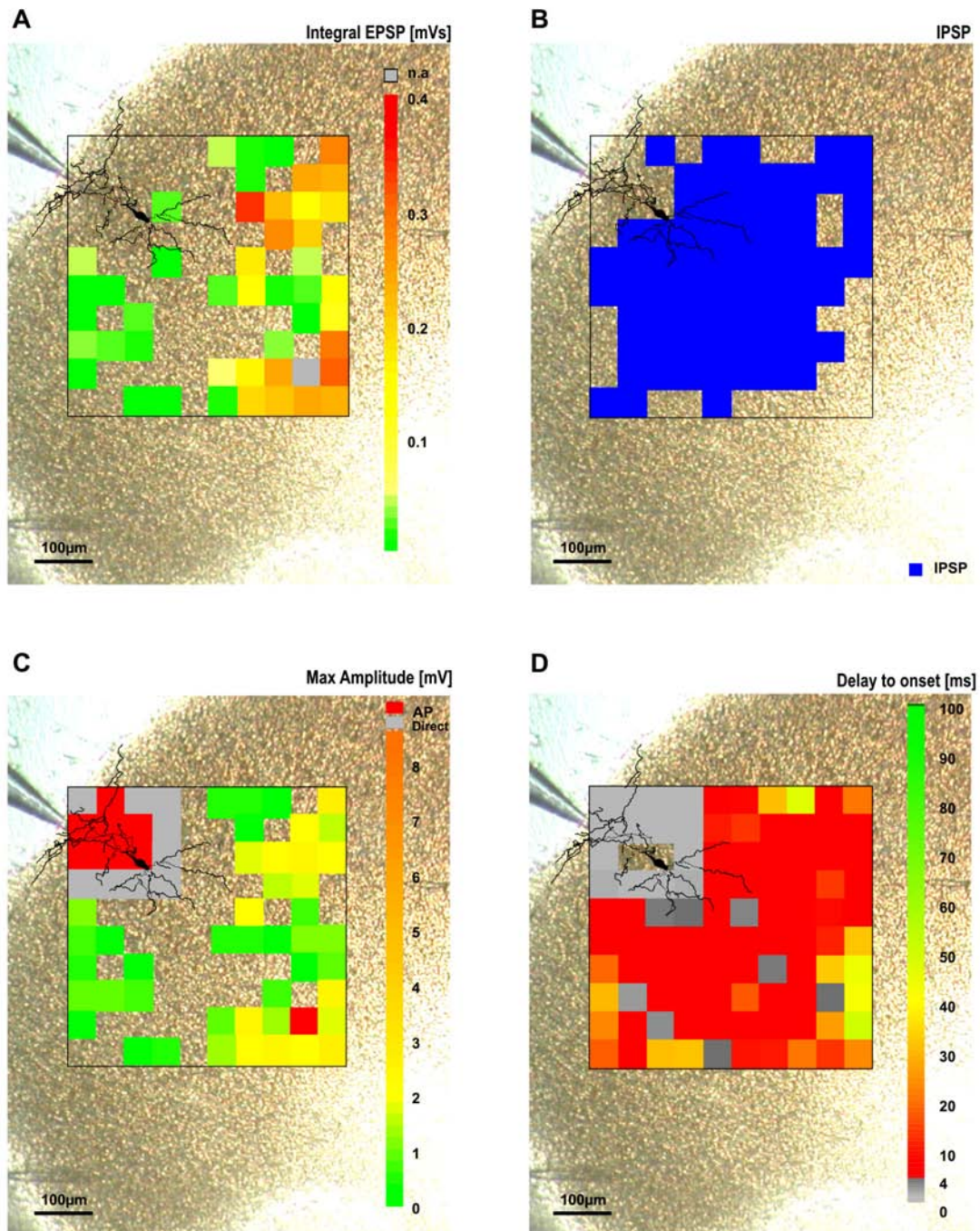


Fig. 3.22: Topographic map of synaptic inputs onto a transplanted heterozygous BDNF knockout neuron in an organotypic slice culture.

The somatodendritic reconstruction of the transplanted pyramidal-like neuron as well as the spatial map of the synaptic input was superimposed on the photomicrograph of the slice culture. The topographic maps illustrate integrals of the recorded EPSPs (A, *green to red*) and fields of origin for IPSPs (B, *blue*). Fields given in *grey* were excluded from analysis because of a strong temporal interaction among direct activation, action potentials and synaptic events. The maximal amplitude of all events (C, *green to orange*) including direct responses (*grey*) and action potentials (*red*) is displayed as well as the delay-to-onset (D, *red to green*). All stimulated fields that did not induce any response are transparent. The black frame indicates the extent of the investigated area (500 μm * 500 μm). Additionally, one field was detected that induced action potentials more than 400 μm away from the soma of the recorded neuron. This could be traced back to the fact that during the mapping the recorded cell was depolarized by up to 10 mV to reach the holding potential of -60 mV.

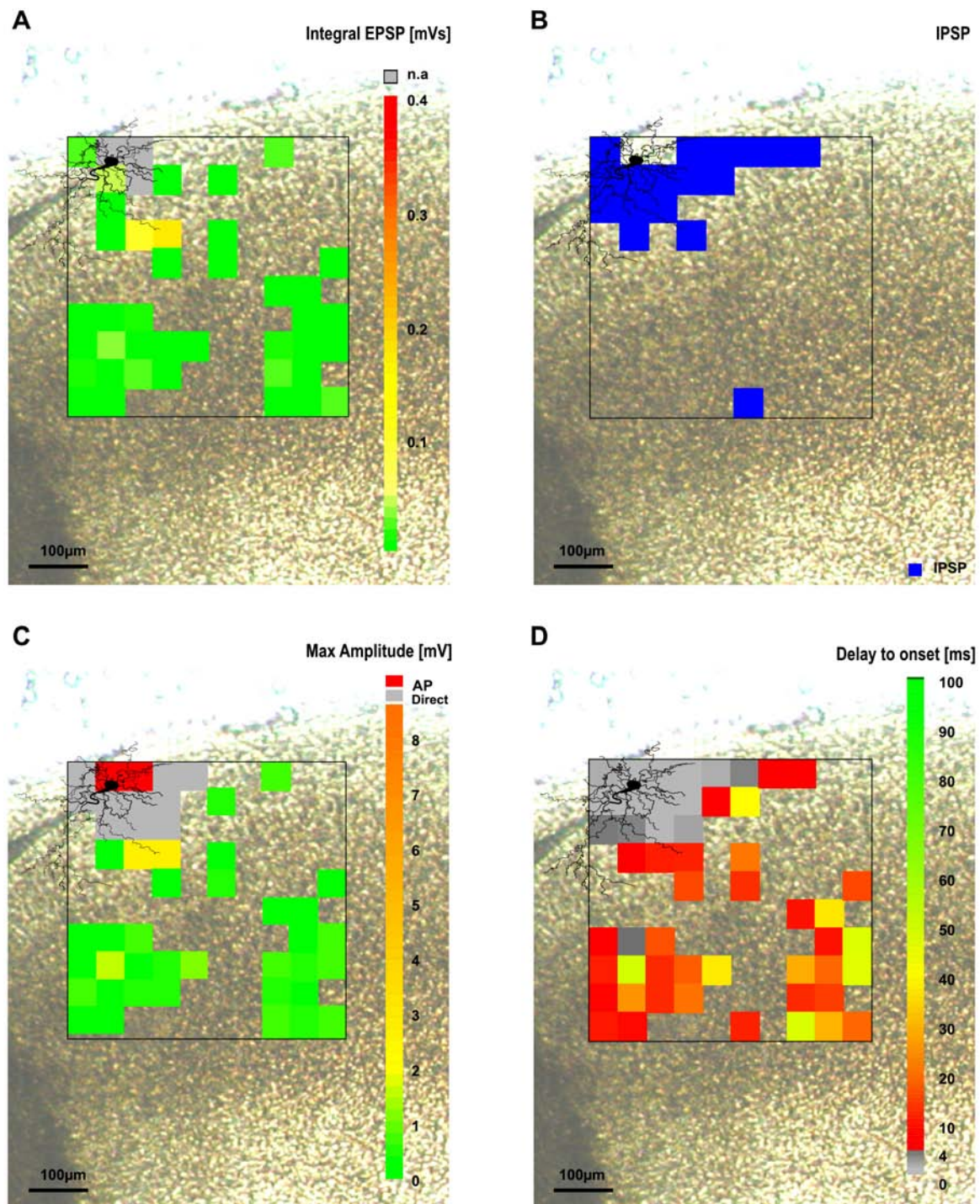


Fig. 3.23: Topographic map of synaptic inputs onto a transplanted homozygous BDNF knockout neuron in an organotypic slice culture.

The somatodendritic reconstruction of the transplanted pyramidal-like neuron as well as the spatial map of the synaptic input was superimposed on the photomicrograph of the slice culture. The topographic maps illustrate integrals of the recorded EPSPs (A, *green to red*) and fields of origin for IPSPs (B, *blue*). Fields given in *grey* were excluded from analysis because of a strong temporal interaction among direct activation, action potentials and synaptic events. The maximal amplitude of all events (C, *green to orange*) including direct responses (*grey*) and action potentials (*red*) is displayed as well as the delay-to-onset (D, *red to green*). All stimulated fields that did not induce any response are transparent. The black frame indicates the extent of the investigated area (500 µm * 500 µm).

In contrast to the EPSPs, the inhibitory inputs were equally distributed to the whole area tested in control neurons ($n = 4$), BDNF wildtype neurons ($n = 3$) and heterozygous BDNF knockout neurons ($n = 2$), but not in the homozygous BDNF knockout neurons ($n = 4$). In the latter, inhibitory inputs were spatially more limited to fields near the recorded neuron. Distal inhibitory inputs were rare and could be observed only in few cases. From these qualitative data the following preliminary conclusions can be drawn: (i) BDNF was not essential for the functional integration of single neurons in a network. (ii) There seems to be no direct relationship between glutamatergic synapses and a lack of BDNF, because the total number of excitatory synaptic inputs was similar in controls and all types of transplanted neurons. (iii) By contrast, the inhibitory inputs were reduced in transplanted BDNF knockout cells, indicating that there might be a smaller number of functional GABAergic synapses on the BDNF knockout neurons.

3.3.4 Comparison of transplanted wildtype and endogenous neurons in organotypic slice cultures

To quantify the spatial distribution of synaptic inputs onto the recorded neuron for different distances to the soma, the mean percentage of fields was calculated, in which the photostimulation caused excitatory or inhibitory postsynaptic currents. Fields, in which EPSPs were overlaid by strong direct activity or action potentials such intensively that a calculation of integrals was impossible, were excluded (only in one or two fields in the perisomatic region in a few mappings (see 2.13)). First of all, it is important to affirm the comparability of endogenous controls and transplanted neurons. Therefore, the relative amount of excitatory and inhibitory inputs onto controls and transplanted wildtype neurons was analyzed depending on the relative distance to the recorded cell. No significant differences in the amount and distribution of excitatory and inhibitory synaptic inputs were found. Transplanted neurons as well as endogenous control neurons received widespread excitatory (fig. 3.24 A) and inhibitory (fig. 3.24 B) inputs from all tested cortical layers. The excitatory input was in all cases most prominent from regions close to the recorded soma ($< 100 \mu\text{m}$: $48,9 \% \pm 24,1$ in controls and $45,3 \% \pm 48,9$ in wildtype; $< 200 \mu\text{m}$: $46,4 \% \pm 15,2$ in controls and $38,6 \% \pm 27,1$ in wildtype), still numerous from medium distances ($< 300 \mu\text{m}$: $35,7 \% \pm 16,4$ in controls and $14,8 \% \pm 7,8$ in wildtype; $< 400 \mu\text{m}$: $29,7 \% \pm 22,0$ in controls and $17,7 \% \pm 5,4$ in wildtype) and at least a few synaptic inputs were detectable from more distant cells ($> 400 \mu\text{m}$: $11,6 \% \pm 23,2$ in controls and $6,5 \% \pm 5,8$ in wildtype). The

inhibitory input also was most prominent from regions close to the recorded soma ($< 100 \mu\text{m}$: $60,9 \% \pm 28,3$ in controls and $52,9 \% \pm 42,4$ in wildtype; $< 200 \mu\text{m}$: $57,7 \% \pm 11,1$ in controls and $54,3 \% \pm 11,6$ in wildtype), still numerous from medium distances ($< 300 \mu\text{m}$: $35,3 \% \pm 17,8$ in controls and $26,4 \% \pm 7,1$ in wildtype; $< 400 \mu\text{m}$: $22,4 \% \pm 14,4$ in controls and $25,4 \% \pm 12,4$ in wildtype) and some synaptic inputs were detectable from more distant cells ($> 400 \mu\text{m}$: $0,9 \% \pm 1,8$ in controls and $14,9 \% \pm 1,0$ in wildtype). Inputs from a distance of more than $500 \mu\text{m}$ were excluded from the quantification because of their rare occurrence. Altogether, the endogenous neurons can be considered as an internal control for the transplanted wildtype and BDNF knockout neurons, because of the similar spatial distribution of synaptic inputs.

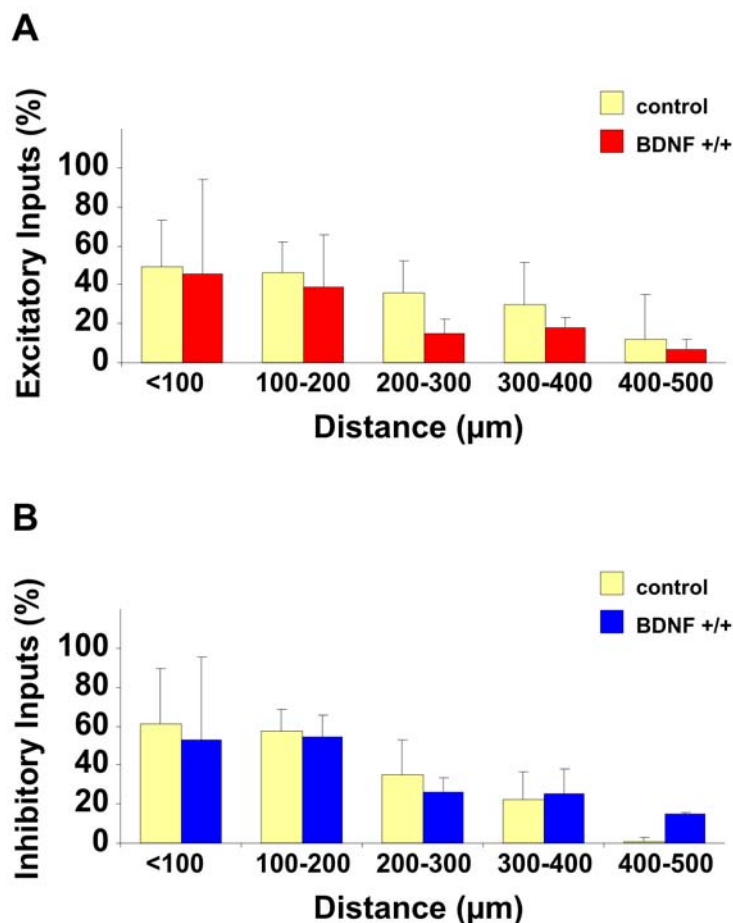


Fig. 3.24: Quantification of synaptic inputs onto endogenous and transplanted neurons in organotypic slice cultures.

Percentages of stimulated presynaptic fields delivering excitatory (A) and inhibitory (B) synaptic responses onto endogenous neurons (*beige*) and transplanted wildtype neurons (*red and blue*, respectively) are shown. No significant differences were observed in the relative amount and distribution of excitatory as well as inhibitory inputs onto endogenous and transplanted neurons. Data are given as mean \pm SD.

3.3.5 Quantitative analysis of synaptic inputs on transplanted BDNF-deficient neurons

For the quantitative analysis of the spatial distribution of synaptic inputs onto endogenous as well as transplanted neurons, the mean percentage of fields, in which the photostimulation caused excitatory (see table 7) or inhibitory inputs (see table 8), was calculated for different distances to the soma. In the overall excitatory input, there did not appear any differences between endogenous and transplanted neurons (fig. 3.25 A). Likewise, there were no significant genotype specific differences found in the distribution of excitatory inputs originating from proximal or distal located presynaptic neurons (see table 7, fig. 3.25 C). Excitatory inputs from all distances are listed for each genotype in table 7:

Distance (μm)	Controls	BDNF +/+	BDNF +/-	BDNF -/-
< 100	48,9 % \pm 24,1	45,3 % \pm 48,9	22,6 % \pm 17,9	40,4 % \pm 37,3
100 - 200	46,4 % \pm 15,2	38,6 % \pm 27,1	27,9 % \pm 14,5	38,4 % \pm 6,3
200 – 300	35,7 % \pm 16,4	14,8 % \pm 7,8	34,1 % \pm 31,6	25,4 % \pm 30,2
300 – 400	29,7 % \pm 22,0	17,7 % \pm 5,4	38,0 % \pm 21,6	12,4 % \pm 7,7
400 – 500	11,6 % \pm 23,2	6,5 % \pm 5,8	51,2 % \pm 32,1	9,3 % \pm 8,5

Table 7: Excitatory inputs onto endogenous and transplanted neurons.

Therefore, the quantitative analysis of the spatial distribution of excitatory synaptic inputs demonstrated that all types of neurons received similar widespread excitatory inputs from all measured regions. In addition, no differences in the strength of excitatory synaptic inputs were observed. The values varied from 0,001 mV*s up to 0,302 mV*s in all recorded endogenous as well as transplanted neurons. Thus, BDNF seems not to play a major role in the formation of excitatory inputs, i.e. BDNF is not compulsory for the receipt of excitatory synaptic inputs during development.

By contrast, in the overall inhibitory input no differences between endogenous and transplanted neurons were observed, but the transplanted BDNF-knockout neurons showed a lower overall input in most neurons tested (fig. 3.25 B). The distribution of inhibitory inputs displayed again no difference between controls, wildtype and heterozygous BDNF knockout neurons, but transplanted homozygous BDNF knockout neurons showed a strong tendency towards lower and more local inhibitory inputs than received by the other cell types (see table 8, fig. 3.25 D). The inhibitory inputs onto each genotype are listed in table 8:

Distance (μm)	Controls	BDNF +/+	BDNF +/-	BDNF -/-
< 100	60,9 % \pm 28,3	52,9 % \pm 42,4	80,0 % \pm 28,3	11,2 % \pm 11,8
100 - 200	57,7 % \pm 11,1	54,3 % \pm 11,6	94,7 % \pm 1,0	26,3 % \pm 12,9
200 - 300	35,3 % \pm 17,8	26,4 % \pm 7,1	74,4 % \pm 5,4	17,2 % \pm 15,3
300 - 400	22,4 % \pm 14,4	25,4 % \pm 12,4	58,8 % \pm 25,3	13,8 % \pm 12,2
400 - 500	0,9 % \pm 1,8	14,9 % \pm 1,0	16,5 % \pm 17,1	1,9 % \pm 3,2

Table 8: Inhibitory inputs onto endogenous and transplanted neurons.

The tendency towards lower values in homozygous BDNF knockout neurons could not be reliably tested because of the small amount of preparations (BDNF -/-: n = 4). The strength of inhibitory synaptic inputs was not quantitatively analyzed, because at a holding potential of -60 mV (close to the equilibrium potential of chloride) inhibitory inputs are most often overlaid by the strong excitatory inputs. However, at -40 mV the inhibitory inputs could be detected without any doubt, but not quantified efficiently, because in most recorded neurons action potentials were elicited at this rather depolarized holding potential.

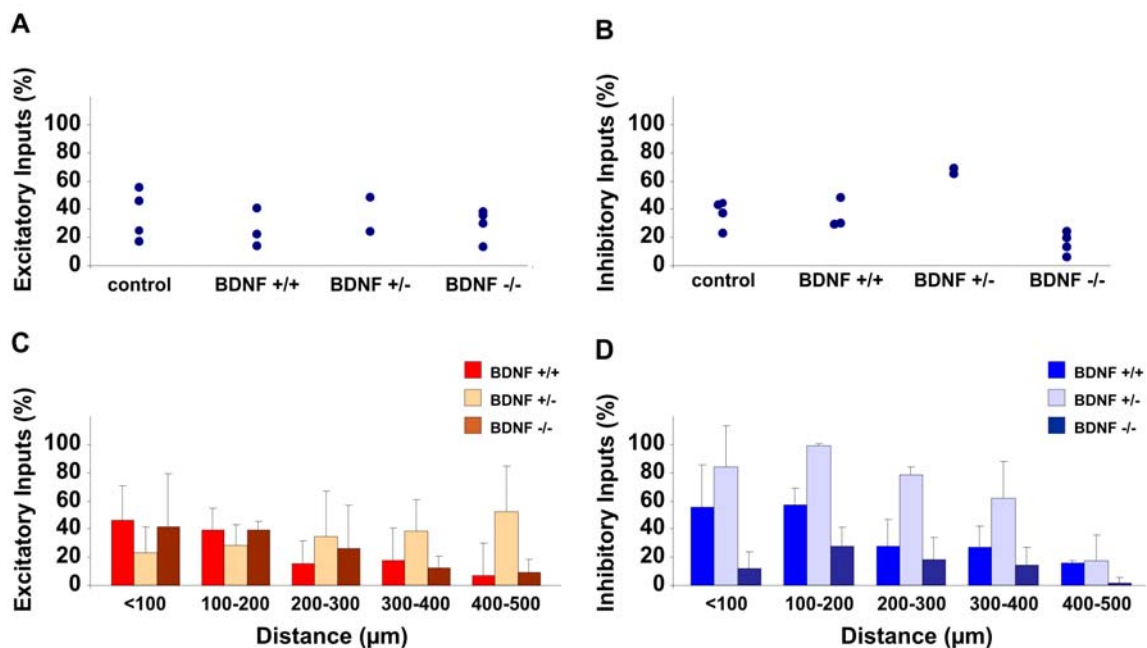


Fig. 3.25: Quantification of synaptic inputs onto transplanted BDNF knockout neurons in organotypic slice cultures.

Percentages of stimulated presynaptic fields delivering excitatory (A, C) and inhibitory (B, D) synaptic responses in transplanted wildtype (*red and blue*), heterozygous (*light red and light blue*) and homozygous BDNF knockout neurons (*dark red and dark blue*) are shown. No differences were observed in the relative amount and distribution of excitatory inputs. Homozygous BDNF knockout neurons showed a strong tendency towards a reduction of inhibitory synaptic inputs. Data are given as mean \pm SD.

As a result of this, only the overall inhibitory synaptic input was analyzed so far from these experiments. Hence, the quantitative analysis of inhibitory synaptic inputs at least suggests an important role of BDNF for the formation of inhibitory synaptic contacts (see 3.3.6).

3.3.6 GABA_A-receptor mediated miniature postsynaptic currents in transplanted BDNF-deficient neurons

Experiments with a single cell gene knockout of BDNF revealed that the number of GABAergic terminals on the soma of BDNF knockout neurons was smaller than on controls (Kohara et al., 2007). To further examine the role of BDNF in the formation of inhibitory networks, spontaneous, GABA receptor mediated miniature PSCs (GABA_A mPSCs) were recorded from transplanted homozygous BDNF knockout (fig. 3.26 A2) and BDNF wildtype (fig. 3.26 A1) neurons (see 2.14) in normal ACSF for mPSCs in organotypic slices (see 2.2 d) containing 10 μ m DNQX to block glutamatergic transmission and 1 μ m TTX at a holding potential of -70 mV. Furthermore the intracellular solution III (see 2.2 h) with symmetric chloride was used. The rise time (2,0 ms \pm 0,3 ms for wildtype and 2,1 ms \pm 0,7 ms for knockout; fig. 3.26 D) as well as the decay kinetics of GABA_A mPSCs (20,8 ms \pm 3,3 ms for wildtype and 17,9 ms \pm 4,7 ms for knockout; fig. 3.26 E) showed no significant differences between the wildtype (n = 11) and BDNF knockout (n = 7) neurons. Intriguingly, the recordings of GABA_A mPSCs revealed a strongly reduced frequency (p < 0,01) in BDNF knockout neurons in comparison to the wildtype neurons (2,1 Hz \pm 0,3 Hz for wildtype and 0,2 Hz \pm 0,1 Hz for knockout; fig. 3.26 C), whereas the mean mPSC amplitude was not significantly different (8,2 pA \pm 0,7 pA for wildtype and 6,3 pA \pm 0,4 pA for knockout; fig. 3.26 B). Because it is known that the frequency of GABA_A mPSCs is related to the total number of functional inhibitory synapses, these results suggest a smaller number of functional GABAergic synapses on the transplanted BDNF knockout neurons. A possible mechanism might be that a release of BDNF from postsynaptic target neurons (impaired in the transplanted BDNF knockout cells) promotes the formation or proliferation of GABAergic synapses through local actions (see 4.3).

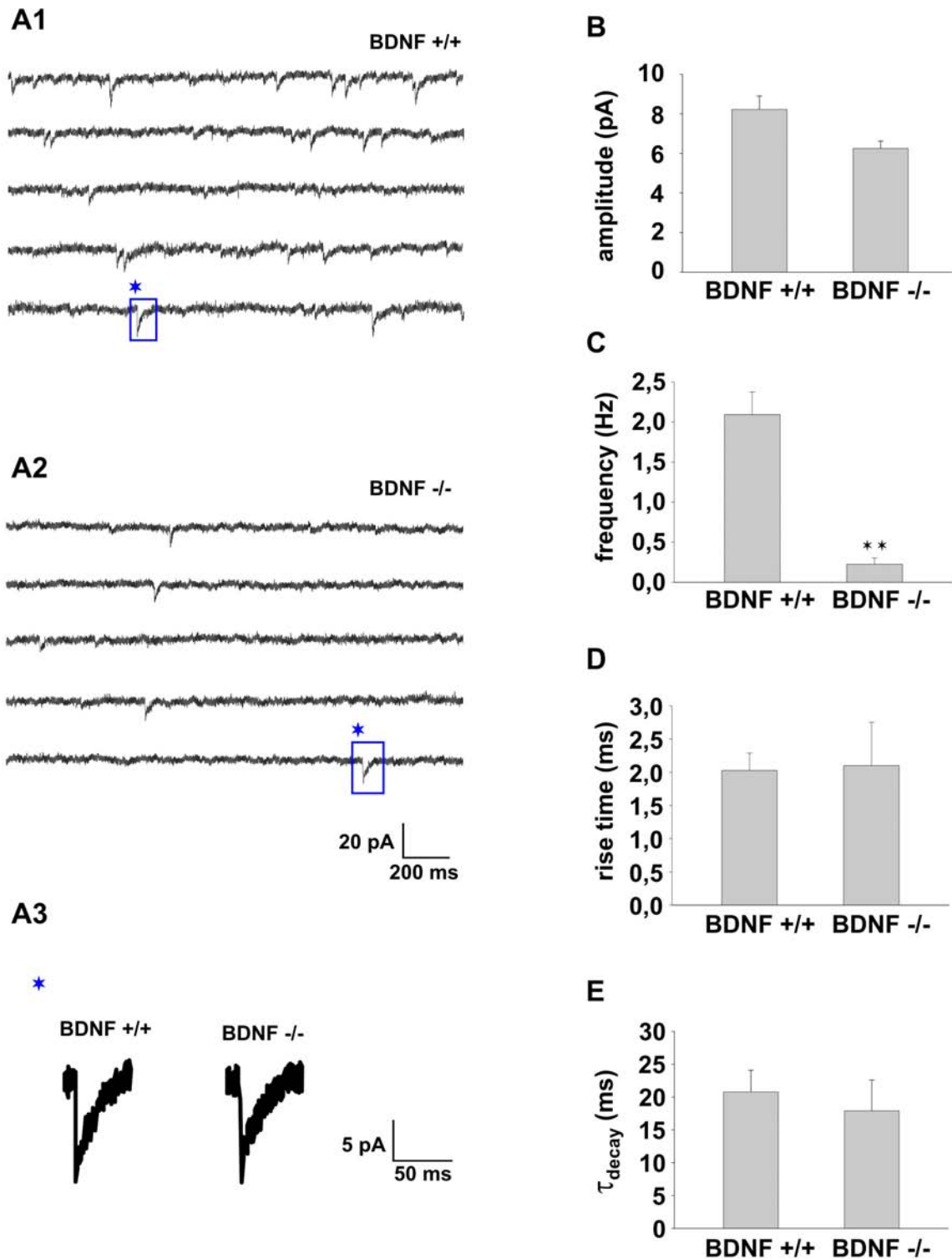


Fig. 3.26: Reduction in the frequency of GABA_A mPSCs in transplanted BDNF knockout neurons.

(A) Representative traces of GABA mPSCs from transplanted BDNF wildtype (A1, n = 11) and BDNF knockout neurons (A2, n = 7) and a magnification of representative individual events (A3). The mean amplitudes (B) did not differ between wildtype and knockout neurons. The mean frequency of GABA mPSCs (C) showed a statistically significant decrease in the BDNF knockout neurons ($p < 0,01$; paired t-test). The mean rise time (D) and the decay time constant (E) showed no differences between wildtype and BDNF knockout neurons. All values are given as mean \pm SD.

4. Discussion

4.1 Presynaptic maturation of glutamatergic synapses in layer Vb pyramidal neurons

The experiments of this study were carried out to investigate the developmental plasticity of glutamatergic synapses in mouse somatosensory cortex. To characterize the presynaptic and postsynaptic properties of these synapses at different developmental stages, layer Vb pyramidal neurons were analyzed in acute slices of young postnatal animals at different ages (P7 and P14). Beside the development of the cortical laminar organization, a progressive differentiation of the cortical neurons takes place as well (Kageyama and Robertson, 1993). Therefore, presynaptic and postsynaptic developmental changes will be discussed, with particular reference to the phenomenon of “silent synapses” in the somatosensory cortex and their conversion into functional ones to persistently increase synaptic efficacy. Foremost, the presynaptically silent synapses and therefore the AMPA receptor mediated postsynaptic currents will be discussed.

4.1.1 Morphology and basic electrophysiology of immature layer Vb pyramidal neurons

The development of the laminar organization in the cortex (Supér and Uylings, 2001; Kageyama and Robertson, 1993) and the appearance of the different cell-types involved (Peters and Kara, 1985; Sur and Cowey, 1995) has been characterized previously for example with the BrdU-method (Takahashi et al., 1999). At postnatal day 7 (P7) all layers and the cortical columns, which have been proposed to be the basic functional units of cortex (Mountcastle, 1997), can be distinguished. The Nissl-staining clearly shows the different laminae in the somatosensory cortex at P7. Below the pial surface the “*molecular layer*”, layer I can be found that consists mostly of glial cells and axons. The “*external granular layer*”, layer II shows a high density of small pyramidal neurons and numerous stellate cells, whereas “*the external pyramidal layer*”, layer III predominantly contains small and middle-sized pyramidal neurons. By contrast, “*the internal granular layer*”, layer IV includes mainly non-pyramidal cells and shows in photomicrographs of native slices the eponymous barrel structure (“barrel cortex”). The “*the internal pyramidal layer*”, layer V contains the biggest pyramidal cells found in the cortex and finally, “*the multiform layer*”, layer VI that is

composed of few big pyramidal neurons as well and many small spindle-like pyramidal and multiform neurons. Below all these layers the white matter can be found, which consists for the most part of myelinated axons. As expected, the layer Vb pyramidal neurons that were investigated in this study, had not yet their final mature appearance despite the almost terminated laminar organization (Kasper et al., 1994). Even the dendritic tree seemed quite complex, except that the apical dendrite had only few collateral branches and a small terminal dendrite tuft. In some cases the apical dendrite left out of the slice before attaining the pial surface without affecting the electrophysiological properties of these cells.

To analyze the active and passive membrane properties of these neurons patch clamp experiments were carried out in the current clamp-mode. Recordings of the membrane potential after hyperpolarizing and depolarizing rectangular pulses showed changes in the membrane potential. At small charges the course of potentials was determined strongly by the passive membrane properties, at higher depolarizations action potentials (AP) were elicited. All characterized neurons showed a regular spiking firing pattern, in line with the fact that only more mature neurons (> P14) can be subdivided into “*Intrinsically Bursting*” (IB) and “*Regular Spiking*” (RS) pyramidal neurons (Amitai, 1994; Chagnac-Amitai et al., 1990; Connors et al., 1982; Hefti and Smith, 2000; Larkman and Mason, 1990; Mason and Larkman, 1990). The further electrophysiological characterization of active and passive membrane properties revealed values, which agreed well with the literature (Kasper et al., 1994). Changes of membrane properties occurring during early postnatal development will be discussed later (see 4.1.3).

4.1.2 Presynaptic properties of immature glutamatergic synapses on layer Vb pyramidal neurons

As described previously, the presynaptic properties are strongly determined by the transmitter release machinery, more precisely amongst others by the release probability. In a presynaptically immature synapse, both AMPA receptors as well as NMDA receptors are postsynaptically present, but they are activated only rarely. This is due to a very low release probability (Pr), because no or very few docked vesicles are present (immature readily releasable pool). At hippocampal developing synapses it has been demonstrated by electron micrographs that presynaptic boutons go through distinct functional states to mature, starting with a complete lack of readily releasable vesicles and a later switch of recycling vesicles to a docked state (Mozhayeva et al., 2002; Hanse and Gustafsson, 2001). These synapses would

not respond if no vesicle release occurs during the experiment and therefore would show a failure rate up to 100%. In the hippocampus, LTP has been shown to increase the Pr and that immature synapses can respond afterwards (Gasparini et al., 2000; Voronin et al., 2004; Walz et al., 2006). In “paired trials” the low release probability increases due to presynaptic paired-pulse facilitation, i.e. if an additional pulse is delivered not more than 50 ms after the first, these synapses respond occasionally to the second pulse, indicating the presence of AMPA receptors (Voronin et al., 2004).

To investigate these presynaptically “silent” synapses, layer 5B pyramidal neurons in mouse somatosensory cortex were analysed using whole-cell patch-clamp-recordings. For extracellular stimulation with a minimal stimulation protocol (Sokolov et al., 2002) a bipolar tungsten electrode was placed in the same layer in a distance of between 50 to 150 μm apart from the soma of interest. To distinguish between “failures” and “successes” the standard deviation (SD) of noise was calculated during the period directly before the stimulation pulse. If the signal amplitude was higher than 2x SD, the signal was rated as “success”, below 2x SD it was rated as “failure”. To ensure, that the signal was a direct synaptic response to the given stimulation, only signals with latencies below 5 ms were analysed. The recording of evoked AMPA receptor mediated EPSCs at a holding potential of -60 mV revealed in some synapses a very high failure rate, a very strong facilitation and thus a reduced failure rate in response to the second pulse, indicating a very low Pr during the first pulse, but synapses showing exclusively “failures” in response to the first pulse (definition: silent synapse) could not be observed. Moreover, responses with a low initial failure rate, which showed a slight reduction in AMPA receptor mediated EPSC amplitude to the second pulse (paired-pulse depression) and no change in failure rate were obtained. Thus, we could not find the in the hippocampus described presynaptically “silent” synapses, but synapses with a very immature release machinery (low Pr) on the presynaptic side. The quantitative analysis of the synaptic responses revealed an amount of about 25% of these presynaptically very immature synapses with failure rates above 30%, whereas the remaining 75% showed quite mature presynaptic properties (high Pr) at the same developmental stage (P7). Instead of the analysis of “failures” that are missing in more mature synaptic responses, the coefficient of variance (CV) was analyzed. As expected, the CV was initially high ($\geq 0,5$) to the first pulse in synaptic responses with a low Pr and initially lower ($\leq 0,6$) in synaptic responses with a high Pr. It has been reported that the paired-pulse behavior varies and depends strongly on the experimental conditions such as the frequency of stimulation (Isaac et al., 1995; Liao et al., 1995; Durand et al., 1996; Gasparini et al., 2000; Montgomery et al., 2001). These findings were confirmed by

experiments with different interpulse intervals (from 25 up to 150 ms) that demonstrated a reduction of facilitation following an increase of the interstimulus intervals.

In the following the synaptic responses with different presynaptic properties were divided into two groups by analyzing the PPR versus the failure rate in response to the first pulse. Two classes of glutamatergic synapses with a low Pr or a high Pr could be formed, with the criteria for a “low Pr synapse” being a PPR of more than 2 and an initial failure rate of at least 30%. Synaptic responses that revealed a PPR of less than 2 and a failure rate below 30% were allocated towards “high Pr synapses”. As a result about 25% of the synapses were defined as “low Pr” and therefore immature synapses and the remaining 75% of the synapses tested were rated as mature synapses with a high Pr. Interestingly, these mature synapses can be found side by side with immature ones simultaneously.

4.1.3 Changes of presynaptic properties in layer Vb pyramidal neurons during postnatal development

In the visual cortex it has been shown that the number of postsynaptically silent synapses is large at birth and decreases during development (Rumpel et al., 1998) as well as on dendritic spines of rat layer II / III pyramidal neurons (Busetto et al., 2008). Synaptic maturation has been proposed to be sequential in the sense that NMDAR-mediated signaling develops initially followed by AMPAR-mediated one (classical postsynaptically silent synapses). Insertion of AMPA-receptors due to a NMDA-receptor-dependent LTP-like process has been proposed as underlying mechanism. However, recent studies suggest additionally a strong involvement of maturation of the presynaptic release machinery. Here, possible developmental changes on the presynaptic side were characterized in more mature pyramidal neurons from P14 mice. The Nissl-staining showed the layers I to VI quite clearly. Below the layers the white matter can be seen. The layer Vb pyramidal neurons have in contrast to those at P7 a mature appearance. The dendritic tree is very complex and the apical dendrite has several collateral branches and an expanded terminal dendrite tuft. Electrophysiologically, at P14 the large pyramidal neurons of layer Vb can be subdivided into “*Intrinsically Bursting*” (IB) and “*Regular Spiking*” (RS) pyramidal neurons, depending on their firing pattern (Amitai, 1994; Chagnac-Amitai et al., 1990; Connors et al., 1982; Hefti and Smith, 2000; Larkman and Mason, 1990; Mason and Larkman, 1990). As mentioned previously, only RS-cells were included for analysis of developmental changes, because in experiments at P7 only RS-cells were found. For the further electrophysiological characterization the active and

passive membrane properties were analyzed as already described. In comparison to P7, several developmental changes were observed. The resting membrane potential was increased as it has been shown similarly for layer V pyramidal neurons in rat visual cortex (Kasper et al., 1994). The membrane resistance was decreased, caused by an enlargement of the cell surface by neuronal growth. Accordingly, the capacitance increased during development. The strong decrease of the membrane time constant during development might result in an elevated excitability of these neurons (McCormick and Prince, 1987). The elicited APs at P14 were hardly adapting in their frequency, showing a “regular spiking” firing pattern (Connors and Gutnick, 1990). The frequency as well as the amplitude was strongly increased at P14, whereas the half width was just about half as much as at P7. This might be caused by a higher density of voltage-dependent channels. These kind of developmental changes correspond well to modifications described in the literature (Kasper et al., 1994; McCormick and Prince, 1997). Recordings of AMPA receptor mediated EPSCs at -60 mV holding potential revealed exclusively responses with no failures, decreased CVs and a clear paired-pulse depression indicating a high Pr and therefore mature presynaptic properties. Thus, we found evidence for presynaptically immature synapses and a developmental maturation from P7 to P14 at glutamatergic synapses on layer Vb pyramidal neurons in mouse somatosensory cortex.

4.2 Developmental changes of postsynaptic NMDA-receptor properties in layer Vb pyramidal neurons

For the analysis of a coupling of presynaptic and postsynaptic maturation corresponding NMDA receptor mediated EPSCs were recorded using the whole-cell patch clamp-technique. Upon identification of the presynaptic properties via AMPA-receptor mediated EPSCs at -70 mV holding potential, the recording was repeated at +40 mV holding potential after addition of 20 μ M DNQX. NMDA receptor mediated responses were observed in case of “failure” as well as in case of “success” in the AMPA component. Therefore, the failure rate of the NMDA receptor mediated responses differed strongly from that of the AMPA receptor mediated ones. NMDA receptor mediated EPSCs exhibited no failures independent of the paired-pulse behavior of AMPA receptor mediated responses. This lack of failures in response to the first pulse at NMDA receptor mediated EPSCs strongly suggests the presence of additionally NMDA receptor only synapses (classical postsynaptically silent synapses). Hence, we found not only evidence for presynaptic immature (low Pr) and mature (high Pr) synapses, but also postsynaptic immature (NMDA receptor only) synapses in parallel. Further

on, differences concerning NMDA receptor kinetics at immature and mature synapses were observed. Synapses with a high Pr, indicating a presynaptically mature state, also showed much faster kinetics than synapses with a low Pr. This acceleration of kinetics from immature (low Pr) to mature (high Pr) synapses might be caused by a change in NMDA-receptor subunit composition during development (Flint et al., 1997; Hoffmann et al., 2000). To analyze, whether a change of NMDA receptor subunit composition is additionally involved in this process of a possibly coupled presynaptic and postsynaptic maturation, the NMDA receptor mediated EPSCs were further investigated in the second part of this study.

As mentioned previously, there seem to be different developmental states present *simultaneously* in mouse somatosensory cortex at P7. So far, we could describe (1) a mature state with a high release probability and postsynaptic AMPA and NMDA receptors and (2) an immature state with a low release probability and postsynaptic AMPA and NMDA receptors. What remained to be shown is (3) an mature state with a high release probability but postsynaptic only NMDA receptors and finally, (4) an immature state with a low release probability and postsynaptic only NMDA receptors. To verify this hypothesis, again layer Vb pyramidal neurons at P7 were chosen for the experiments, because the anatomical development of the somatosensory cortex then is almost finished, but developmental maturation like the conversion of “silent synapses” into functional ones still can be detected as already demonstrated in visual cortex (Rumpel et al., 1998). These postsynaptically silent synapses are well known as NMDA receptor only synapses, i.e. they are lacking AMPA receptors, but express functional NMDA receptors. Functional AMPA receptors are delivered to the subsynaptic membrane after LTP induction. This process seems to be characteristic for this early postnatal development in the brain, where a quite intensive synaptogenesis takes place (Malenka and Nicoll, 1997; Feldman and Knudsen, 1998; Feldman et al., 1999; Atwood and Wojtowicz, 1999). Another indicator for postsynaptic maturation is the change of NMDA receptor subunit composition from NR2B to NR2B/NR2A containing receptors (Flint et al., 1997; Hoffmann et al., 2000) that fastens NMDA receptor kinetics.

To characterize the postsynaptic development and to ascertain, if there might exist a coupling between presynaptic (low Pr to high Pr) and postsynaptic (NMDA receptor only to AMPA receptors and NMDA receptors) developmental maturation, NMDA receptor mediated currents were investigated at different maturational conditions (at low Pr and high Pr synapses).

4.2.1 NMDA receptor only synapses on immature layer Vb pyramidal neurons

Synapses with a purely NMDA receptor mediated transmission have been described frequently in the developing cortex. To analyze these postsynaptically silent synapses in immature layer Vb pyramidal neurons, whole-cell patch clamp recordings were performed at P7. Glutamatergic EPSCs were elicited by extracellular stimulation as previously described and pharmacologically isolated. The stimulation strength was adjusted according to the minimal stimulation protocol. At a holding potential of +40 mV a response was elicited in all cases, whereas at -70 mV in some cases no response was detectable. In the latter cases the responses comply with NMDA receptor only synapses. These immature silent synapses might not only contain just NMDA receptors but further, only NMDA receptors with an immature subunit composition, i.e. NR2B subunits. This was demonstrated by a complete block of the NMDA receptor mediated response using the NR2B-specific blocker Ro 25-6981. These findings are consistent with those of Kimiko Nakayama, who has shown that diminished neuronal activity promotes silent synapse formation via the surface delivering of NR2B containing NMDA receptors (Nakayama et al., 2005) and further that these receptors are important for the conversion of silent synapses into functional ones in mature neuronal circuits.

4.2.2 Changes in NMDA-receptor subunit composition during developmental maturation of glutamatergic synapses

As already depicted, the duration of NMDA receptor mediated EPSCs is thought to be determined by intrinsic receptor properties (Lester et al., 1990; Lester and Jahr, 1992) rather than the persistence of glutamate in the synaptic cleft (Clements et al., 1992). Therefore, changes in NMDA receptor mediated EPSC duration are likely to result from alterations of the NMDA receptor complex itself (Hestrin, 1992; Crair and Malenka, 1995). Several studies (Monyer et al., 1994; Zhong et al., 1995; Sheng et al., 1994) have demonstrated that NR2 subunit expression is developmentally regulated. One week after birth all four NR2 subunits are expressed in cortex at different levels (Monyer et al., 1994). These data suggest that changes in subunit expression during cortical development might regulate the function of cortical NMDA receptors. The proportion of cells expressing NR2A and thus, displaying faster NMDA receptor mediated EPSCs, increases during postnatal development, thereby providing a molecular basis for the developmental changes in EPSCs (Flint et al., 1997).

Actually, recent evidence supports the notion that NR2A expression is controlled by neuronal activity. Depolarization of cerebellar granule cells in culture has been shown to lead to a significant upregulation of NR2A subunit expression (Vallano et al., 1996). Moreover, changes in NMDA receptor efficacy have been proposed as a mechanism establishing critical periods for plasticity in neocortex (Fox et al., 1992; Crair and Malenka, 1995).

To analyze if changes in NMDA receptor mediated EPSC kinetics are caused by a change of NMDA receptor subunit composition, whole-cell patch-clamp recordings were performed in acute slices at P7. After detection of immature (low Pr) and mature (high Pr) synapses at -60 mV, SYM 2206 was added to the ACSF to eliminate any possibility of an influence of AMPA receptor mediated currents. NMDA receptor mediated EPSCs then were recorded with identical stimulation strength at a holding potential of +40 mV. To evaluate the amount of NR2B-containing NMDA receptors, the specific NR2B subunit antagonist Ro 25-6981 was added to the ACSF. The addition of this very potent antagonist (Fischer et al., 1997) led to a reduction of the NMDA receptor mediated EPSCs to 20% in immature, but only to 80% in mature synapses. These findings indicate a large amount of NR2B subunit-containing NMDA receptors in immature synapses and a significantly smaller amount of these subunits in the more mature ones. The other way around, NMDA receptors at immature synapses contain only few NR2A subunits, whereas at mature synapses the amount of NR2A subunits is quite large. In a second approach the NR2A subunit was selectively blocked by addition of Zn^{2+} (Paoletti et al., 1997) to the ACSF. As a result of this, the NMDA receptor EPSCs were not reduced at all in immature synapses, whereas mature ones showed a strongly reduced response of only 30%. These findings suggest a large amount of NR2A subunits at mature synapses and a lack of these subunits in the immature ones. The change of the decay kinetics, caused by a developmental change of subunit composition, has been described previously (Carminigno and Vicini, 1992; Hestrin, 1992b; Khazipov et al., 1995; Gottmann et al., 1997; Hoffmann et al., 2000). Therefore, the observed changes in NMDA receptor kinetics at immature (low Pr) and mature (high Pr) synapses were further analyzed. Mature synapses always revealed NMDA receptor mediated responses with a faster decay than the immature ones, indicating the presence of NR2A subunit containing NMDA receptors at mature synapses. Thus, we found evidence that a coupling between presynaptic and postsynaptic maturation exists in a way that presynaptically immature synapses (low Pr) also exhibit only NR2B subunit containing (immature) NMDA receptors on the postsynaptic side. The other way around, presynaptically mature (high Pr) synapses also revealed a mature postsynaptic side with mature NR2A subunit containing NMDA receptors. This coupling may be mediated

by an activity-dependent expression of NR2A subunits that is only sufficiently activated at high Pr synapses with postsynaptic AMPA receptors (pre- and postsynaptically mature).

4.2.3 Changes in release probability at different developmental stages

The strength (efficacy) of a synapse can be modified by variation of its Pr (Bekkers and Stevens, 1990; Bolshakov and Siegelbaum, 1995; Magleby, 1987; Malinow and Tsien 1990; Manabe et al., 1993; Stevens and Wang 1994; Zucker, 1989). Because synaptic efficacy is that important for the function of neuronal circuits, a fundamental question is how Pr is distributed in these synapses. As already described in hippocampal synapses in culture and in slices (Hessler et al., 1993; Rosenmund et al., 1993), the progressive decrease of NMDA receptor mediated currents was analyzed in the presence of the open-channel NMDA receptor blocker MK-801 what provides an indirect measure of the transmitter Pr (Huang and Stevens, 1997). For further analysis of the observed changes in Pr at immature and mature synapses at P7, whole-cell patch-clamp recordings were obtained as already described. Again after detection of immature and mature synapses at -60mV, SYM 2206 was added to the ACSF to block the AMPA receptor mediated components. Without changing the stimulation strength, single evoked NMDA receptor mediated EPSCs at +40 mV were elicited every 10 s and, after recording of 10 controls, 20 μ M MK-801 was washed into the slice. The progressive block was subsequently recorded for at least another 40 stimulations until a saturated block was reached. Immature synapses revealed a significantly slower block by MK-801 than mature ones. Because the synaptic Pr plays a major role in determining the strength of a synapse and the strength (efficacy) of a synapse can be modified by variation of its Pr, our findings suggest that an increasing Pr occurs during development and that this higher Pr leads to an improved efficacy (heightened strength) and therefore, a maturation of the synapse. An influence of the higher open probability of NR2A subunit containing NMDA receptors on the kinetics of the MK801 block has been suggested to be compensated by the obvious faster decay kinetics of these subunits (Huang and Stevens, 1997). Therefore, the MK-801 block can be regarded as a good estimate of differences in Pr.

4.3 Pairing-induced potentiation of immature synapses in layer Vb pyramidal neurons

Conversion of a silent synapse into a functional one is one way to persistently increase synaptic efficacy (strength). In principle, synapses can be silent through postsynaptic as well as presynaptic mechanisms. Postsynaptically silent synapses are unable to detect glutamate release and do not conduct at rest due to the lack of AMPA-receptors in the subsynaptic membrane (Malenka and Nicoll, 1997; Feldman and Knudsen, 1998; Rumpel et al., 1998; Feldman et al., 1999; Atwood and Wojtowicz, 1999). By contrast, presynaptically silent synapses do not conduct, because their probability of glutamate release (Pr) is close to zero (Voronin and Cherubini, 2004). The conversion of postsynaptically silent synapses into functional ones, due to insertion of AMPA receptors, has been suggested to be particularly relevant during postnatal development, when a significant fraction of synapses contains only NMDA receptors (Durand et al., 1996; Rumpel et al., 1998). The existence of presynaptically silent synapses (low Pr) has been proofed by experiments with minimal paired-pulse stimulation delivered to Schaffer collateral or to mossy fibres (Gasparini et al., 2000; Maggi et al., 2003). Synaptic responses revealed a strong paired-pulse facilitation that is known to depend largely on an increase in Pr. Furthermore, a pairing of afferent stimulation with postsynaptic depolarization has been shown to convert these silent synapses into fully functional synapses and thus, to induce or to contribute to LTP where some synapses are already active at rest. Experiments in cultured hippocampal neurons have demonstrated that a potentiation is accompanied by a transmitter release increase through Pr increase at pre-existing functional synapses in an NMDA receptor dependent manner (Ninan et al., 2006). The relative contribution of presynaptic and postsynaptic mechanisms seem to vary according to the initial state of the synapse, experimental protocol and time after induction as already shown in CA1 pyramidal neurons (Palmer et al., 2004).

To investigate a possible potentiation of the previously described presynaptically silent synapses, a pairing of extracellular stimulation combined with postsynaptic depolarization has been carried out in immature layer Vb pyramidal neurons at P7. Following this protocol, the immature synapses at P7 with a low Pr were potentiated and showed afterwards significantly increased EPSC amplitudes. A strongly reduced failure rate was observed in these synapses and hence, the paired-pulse behaviour revealed an evidentiary reduced facilitation after the pairing. Thus, an activity-dependent conversion of presynaptically immature synapses towards more mature ones with a higher Pr can be assumed. However, the potentiation might also be caused by an activation of postsynaptically silent synapses as it has been demonstrated

previously (Malenka and Nicoll, 1997; Feldman and Knudsen, 1998; Feldman et al., 1999; Atwood and Wojtowicz, 1999). Neither the hypothesis of a purely presynaptic, nor postsynaptic potentiation, i.e. an increase in Pr or the delivery of AMPA receptors, can be confirmed. Even a composition of both is supposably. As mentioned previously, this kind of potentiation should be NMDA receptor dependent. On that account, the pairing of extracellular stimulation combined with postsynaptic depolarization in immature layer Vb pyramidal neurons at P7 was repeated in the presence of the NMDA receptor specific antagonist D-AP5. The pairing protocol did not induce any changes in EPSC amplitudes and accordingly, these synapses still revealed a high initial failure rate and therefore a low Pr. Finally, we found evidence that immature (silent) synapses can be potentiated and converted into more mature ones. Furthermore, this kind of potentiation depends strongly on NMDA receptor activation, as demonstrated by addition of the specific NMDA receptor antagonist D-AP5.

Recapitulatory, it could be adopted that immature synapses with a low Pr on layer Vb pyramidal neurons in mouse somatosensory cortex disappear during early maturation. Additionally, NMDA receptor only synapses (= postsynaptically silent synapses) are present at very young ages. In parallel, the NMDA receptor subunit composition changes during early maturation suggesting a coupling of presynaptic and postsynaptic maturation. All of the described developmental states are present simultaneously in the developing mouse somatosensory cortex.

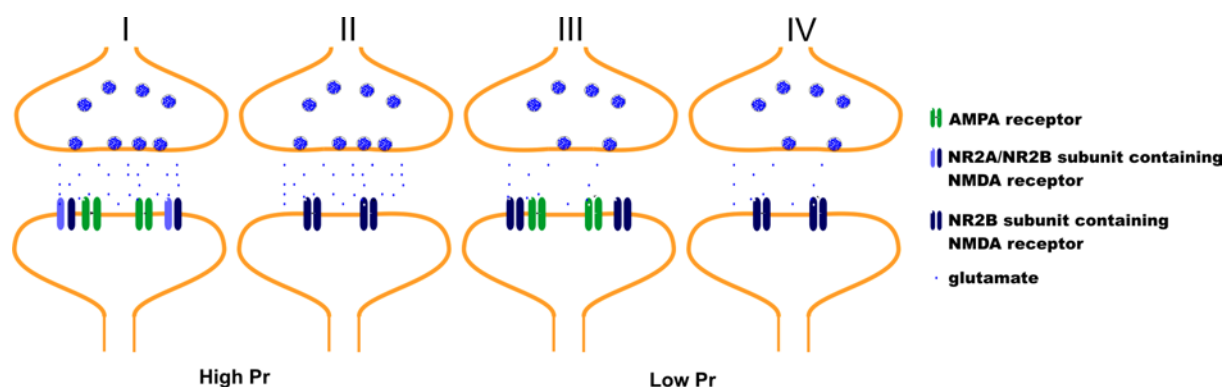


Fig. 4.1: Different maturational states of glutamatergic synapses on layer Vb pyramidal neurons.

The different developmental states of glutamatergic synapses on layer Vb pyramidal neurons in mouse somatosensory cortex are present simultaneously. Presynaptically mature synapses with a high Pr can show a mature (I: NR2A receptors and AMPA receptors) or an immature (II: NR2B receptors and no AMPA receptors) postsynaptic side. On the other hand, a presynaptically immature synapse with a low Pr is always coupled with a postsynaptically immature (III: NR2B receptors and AMPA receptors, or IV: NR2B receptors and no AMPA receptors) side. Type IV remains to be demonstrated.

4.4 Spatial mapping of synaptic inputs onto single BDNF-deficient neurons transplanted to wildtype organotypic slice cultures

Synapse formation and stabilization in the vertebrate central nervous system is a dynamic process, requiring bi-directional communication between pre- and postsynaptic partners (Cohen-Cory, 2002). A favoured candidate molecule to modulate synaptogenesis in the developing brain is BDNF. BDNF plays a crucial role in synaptic development and plasticity in the CNS (for review, see Bibel and Barde, 2000; Huang and Reichardt, 2001; Poo, 2001; Lu, 2003). The question, whether BDNF acts via a retrograde messenger onto presynaptic cells in the neocortex, has not been fully addressed previously. A reason therefore is that experiments were carried out by application of exogenous BDNF and often with presumably nonphysiological levels of BDNF. To investigate the possibility of local retrograde actions of endogenous BDNF onto presynaptic cells, it is also inappropriate to use preparations derived from conventional or even area-specific BDNF knockout mice, because in all of these preparations, all neurons in a given area of the cortex lack BDNF and thus, it is difficult to examine the direction of endogenous BDNF actions onto synapses at particular neurons. To overcome these problems, in this study relatively few, EGFP-expressing BDNF knockout neurons were transplanted to organotypic slice cultures of somatosensory cortex. In this kind of preparation endogenous BDNF is lacking in a single neuron or at least a very small number of distributed cells. To characterize the role of BDNF in developmental plasticity, especially as a retrograde messenger, synaptic inputs on transplanted BDNF-deficient neurons in organotypic slice cultures were analyzed using the patch clamp-technique in combination with photolysis of *caged* glutamate.

4.4.1 Morphology and basic electrophysiology of transplanted BDNF-deficient neurons

In the third part of this study, single BDNF knockout neurons were transplanted to organotypic slice cultures of mouse somatosensory cortex. In these preparations endogenous BDNF was lacking in a single cell or a small number of cells, more precisely, not more than 3 neurons were integrated into the cultured slices. After 28 DIV the transplanted neurons were functionally integrated into the organotypic slice culture. To identify the transplanted EGFP-expressing neurons, the EGFP signal of the cell of interest was detected under UV-light and then the cell was patched under visual control in the infrared contrast. The exchange of pipette

solution and intracellular space after reaching the whole-cell configuration led to a rapid decrease of the fluorescence. In most experiments a transplanted and an endogenous neuron (as internal control) were recorded from the same slice culture. More than 70% of the transplanted cells were located in a region corresponding to layers II/III, only some single neurons were integrated in the region of layer IV to VI. The type of neuron was identified after filling with biocytin in the subsequent morphological analysis, whereas most of the cells displayed a pyramidal-like morphology.

In general, no changes in morphology were observed between controls and transplanted neurons, as well as between homozygous BDNF knockout, heterozygous BDNF knockout and BDNF wildtype. The morphology was not examined more closely, since it has been described in a single-cell gene knockout preparation in detail. There, a local reduction of GABAergic presynaptic terminals was observed, but no differences in dendritic morphology (Kohara et al., 2007). Furthermore, an overexpression of BDNF via biolistic transfection in organotypic slice cultures has been shown to increase dendritic length and number of segments in pyramidal neurons without affecting maximum branch order and number of primary dendrites, whereas the neutralization of BDNF had no effect (Wirth et al., 2003; Mc Allister et al., 1995). All of the different neurotrophic actions in mammalian neocortex were lamina-specific and besides, required activity (Mc Allister et al., 1996).

To compare the active and passive membrane properties the membrane potential was recorded in the current clamp- mode after application of hyperpolarizing and depolarizing current pulses. According to the previously described morphology, neurons with a regular spiking (RS) as well as a fast spiking (FS) firing pattern (interneurons) were detected. The electrophysiological properties for each genotype showed no significant differences in either transplanted or endogenous neurons. All characteristic parameters in the organotypic slice cultures were according to literature (Gorba et al., 1999; Klostermann and Wahle, 1999). Therefore, all recorded neurons seemed to be functionally integrated into the slice culture and hence, can be compared to endogenous cells of the organotypic slice culture.

4.4.2 Properties of photolysis-induced synaptic activity

The object of the spatial mapping using *caged* glutamate photolysis was to characterize the amount of synaptic inputs onto transplanted BDNF knockout and BDNF wildtype neurons as well as onto endogenous controls in organotypic slice cultures. The topographic acquisition of photolysis induced activity was recorded following double flashes at -60 mV and -40 mV

holding potential, respectively. As already mentioned, analysis of the photolysis induced activity was carried out concerning (a) the latency between stimulus and onset of activity, (b) the maximal amplitude of excitatory postsynaptic potentials (EPSPs), (c) the integral of EPSPs during the period of 150 ms after stimulation and (d) the occurrence of inhibitory postsynaptic potentials (IPSPs). For quantification of the EPSPs the integral of all depolarizing events during the 150 ms *post stimulus* were included. The result provided information about the strength of the elicited excitatory activity. The recorded cells received distinct excitatory and inhibitory synaptic inputs from presynaptically activated neurons. This kind of topographic mapping of synaptic connectivity has already been used to identify the principles underlying the construction of columnar architecture in the rat barrel cortex (Bureau et al., 2004) as well as to analyze the functional organization of cortical circuits (Shepherd et al., 2005; Shepherd and Svoboda, 2005; Bureau et al., 2006). Moreover, it has been demonstrated that repetitive stimulation of some fields reliably elicited IPSPs with stable rise-time and delay-to-onset time, but the amplitude of the IPSPs varied from trial to trial with a tendency to decrease (Schubert et al., 2001). Therefore, only the occurrence of IPSPs was analyzed, but not the strength of the synaptic input. EPSPs were elicited reliably and from there were analyzed concerning their strength.

The different recorded types of photolysis induced activity included the direct activity that occurred with very short latencies (below 4 ms) after photostimulation of proximal dendrites as well as synaptic mediated activity in the recorded neuron. The synaptic mediated EPSPs and IPSPs usually showed much longer latencies (up to 50 ms) than the direct activity. These longer latencies were caused by very long and variable latencies until generation of action potentials in the presynaptic neurons after photostimulation (Katz and Dalva, 1994; Molnar and Nadler, 1999). Most likely, more than one action potential was elicited in the presynaptic neuron by photostimulation (Molnar and Nadler, 1999), so that excitatory inputs composed of several EPSPs might have been elicited by activation of one presynaptic neuron. Therefore, the amount of EPSPs does not necessarily reveal the amount of activated presynaptic neurons, i.e. the spatial distribution of connected neurons could be interpreted, but not their absolute amount or the timing properties of their inputs.

A long lasting recording and therefore long lasting exposition to *caged* glutamate and multiple photostimulations did neither influence the electrophysiological properties of the neurons nor damage them (Callaway and Katz, 1993; Katz and Dalva, 1994).

4.4.3 Comparison of transplanted and endogenous neurons in organotypic slice cultures

To quantify the spatial distribution of synaptic inputs onto the recorded neuron for different distances to the soma, the mean percentage of fields was detected, in which the photostimulation caused excitatory or inhibitory inputs. To affirm the comparability of endogenous controls and the transplanted neurons, the excitatory and inhibitory inputs onto controls and transplanted BDNF wildtype neurons were quantitatively analyzed. No significant differences were detected in the amount and distribution of excitatory and inhibitory synaptic inputs between endogenous controls and transplanted wildtype neurons. Both received widespread excitatory and inhibitory inputs from all tested proximal and more distal regions. The input was in all cases more prominent from regions close to the recorded soma ($< 200 \mu\text{m}$), still numerous inputs from medium distances (200 to $400 \mu\text{m}$) and at least few synaptic inputs from more distant cells ($> 400 \mu\text{m}$). Inputs from a distance of more than $500 \mu\text{m}$ were excluded from the quantification because of their unsteady occurrence. Altogether, the endogenous neurons can be considered as internal controls for the transplanted BDNF wildtype and knockout neurons. This is consistent with previous studies that have demonstrated by transplantation of embryonic stem cell-derived neurons in hippocampal slice cultures that these integrated cells expressed AMPA and GABA_A receptor subunits. Moreover, these cells received functional glutamatergic and GABAergic synapses from host neurons and the synapses between host and embryonic stem cell-derived neurons displayed pronounced paired-pulse facilitation indicative of intact presynaptic short-term plasticity (Benninger et al., 2003; Rüschemschmidt et al., 2005; Scheffler et al., 2006).

4.4.4 Synaptic inputs on transplanted BDNF-deficient neurons

To investigate the typical spatial distribution and strength of synaptic inputs onto transplanted as well as endogenous cells, mapping of different transplanted genotypes and endogenous neurons was performed. Only pyramidal-like neurons with a RS firing pattern were included in the analysis of the synaptic inputs, because inhibitory neurons are not able to produce and release BDNF by themselves. The resulting maps of all neurons clearly indicate that all recorded cells received widely distributed excitatory synaptic inputs. A layer specific functional connectivity as reported from acute slices (Schubert et al., 2001) could not be confirmed in organotypic slice cultures, *most likely* because of the lack of laminar organization after longer cultivation periods.

In contrast to the excitatory inputs, the inhibitory inputs were equally distributed to the whole area tested in endogenous cells, transplanted BDNF wildtype *and* heterozygous BDNF knockout neurons. In the transplanted homozygous BDNF knockout neurons the inhibitory inputs were strongly reduced and spatially more limited to fields near the recorded neuron. Distal inhibitory inputs were pretty rare and could be observed only in few cases. These results suggest that BDNF is not crucial for the functional integration of single neurons in a network or receiving input from presynaptic neurons in general. Furthermore, there seems to be no direct influence on glutamatergic receptors during development (synaptogenesis), because the total number of excitatory synaptic inputs remained constant in controls and all types of transplanted neurons. By contrast, the inhibitory inputs were clearly reduced in transplanted homozygous BDNF knockout cells, indicating a smaller number of functional GABAergic synapses on the BDNF knockout neurons. These results are in accordance with previous studies that showed a reduced number of GABAergic terminals on the soma of BDNF knockout neurons in a single-cell gene knockout by using immunohistochemical analysis. Additional recordings of miniature IPSCs revealed a lower frequency of mIPSCs of BDNF-deficient neurons in the single-cell gene knockout model, although the amplitude was not significantly different from controls (Kohara et al., 2007).

Therefore, in our study the differences in inhibitory inputs onto transplanted homozygous BDNF knockout neurons were further analyzed by recording of *GABA_A receptor mediated* PSCs because of the lack of reliability of *the determination of* inhibitory input strength.

4.4.5 Quantitative analysis of synaptic inputs onto transplanted BDNF-deficient neurons

For the quantitative analysis of the spatial distribution of synaptic inputs onto transplanted neurons, the mean percentage of fields, in which the photostimulation caused excitatory or inhibitory inputs, was detected for different distances to the soma. No significant genotype specific differences were found in the distribution of excitatory inputs originating from proximal or distal located presynaptic neurons. Inputs from all different distances varied between 12,7 and 53,3% in all transplanted as well as control neurons. Therefore, the quantitative analysis of the spatial distribution of excitatory synaptic inputs demonstrates that all types of neurons received similar widespread excitatory inputs from all tested regions. In addition, no differences in the strength of excitatory synaptic inputs were observed. Thus, BDNF seems not to play a major role in the synaptogenesis of excitatory inputs, i.e. BDNF is

not compulsory for the receipt of excitatory synaptic inputs during development. In contrast, the distribution of inhibitory inputs shows the tendency towards spatially more local restricted inputs in transplanted homozygous BDNF knockout neurons, but not in all other genotypes and endogenous cells. The inhibitory inputs onto homozygous BDNF knockout neurons varied between 5,8 and 23,6%, whereas the inhibitory input onto the other genotypes and controls varied between 21,9 and 66,8%. The very small amount of neurons tested allowed no statistical tests concerning significant differences, but further experiments (GABA receptor mediated miniature currents) confirmed the suspicion of a strong influence of BDNF on GABAergic transmission (see 4.3.6). Furthermore, the strength of inhibitory synaptic inputs was not quantitatively analyzed, because at a holding potential of -60 mV (close to the equilibrium potential of chloride) inhibitory inputs were most often overlaid by the strong excitatory inputs. However, at -40 mV the inhibitory inputs could be detected without any doubt, but not quantified efficiently, because in most recorded neurons action potentials were elicited by this rather strong depolarization. As a result of this, only the percentage of inhibitory synaptic input was analyzed in these experiments. Anyway, the quantitative analysis of inhibitory synaptic inputs at least suggests an important role of BDNF for the formation of inhibitory synaptic contacts (see 4.3.6).

4.4.6 GABA_A-receptor mediated miniature currents in transplanted BDNF-deficient neurons

As demonstrated previously in a single cell gene knockout of BDNF, the number of GABAergic terminals on the soma of BDNF knockout neurons is smaller than on controls (Kohara et al., 2007). To examine more closely the role of BDNF on the formation of inhibitory networks after transplantation, spontaneous GABA receptor mediated miniature PSCs (GABA_A mPSCs) were recorded from transplanted homozygous BDNF knockout and BDNF wildtype neurons at a holding potential of -70 mV. The subsequent analysis of the recorded GABA_A mPSCs revealed no differences between wildtype and knockout neurons concerning their rise times as well as their decay kinetics. By contrast, the frequency of GABA mPSCs was strongly reduced in BDNF knockout neurons in comparison to the wildtype neurons, although the mean amplitudes remained constant. It is well known that the frequency of mPSCs is related to the total number of functional inhibitory synapses. Therefore, these results suggest a smaller amount of functional GABAergic synapses on the transplanted BDNF knockout neurons. However, a functional defect in release probability

would result in a similar mPSC phenotype. To decide between these alternatives, a further functional and morphological analysis of GABAergic synapses is needed.

A possible mechanism for this action of BDNF might be that a release of BDNF from postsynaptic target neurons, which is impaired in the transplanted BDNF knockout neurons, promotes the formation or functional maturation of GABAergic synapses through local actions (fig. 4.2). GABAergic neurons do not express BDNF-related mRNA and thus do not produce BDNF by themselves (Ernfors et al., 1990; Cellerino et al., 1996; Rocamora et al., 1996; Gorba and Wahle, 1999). An activity dependent (Kohara et al., 2001) transfer of BDNF from surrounding (wildtype) excitatory neurons that are known to produce and secrete BDNF (Yan et al., 1997; Friedman et al., 1998; Lessmann, 1998; Hartmann et al., 2001; Lessmann et al., 2003) might be crucial for the development of GABAergic synapses. This very local action of BDNF onto GABAergic synapses is consistent with previous studies on neuromuscular synapses, in which actions of BDNF were restricted to nearby synapses at the BDNF application site (Zhang and Poo, 2002). Because it was previously reported that exogenously applied BDNF attracts axonal growth cones (Song et al., 1997; Ming et al., 2002; Li et al., 2005), the results in this study suggest that postsynaptically released BDNF might attract GABAergic growth cones and result in an increase of GABAergic synapses. Therefore, a loss of retrograde actions of BDNF in the transplanted BDNF knockout neurons might impair the formation of functional GABAergic synapses. This is corroborated by former studies in hippocampal neurons which suggested that BDNF transferred retrogradely from excitatory to GABAergic neurons promotes dendritic growth of the latter neurons (Marty et al., 1996; Marty et al., 1997). Still it remains unclear, whether transplanted GABAergic neurons would reveal a similar low inhibitory input as it has been shown for transplanted excitatory BDNF deficient neurons. Another question that has to be addressed is the normal excitatory input onto transplanted BDNF knockout neurons. A possible explanation therefore would be a minor role of BDNF in formation of excitatory synapses. Another reason might be that glutamatergic growth cones do not depend exclusively on postsynaptically released BDNF, but may presynaptically release BDNF by themselves (Kolarow et al., 2007). Thus, the final concentration of BDNF between glutamatergic growth cones and postsynaptic target neurons would be higher than between GABAergic growth cones and postsynaptic target neurons, respectively. However, by transplantation of single EGFP-expressing BDNF deficient neurons into organotypic slice cultures, retrograde actions of BDNF could be investigated at particular neurons. Actually, by generating topographic maps of synaptic inputs onto these transplanted

neurons, it could be demonstrated that the formation and proliferation of GABAergic synapses is strongly influenced by postsynaptically released BDNF.

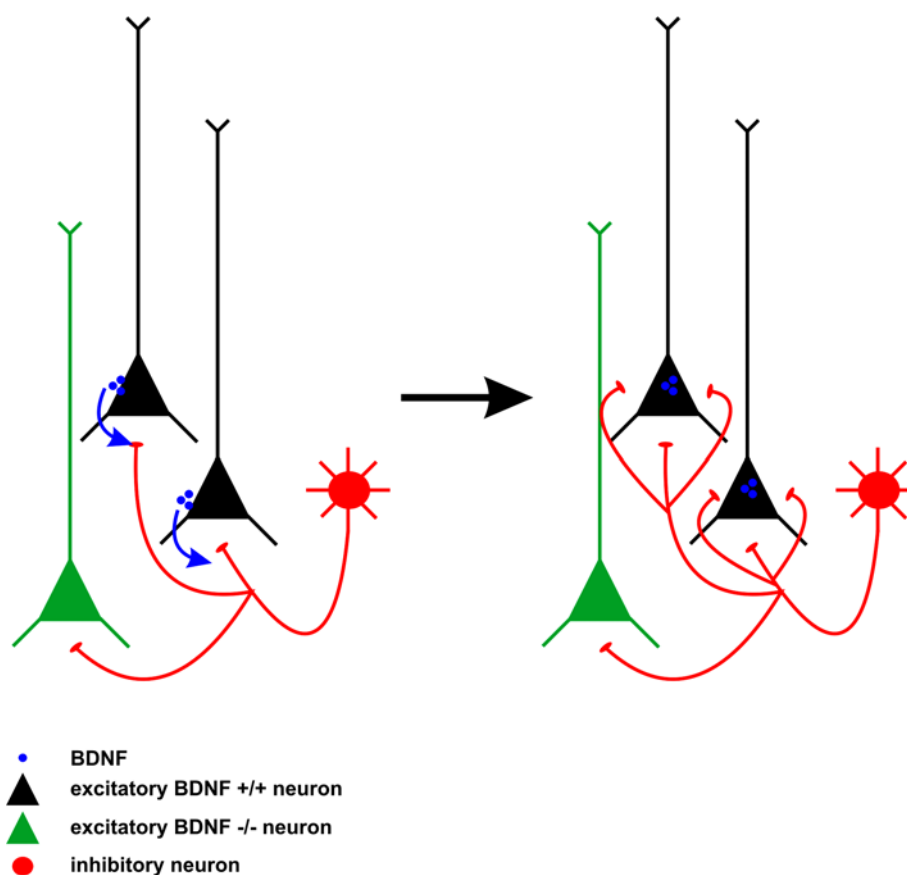


Fig. 4.2: Retrograde action of BDNF onto inhibitory GABAergic synapses.

Schematically shown is the retrograde action of BDNF onto GABAergic synapses attached to excitatory neurons. During cortical development BDNF (*blue*) increases the amount of GABAergic contacts (*red*) on excitatory neurons (*black*), whereas the number of synapses remains constant in case of a transplanted BDNF-deficient (*green*) target neuron (modified after Kohara et al., 2007).

These results also support findings of previous studies in the primary visual cortex that during the critical period the activity-dependent development is triggered by the functional maturation of local inhibitory connections and driven by a specific, late-developing subset of interneurons (Hensch et al., 1998; Hensch, 2005). Moreover, it has been proposed that BDNF promotes the maturation of cortical inhibition during the critical period (Berardi et al., 1994; Bonhoeffer, 1996; Cellerino and Maffei, 1996; Domenici et al., 1994; Galuske et al., 1996; Katz and Shatz, 1996; Maffei et al., 1992; Pizzorusso and Maffei, 1996; Thoenen, 1995), because an accelerated rise of BDNF in transgenic mice led to an accelerated inhibition and maturation of GABAergic innervation (Huang et al., 1999). Also an overexpression of BDNF accelerated the time course of the critical period for monocular deprivation, and exogenous administration of BDNF altered the outcome of monocular deprivation (Bartoletti et al.,

2002). Furthermore, in the absence of visual experience (dark rearing), BDNF overexpression was sufficient for the development of aspects of visual cortex, suggesting that reduced BDNF expression contributes to retarded maturation of GABAergic inhibition and delayed development of visual cortex during visual deprivation (Gianfranceschi et al., 2003). Therefore, the development of inhibition is an important factor of the time course of visual cortical plasticity and BDNF strongly affects interneuron development and the onset and closure of the critical period for ocular dominance plasticity (Engelhardt et al., 2007). A highly local action of BDNF in strengthening and maintaining active synapses during ocular dominance column formation can be assumed (Lein and Shatz, 2000).

5. References

- Adam G, Matus A (1996) Role of actin in the organisation of brain postsynaptic densities. *Brain Res Mol Brain Res.* 43(1-2):246-50
- Agmon A, Connors BW (1991) Thalamocortical responses of mouse somatosensory (barrel) cortex in vitro. *Neuroscience.* 41(2-3):365-79
- Amitai Y (1994) Membrane potential oscillations underlying firing patterns in neocortical neurons. *Neuroscience.* 63(1):151-61
- Angulo MC, Staiger JF, Rossier J, Audinat E (1999) Developmental synaptic changes increase the range of integrative capabilities of an identified excitatory neocortical connection. *J Neurosci.* 19(5):1566-76
- Ascher P, Nowak L (1988) The role of divalent cations in the N-methyl-D-aspartate responses of mouse central neurones in culture. *J Physiol.* 399:247-66
- Atwood HL, Wojtowicz JM (1999) Silent synapses in neural plasticity: current evidence. *Learn Mem.* 6(6):542-71
- Auger C, Marty A (2000) Quantal currents at single-site central synapses. *J Physiol.* 526 Pt 1:3-11
- Augustine GJ, Charlton MP, Smith SJ (1987) Calcium action in synaptic transmitter release. *Annu Rev Neurosci.* 10:633-93
- Bajjalieh SM, Scheller RH (1995) The biochemistry of neurotransmitter secretion. *J Biol Chem.* 270(5):1971-4
- Balkowiec A, Katz DM (2000) Activity-dependent release of endogenous brain-derived neurotrophic factor from primary sensory neurons detected by ELISA in situ. *J Neurosci.* 20(19):7417-23
- Barbacid M (1994) The Trk family of neurotrophin receptors. *J Neurobiol.* 25(11):1386-403
- Barde YA, Edgar D, Thoenen H (1982) Purification of a new neurotrophic factor from mammalian brain. *EMBO J.* 1(5):549-53
- Barde YA (1990) The nerve growth factor family. *Prog Growth Factor Res.* 2(4):237-48
- Barria A, Muller D, Derkach V, Griffith LC, Soderling TR (1997) Regulatory phosphorylation of AMPA-type glutamate receptors by CaM-KII during long-term potentiation. *Science.* 276(5321):2042-5
- Barry PH (1994) JPCalc, a software package for calculating liquid junction potential corrections in patch-clamp, intracellular, epithelial and bilayer measurements and for correcting junction potential measurements. *J Neurosci Methods.* 51(1):107-16

- Bartoletti A, Cancedda L, Reid SW, Tessarollo L, Porciatti V, Pizzorusso T, Maffei L (2002) Heterozygous knock-out mice for brain-derived neurotrophic factor show a pathway-specific impairment of long-term potentiation but normal critical period for monocular deprivation. *J Neurosci.* 22(23):10072-7
- Bekkers JM, Stevens CF (1989) NMDA and non-NMDA receptors are co-localized at individual excitatory synapses in cultured rat hippocampus. *Nature.* 341(6239):230-3
- Benfenati F, Onofri F, Giovedì S (1999) Protein-protein interactions and protein modules in the control of neurotransmitter release. *Philos Trans R Soc Lond B Biol Sci.* 354(1381):243-57
- Bennett MV, Zukin RS (2004) Electrical coupling and neuronal synchronization in the Mammalian brain. *Neuron.* 41(4):495-511
- Benninger F, Beck H, Wernig M, Tucker KL, Brüstle O, Scheffler B (2003) Functional integration of embryonic stem cell-derived neurons in hippocampal slice cultures. *J Neurosci.* 23(18):7075-83
- Berardi N, Cellerino A, Domenici L, Fagiolini M, Pizzorusso T, Cattaneo A, Maffei L (1994) Monoclonal antibodies to nerve growth factor affect the postnatal development of the visual system. *Proc Natl Acad Sci U S A.* 91(2):684-8
- Berninger B, Poo M (1999) Exciting neurotrophins. *Nature.* 401(6756):862-3
- Berninger B, Schinder AF, Poo MM (1999) Synaptic reliability correlates with reduced susceptibility to synaptic potentiation by brain-derived neurotrophic factor. *Learn Mem.* 6(3):232-42
- Biou V, Bhattacharyya S, Malenka RC (2008) Endocytosis and recycling of AMPA receptors lacking GluR2/3. *Proc Natl Acad Sci U S A.* 105(3):1038-43
- Bliss TV (1990) Long-term potentiation. *Science.* 249(4972):973
- Bliss TV (1990) Maintenance is presynaptic. *Nature.* 346(6286):698-9
- Boller M, Schmidt M (2001) Postnatal maturation of GABA(A) and GABA(C) receptor function in the mammalian superior colliculus. *Eur. J. Neurosci.* 14(8):1185-93
- Bolshakov VY, Siegelbaum SA (1995) Regulation of hippocampal transmitter release during development and long-term potentiation. *Science.* 269(5231):1730-4
- Bonhoeffer T (1996) Neurotrophins and activity-dependent development of the neocortex. *Curr Opin Neurobiol.* 6(1):119-26
- Bormann J (1988) Electrophysiology of GABAA and GABAB receptor subtypes. *Trends Neurosci.* 11(3):112-6
- Bormann J (2000) The 'ABC' of GABA receptors. *Trends Pharmacol Sci.* 21(1):16-9

- Bortolotto ZA, Bashir ZI, Davies CH, Collingridge GL (1994) A molecular switch activated by metabotropic glutamate receptors regulates induction of long-term potentiation. *Nature*. 368(6473):740-3
- Bowery, NG (1989) GABAB receptors and their significance in mammalian pharmacology. *Trends Pharmacol. Sci.* 10, 401-407
- Bowery NG, Bettler B, Froestl W, Gallagher JP, Marshall F, Raiteri M, Bonner TI, Enna SJ (2002) International Union of Pharmacology. XXXIII. Mammalian gamma-aminobutyric acid(B) receptors: structure and function. *Pharmacol Rev.* 54(2):247-64
- Braga MF, Aroniadou-Anderjaska V, Xie J, Li H (2003) Bidirectional modulation of GABA release by presynaptic glutamate receptor 5 kainate receptors in the basolateral amygdala. *J Neurosci.* 23(2):442-52
- Braithwaite SP, Meyer G, Henley JM (2000) Interactions between AMPA receptors and intracellular proteins. *Neuropharmacology.* 39(6):919-30
- Bureau I, Shepherd GM, Svoboda K (2004) Precise development of functional and anatomical columns in the neocortex. *Neuron.* 42(5):789-801
- Bureau I, von Saint Paul F, Svoboda K (2006) Interdigitated paralemniscal and lemniscal pathways in the mouse barrel cortex. *PLoS Biol.* 4(12):e382
- Busetto G, Higley MJ, Sabatini BL (2008) Developmental presence and disappearance of postsynaptically silent synapses on dendritic spines of rat layer 2/3 pyramidal neurons. *J Physiol.* Epub
- Cabelli RJ, Shelton DL, Segal RA, Shatz CJ (1997) Blockade of endogenous ligands of trkB inhibits formation of ocular dominance columns. *Neuron.* 19(1):63-76
- Callaway EM, Katz LC (1993) Photostimulation using caged glutamate reveals functional circuitry in living brain slices. *Proc Natl Acad Sci U S A.* 90(16):7661-5
- Canossa M, Griesbeck O, Berninger B, Campana G, Kolbeck R, Thoenen H (1997) Neurotrophin release by neurotrophins: implications for activity-dependent neuronal plasticity. *Proc Natl Acad Sci U S A.* 94(24):13279-86
- Carmignoto G, Vicini S (1992) Activity-dependent decrease in NMDA receptor responses during development of the visual cortex. *Science.* 258(5084):1007-11
- Cellerino A, Maffei L, Domenici L (1996) The distribution of brain-derived neurotrophic factor and its receptor trkB in parvalbumin-containing neurons of the rat visual cortex. *Eur J Neurosci.* 8(6):1190-7
- Cellerino A, Maffei L (1996) The action of neurotrophins in the development and plasticity of the visual cortex. *Prog Neurobiol.* 49(1):53-71
- Chagnac-Amitai Y, Luhmann HJ, Prince DA (1990) Burst generating and regular spiking layer 5 pyramidal neurons of rat neocortex have different morphological features. *J Comp Neurol.* 296(4):598-613

- Cherubini E, Gaiarsa JL, Ben-Ari Y (1991) GABA: an excitatory transmitter in early postnatal life. *Trends Neurosci.* 14(12):515-9
- Cheyne JE, Montgomery JM (2007) Plasticity-dependent changes in metabotropic glutamate receptor expression at excitatory hippocampal synapses. *Mol Cell Neurosci.* Epub
- Christine CW, Choi DW (1990) Effect of zinc on NMDA receptor-mediated channel currents in cortical neurons. *J Neurosci.* 10(1):108-16
- Clements JD, Lester RA, Tong G, Jahr CE, Westbrook GL (1992) The time course of glutamate in the synaptic cleft. *Science.* 258(5087):1498-501
- Cohen-Cory S, Fraser SE (1995) Effects of brain-derived neurotrophic factor on optic axon branching and remodelling in vivo. *Nature.* 378(6553):192-6
- Collingridge GL, Lester RA (1989) Excitatory amino acid receptors in the vertebrate central nervous system. *Pharmacol Rev.* 41(2):143-210
- Connors BW, Gutnick MJ, Prince DA (1982) Electrophysiological properties of neocortical neurons in vitro. *J Neurophysiol.* 48(6):1302-20
- Connors BW, Gutnick MJ (1990) Intrinsic firing patterns of diverse neocortical neurons. *Trends Neurosci.* 13(3):99-104
- Conti F, Weinberg RJ (1999) Shaping excitation at glutamatergic synapses. *Trends Neurosci.* 22(10):451-8
- Crair MC, Malenka RC (1995) A critical period for long-term potentiation at thalamocortical synapses. *Nature.* 375(6529):325-8
- Dakoji S, Tomita S, Karimzadegan S, Nicoll RA, Brecht DS (2003) Interaction of transmembrane AMPA receptor regulatory proteins with multiple membrane associated guanylate kinases. *Neuropharmacology.* 45(6):849-56
- Dalva MB, Katz LC (1994) Rearrangements of synaptic connections in visual cortex revealed by laser photostimulation. *Science.* 265(5169):255-8
- Debanne D, Russier M (2003) Axonal propagation: does the spike stop here? *J Physiol.* 548(Pt 3):663
- Demarque M, Villeneuve N, Manent JB, Becq H, Represa A, Ben-Ari Y, Aniksztejn L (2004) Glutamate transporters prevent the generation of seizures in the developing rat neocortex. *J Neurosci.* 24(13):3289-94
- Domenici L, Cellerino A, Berardi N, Cattaneo A, Maffei L (1994) Antibodies to nerve growth factor (NGF) prolong the sensitive period for monocular deprivation in the rat. *Neuroreport.* 5(16):2041-4

- Dong H, O'Brien RJ, Fung ET, Lanahan AA, Worley PF, Huganir RL (1997) GRIP: a synaptic PDZ domain-containing protein that interacts with AMPA receptors. *Nature*. 386(6622):279-84
- Dragunow M, Beilharz E, Mason B, Lawlor P, Abraham W, Gluckman P (1993) Brain-derived neurotrophic factor expression after long-term potentiation. *Neurosci Lett*. 160(2):232-6
- Durand GM, Kovalchuk Y, Konnerth A (1996) Long-term potentiation and functional synapse induction in developing hippocampus. *Nature*. 381(6577):71-5
- Edmonds B, Gibb AJ, Colquhoun D (1995) Mechanisms of activation of glutamate receptors and the time course of excitatory synaptic currents. *Annu Rev Physiol*. 57:495-519
- Elgersma Y, Silva AJ (1999) Molecular mechanisms of synaptic plasticity and memory. *Curr Opin Neurobiol*. 9(2):209-13
- El-Husseini AE, Schnell E, Chetkovich DM, Nicoll RA, Brecht DS (2000) PSD-95 involvement in maturation of excitatory synapses. *Science*. 290(5495):1364-8
- Elias GM, Funke L, Stein V, Grant SG, Brecht DS, Nicoll RA (2006) Synapse-specific and developmentally regulated targeting of AMPA receptors by a family of MAGUK scaffolding proteins. *Neuron*. 52(2):307-20
- Engelhardt M, Di Cristo G, Berardi N, Maffei L, Wahle P (2007) Differential effects of NT-4, NGF and BDNF on development of neurochemical architecture and cell size regulation in rat visual cortex during the critical period. *Eur J Neurosci*. 25(2):529-40
- Ernfors P, Bengzon J, Kokaia Z, Persson H, Lindvall O (1991) Increased levels of messenger RNAs for neurotrophic factors in the brain during kindling epileptogenesis. *Neuron*. 7(1):165-76.
- Erreger K, Geballe MT, Kristensen A, Chen PE, Hansen KB, Lee CJ, Yuan H, Le P, Lyuboslavsky PN, Micale N, Jørgensen L, Clausen RP, Wyllie DJ, Snyder JP, Traynelis SF (2007) Subunit-specific agonist activity at NR2A-, NR2B-, NR2C-, and NR2D-containing N-methyl-D-aspartate glutamate receptors. *Mol Pharmacol*. 72(4):907-20
- Essrich, C., Lorez, M., Benson, J. A., Fritschy, J. M., Luscher, B (1998) Postsynaptic clustering of major GABAA receptor subtypes requires the gamma 2 subunit and gephyrin, *Nat. Neurosci*. 1,563-571
- Faber DS, Lin JW, Korn H (1991) Silent synaptic connections and their modifiability. *Ann N Y Acad Sci*. 627:151-64
- Fagg GE, Foster AC (1983) Amino acid neurotransmitters and their pathways in the mammalian central nervous system. *Neuroscience*. 9(4):701-19
- Feigenspan, A, and Bormann, J (1994) Differential pharmacology of GABAA and GABAC receptors on rat bipolar cells. *Eur.J.Pharmacol./Mol.Pharmacol*. 288: 97-104

- Feldman DE, Knudsen EI (1998) Experience-dependent plasticity and the maturation of glutamatergic synapses. *Neuron*. 20(6):1067-71
- Feldman DE, Nicoll RA, Malenka RC (1999) Synaptic plasticity at thalamocortical synapses in developing rat somatosensory cortex: LTP, LTD, and silent synapses. *J Neurobiol*. 41(1):92-101
- Feldman DE, Nicoll RA, Malenka RC, Isaac JT (1998) Long-term depression at thalamocortical synapses in developing rat somatosensory cortex. *Neuron*. 21(2):347-57
- Fillenz M (1995) Physiological release of excitatory amino acids. *Behav Brain Res*. 71(1-2):51-67
- Fischer G, Mutel V, Trube G, Malherbe P, Kew JN, Mohacsi E, Heitz MP, Kemp JA (1997) Ro 25-6981, a highly potent and selective blocker of N-methyl-D-aspartate receptors containing the NR2B subunit. Characterization in vitro. *J Pharmacol Exp Ther*. 283(3):1285-92
- Fleiderman IA, Binshtok AM, Gutnick MJ (1998) Functionally distinct NMDA receptors mediate horizontal connectivity within layer 4 of mouse barrel cortex. *Neuron*. 21(5):1055-65
- Flint AC, Maisch US, Weishaupt JH, Kriegstein AR, Monyer H (1997) NR2A subunit expression shortens NMDA receptor synaptic currents in developing neocortex. *J Neurosci*. 17(7):2469-76
- Forsythe ID, Westbrook GL (1988) Slow excitatory postsynaptic currents mediated by N-methyl-D-aspartate receptors on cultured mouse central neurones. *J Physiol*. 396:515-33
- Fox K, Daw N, Sato H, Czepita D (1992) The effect of visual experience on development of NMDA receptor synaptic transmission in kitten visual cortex. *J Neurosci*. 12(7):2672-84
- Friedman WJ, Black IB, Kaplan DR (1998) Distribution of the neurotrophins brain-derived neurotrophic factor, neurotrophin-3, and neurotrophin-4/5 in the postnatal rat brain: an immunocytochemical study. *Neuroscience*. 84(1):101-14
- Gaiarsa JL, Caillard O, Ben-Ari Y (2002) Long-term plasticity at GABAergic and glycinergic synapses: mechanisms and functional significance. *Trends Neurosci*. 25(11):564-70
- Galuske RA, Kim DS, Castren E, Thoenen H, Singer W (1996) Brain-derived neurotrophic factor reversed experience-dependent synaptic modifications in kitten visual cortex. *Eur J Neurosci*. 8(7):1554-9
- Gardoni F, Schrama LH, Kamal A, Gispen WH, Cattabeni F, Di Luca M (2001) Hippocampal synaptic plasticity involves competition between Ca²⁺/calmodulin-dependent protein kinase II and postsynaptic density 95 for binding to the NR2A subunit of the NMDA receptor. *J Neurosci*. 21(5):1501-9
- Gasic GP, Hollmann M (1992) Molecular neurobiology of glutamate receptors. *Annu Rev Physiol*. 54:507-36

- Gasparini S, Saviane C, Voronin LL, Cherubini E (2000) Silent synapses in the developing hippocampus: lack of functional AMPA receptors or low probability of glutamate release? *Proc Natl Acad Sci U S A.* 97(17):9741-6
- Gianfranceschi L, Siciliano R, Walls J, Morales B, Kirkwood A, Huang ZJ, Tonegawa S, Maffei L (2003) Visual cortex is rescued from the effects of dark rearing by overexpression of BDNF. *Proc Natl Acad Sci U S A.* 100(21):12486-91
- Giese KP, Fedorov NB, Filipkowski RK, Silva AJ (1998) Autophosphorylation at Thr286 of the alpha calcium-calmodulin kinase II in LTP and learning. *Science.* 279(5352):870-3
- Gomes AR, Ferreira JS, Paternain AV, Lerma J, Duarte CB, Carvalho AL (2007) Characterization of alternatively spliced isoforms of AMPA receptor subunits encoding truncated receptors. *Mol Cell Neurosci.* Epub
- Gorba T, Wahle P (1999) Expression of TrkB and TrkC but not BDNF mRNA in neurochemically identified interneurons in rat visual cortex in vivo and in organotypic cultures. *Eur J Neurosci.* 11(4):1179-90
- Gorba T, Klostermann O, Wahle P (1999) Development of neuronal activity and activity-dependent expression of brain-derived neurotrophic factor mRNA in organotypic cultures of rat visual cortex. *Cereb Cortex.* 9(8):864-77
- Gottmann K, Mehrle A, Gisselmann G, Hatt H (1997) Presynaptic control of subunit composition of NMDA receptors mediating synaptic plasticity. *J Neurosci.* 17(8):2766-74.
- Gray EG (1959) Axo-somatic and axo-dendritic synapses of the cerebral cortex: an electron microscope study. *J Anat.* 93:420-33
- Greger IH, Ziff EB, Penn AC (2007) Molecular determinants of AMPA receptor subunit assembly. *Trends Neurosci.* 30(8):407-16
- Hadjantonakis AK, Gertsenstein M, Ikawa M, Okabe M, Nagy A (1998) Generating green fluorescent mice by germline transmission of green fluorescent ES cells. *Mech Dev.* 76(1-2):79-90
- Hamill OP, Marty A, Neher E, Sakmann B, Sigworth FJ (1981) Improved patch-clamp techniques for high-resolution current recording from cells and cell-free membrane patches. *Pflugers Arch.* 391(2):85-100
- Hanley, J. G., Koulen, P., Bedford, F., Gordon-Weeks, P. R., Moss, S. J. (1999) The protein MAP-1B links GABA(C) receptors to the cytoskeleton at retinal synapses. *Nature.* 397, 66-69
- Hanse E, Gustafsson B (2001) Vesicle release probability and pre-primed pool at glutamatergic synapses in area CA1 of the rat neonatal hippocampus. *J Physiol.* 531(Pt 2):481-93
- Harney SC, Rowan M, Anwyl R (2006) Long-term depression of NMDA receptor-mediated synaptic transmission is dependent on activation of metabotropic glutamate receptors and is altered to long-term potentiation by low intracellular calcium buffering. *J Neurosci.* 26(4):1128-32

- Hartmann M, Heumann R, Lessmann V (2001) Synaptic secretion of BDNF after high-frequency stimulation of glutamatergic synapses. *EMBO J.* 20(21):5887-97
- Hefli BJ, Smith PH (2000) Anatomy, physiology, and synaptic responses of rat layer V auditory cortical cells and effects of intracellular GABA(A) blockade. *J Neurophysiol.* 83(5):2626-38
- Hensch TK, Fagiolini M, Mataga N, Stryker MP, Baekkeskov S, Kash SF (1998) Local GABA circuit control of experience-dependent plasticity in developing visual cortex. *Science.* 282(5393):1504-8
- Hensch TK (2005) Critical period plasticity in local cortical circuits. *Nat Rev Neurosci.* 6(11):877-88
- Hessler NA, Shirke AM, Malinow R (1993) The probability of transmitter release at a mammalian central synapse. *Nature.* 366(6455):569-72
- Hestrin S (1993) Different glutamate receptor channels mediate fast excitatory synaptic currents in inhibitory and excitatory cortical neurons. *Neuron.* 11(6):1083-91
- Hestrin S (1992) Activation and desensitization of glutamate-activated channels mediating fast excitatory synaptic currents in the visual cortex. *Neuron.* 9(5):991-9
- Hestrin S (1992) Developmental regulation of NMDA receptor-mediated synaptic currents at a central synapse. *Nature.* 357(6380):686-9
- Heumann R (1994) Neurotrophin signalling. *Curr Opin Neurobiol.* 4(5):668-79
- Hofer M, Pagliusi SR, Hohn A, Leibrock J, Barde YA (1990) Regional distribution of brain-derived neurotrophic factor mRNA in the adult mouse brain. *EMBO J.* 9(8):2459-64
- Hoffmann H, Gremme T, Hatt H, Gottmann K (2000) Synaptic activity-dependent developmental regulation of NMDA receptor subunit expression in cultured neocortical neurons. *J Neurochem.* 75(4):1590-9
- Hollmann M, Heinemann S (1994) Cloned glutamate receptors. *Annu Rev Neurosci.* 17:31-108
- Hormuzdi SG, Filippov MA, Mitropoulou G, Monyer H, Bruzzone R (2004) Electrical synapses: a dynamic signaling system that shapes the activity of neuronal networks. *Biochim Biophys Acta.* 1662(1-2):113-37
- Huang YY, Zakharenko SS, Schoch S, Kaeser PS, Janz R, Südhof TC, Siegelbaum SA, Kandel ER (2005) Genetic evidence for a protein-kinase-A-mediated presynaptic component in NMDA-receptor-dependent forms of long-term synaptic potentiation. *Proc Natl Acad Sci U S A.* 102(26):9365-70
- Huang ZJ, Kirkwood A, Pizzorusso T, Porciatti V, Morales B, Bear MF, Maffei L, Tonegawa S (1999) BDNF regulates the maturation of inhibition and the critical period of plasticity in mouse visual cortex. *Cell.* 98(6):739-55

- Hubel DH, Wiesel TN (1959) Receptive fields of single neurones in the cat's striate cortex. *J Physiol.* 148:574-91
- Huettner JE (2003) Kainate receptors and synaptic transmission. *Prog Neurobiol.* 70(5):387-407
- Isaac JT, Nicoll RA, Malenka RC (1995) Evidence for silent synapses: implications for the expression of LTP. *Neuron.* 15(2):427-34
- Isaac JT, Crair MC, Nicoll RA, Malenka RC (1997) Silent synapses during development of thalamocortical inputs. *Neuron.* 18(2):269-80
- Jentsch TJ, Stein V, Weinreich F, Zdebik AA (2002) Molecular structure and physiological function of chloride channels. *Physiol Rev.* 82(2):503-68
- Johnson JW, Ascher P (1987) Glycine potentiates the NMDA response in cultured mouse brain neurons. *Nature.* 325(6104):529-31
- Kafitz KW, Rose CR, Thoenen H, Konnerth A (1999) Neurotrophin-evoked rapid excitation through TrkB receptors. *Nature.* 401(6756):918-21
- Kageyama GH, Robertson RT (1993) Development of geniculocortical projections to visual cortex in rat: evidence early ingrowth and synaptogenesis. *J Comp Neurol.* 335(1):123-48
- Kaila, K. (1994) Ionic basis of GABAA receptor channel function in the nervous system. *Prog. Neurobiol.* 42: 489-537
- Kandel ER, Schwartz JH, Jessell TM (2002) Principles of neural science. *McGraw-Hill Professional*
- Kang H, Schuman EM (1995) Long-lasting neurotrophin-induced enhancement of synaptic transmission in the adult hippocampus. *Science.* 267(5204):1658-62
- Kaplan DR, Miller FD (2000) Neurotrophin signal transduction in the nervous system. *Curr Opin Neurobiol.* 10(3):381-91
- Katz LC, Shatz CJ (1996) Synaptic activity and the construction of cortical circuits. *Science.* 274(5290):1133-8
- Katz LC, Dalva MB (1994) Scanning laser photostimulation: a new approach for analyzing brain circuits. *J Neurosci Methods.* 54(2):205-18
- Kauer JA, Malenka RC, Nicoll RA (1988) A persistent postsynaptic modification mediates long-term potentiation in the hippocampus. *Neuron.* 1(10):911-7
- Kauer JA, Malenka RC, Nicoll RA (1988) NMDA application potentiates synaptic transmission in the hippocampus. *Nature.* 334(6179):250-2
- Kennedy MB (1997) The postsynaptic density at glutamatergic synapses. *Trends Neurosci.* 20(6):264-8

- Khazipov R, Ragozzino D, Bregestovski P (1995) Kinetics and Mg²⁺ block of N-methyl-D-aspartate receptor channels during postnatal development of hippocampal CA3 pyramidal neurons. *Neuroscience*. 69(4):1057-65
- Kidd FL, Isaac JT (1999) Developmental and activity-dependent regulation of kainate receptors at thalamocortical synapses. *Nature*. 400(6744):569-73
- Kleckner NW, Dingledine R (1988) Requirement for glycine in activation of NMDA-receptors expressed in *Xenopus* oocytes. *Science*. 241(4867):835-7
- Klostermann O, Wahle P (1999) Patterns of spontaneous activity and morphology of interneuron types in organotypic cortex and thalamus-cortex cultures. *Neuroscience*. 92(4):1243-59
- Kneussel M, Brandstatter JH, Laube B, Stahl S, Muller U, Betz H (1999) Loss of postsynaptic GABAA receptor clustering in gephyrin-deficient mice. *J. Neurosci.* 19, 9289-9297
- Kneussel M, Betz H (2000) Clustering of inhibitory neurotransmitter receptors at developing postsynaptic sites: the membrane activation model. *Trends Neurosci.* 23, 429-435
- Kohara K, Yasuda H, Huang Y, Adachi N, Sohya K, Tsumoto T (2007) A local reduction in cortical GABAergic synapses after a loss of endogenous brain-derived neurotrophic factor, as revealed by single-cell gene knock-out method. *J Neurosci.* 27(27):7234-44
- Kolarow R, Brigadski T, Lessmann V (2007) Postsynaptic secretion of BDNF and NT-3 from hippocampal neurons depends on calcium calmodulin kinase II signaling and proceeds via delayed fusion pore opening. *J Neurosci.* 27(39):10350-64
- Kornau HC, Schenker LT, Kennedy MB, Seeburg PH (1995) Domain interaction between NMDA receptor subunits and the postsynaptic density protein PSD-95. *Science*. 269(5231):1737-40
- Korte M, Carroll P, Wolf E, Brem G, Thoenen H, Bonhoeffer T (1995) Hippocampal long-term potentiation is impaired in mice lacking brain-derived neurotrophic factor. *Proc Natl Acad Sci U S A.* 92(19):8856-60
- Kötter R, Staiger JF, Zilles K, Luhmann HJ (1998) Analysing functional connectivity in brain slices by a combination of infrared video microscopy, flash photolysis of caged compounds and scanning methods. *Neuroscience*. 86(1):265-77
- Krnjević K (1974) Some neuroactive compounds in the substantia nigra. *Adv Neurol.* 5:145-52
- Kulla A, Manahan-Vaughan D (2008) Modulation by group 1 metabotropic glutamate receptors of depotentiation in the dentate gyrus of freely moving rats. *Hippocampus*. 18(1):48-54
- Kullmann DM (2001) Presynaptic kainate receptors in the hippocampus: slowly emerging from obscurity. *Neuron*. 32(4):561-4

- Kullmann DM, Lamsa KP (2008) Roles of distinct glutamate receptors in induction of anti-Hebbian long-term potentiation. *J Physiol.* Epub
- Kullmann DM, Siegelbaum SA (1995) The site of expression of NMDA receptor-dependent LTP: new fuel for an old fire. *Neuron.* 15(5):997-1002
- Larkman A, Mason A (1990) Correlations between morphology and electrophysiology of pyramidal neurons in slices of rat visual cortex. I. Establishment of cell classes. *J Neurosci.* 10(5):1407-14
- Lee HK, Barbarosie M, Kameyama K, Bear MF, Huganir RL (2000) Regulation of distinct AMPA receptor phosphorylation sites during bidirectional synaptic plasticity. *Nature.* 405(6789):955-9
- Legendre P, Westbrook GL (1990) The inhibition of single N-methyl-D-aspartate-activated channels by zinc ions on cultured rat neurons. *J Physiol.* 429:429-49
- Leibrock J, Lottspeich F, Hohn A, Hofer M, Hengerer B, Masiakowski P, Thoenen H, Barde YA (1989) Molecular cloning and expression of brain-derived neurotrophic factor. *Nature.* 341(6238):149-52
- Lein ES, Shatz CJ (2000) Rapid regulation of brain-derived neurotrophic factor mRNA within eye-specific circuits during ocular dominance column formation. *J Neurosci.* 20(4):1470-83
- Lessmann V, Gottmann K, Heumann R (1994) BDNF and NT-4/5 enhance glutamatergic synaptic transmission in cultured hippocampal neurones. *Neuroreport.* 6(1):21-5
- Lessmann V, Heumann R (1998) Modulation of unitary glutamatergic synapses by neurotrophin-4/5 or brain-derived neurotrophic factor in hippocampal microcultures: presynaptic enhancement depends on pre-established paired-pulse facilitation. *Neuroscience.* 86(2):399-413
- Lessmann V (1998) Neurotrophin-dependent modulation of glutamatergic synaptic transmission in the mammalian CNS. *Gen Pharmacol.* 31(5):667-74
- Lester RA, Jahr CE (1992) NMDA channel behavior depends on agonist affinity. *J Neurosci.* 12(2):635-43
- Lester RA, Clements JD, Westbrook GL, Jahr CE (1990) Channel kinetics determine the time course of NMDA receptor-mediated synaptic currents. *Nature.* 346(6284):565-7
- Lewin GR, Barde YA (1996) Physiology of the neurotrophins. *Annu Rev Neurosci.* 19:289-317
- Li P, Wilding TJ, Kim SJ, Calejesan AA, Huettner JE, Zhuo M (1999) Kainate-receptor-mediated sensory synaptic transmission in mammalian spinal cord. *Nature.* 397(6715):161-4
- Li Y, Jia YC, Cui K, Li N, Zheng ZY, Wang YZ, Yuan XB (2005) Essential role of TRPC channels in the guidance of nerve growth cones by brain-derived neurotrophic factor. *Nature.* 434(7035):894-8

- Liao D, Hessler NA, Malinow R (1995) Activation of postsynaptically silent synapses during pairing-induced LTP in CA1 region of hippocampal slice. *Nature*. 375(6530):400-4
- Lindsay RM, Thoenen H, Barde YA (1985) Placode and neural crest-derived sensory neurons are responsive at early developmental stages to brain-derived neurotrophic factor. *Dev Biol*. 112(2):319-28
- Lisman JE, Fallon JR (1999) What maintains memories? *Science*. 283(5400):339-40
- Lodge D, Johnson KM (1990) Noncompetitive excitatory amino acid receptor antagonists. *Trends Pharmacol Sci*. 11(2):81-6
- Lu B, Gottschalk W (2000) Modulation of hippocampal synaptic transmission and plasticity by neurotrophins. *Prog Brain Res*. 128:231-41
- MacDermott AB, Mayer ML, Westbrook GL, Smith SJ, Barker JL (1986) NMDA-receptor activation increases cytoplasmic calcium concentration in cultured spinal cord neurones. *Nature*. 321(6069):519-22
- Maffei L, Berardi N, Domenici L, Parisi V, Pizzorusso T (1992) Nerve growth factor (NGF) prevents the shift in ocular dominance distribution of visual cortical neurons in monocularly deprived rats. *J Neurosci*. 12(12):4651-62
- Maggi L, Le Magueresse C, Changeux JP, Cherubini E (2003) Nicotine activates immature "silent" connections in the developing hippocampus. *Proc Natl Acad Sci U S A*. 100(4):2059-64
- Magleby KL, Zengel JE (1982) A quantitative description of stimulation-induced changes in transmitter release at the frog neuromuscular junction. *J Gen Physiol*. 80(4):613-38
- Mainen ZF, Sejnowski TJ (1996) Influence of dendritic structure on firing pattern in model neocortical neurons. *Nature*. 382(6589):363-6
- Maisonpierre PC, Belluscio L, Friedman B, Alderson RF, Wiegand SJ, Furth ME, Lindsay RM, Yancopoulos GD (1990) NT-3, BDNF, and NGF in the developing rat nervous system: parallel as well as reciprocal patterns of expression. *Neuron*. 5(4):501-9
- Malenka RC, Nicoll RA (1993) NMDA-receptor-dependent synaptic plasticity: multiple forms and mechanisms. *Trends Neurosci*. 16(12):521-7
- Malenka RC, Nicoll RA (1997) Silent synapses speak up. *Neuron*. 19(3):473-6
- Malenka RC, Nicoll RA (1999) Long-term potentiation--a decade of progress? *Science*. 285(5435):1870-4
- Malinow R (1994) LTP: desperately seeking resolution. *Science*. 266(5188):1195-6
- Malinow R, Tsien RW (1990) Presynaptic enhancement shown by whole-cell recordings of long-term potentiation in hippocampal slices. *Nature*. 346(6280):177-80

- Manabe T, Wyllie DJ, Perkel DJ, Nicoll RA (1993) Modulation of synaptic transmission and long-term potentiation: effects on paired pulse facilitation and EPSC variance in the CA1 region of the hippocampus. *J Neurophysiol.* 70(4):1451-9
- Manabe T, Nicoll RA (1994) Long-term potentiation: evidence against an increase in transmitter release probability in the CA1 region of the hippocampus. *Science.* 265(5180):1888-92
- Manahan-Vaughan D, Braunewell KH (2005) The metabotropic glutamate receptor, mGluR5, is a key determinant of good and bad spatial learning performance and hippocampal synaptic plasticity. *Cereb Cortex.* 15(11):1703-13
- Mandolesi G, Menna E, Harauzov A, von Bartheld CS, Caleo M, Maffei L (2005) A role for retinal brain-derived neurotrophic factor in ocular dominance plasticity. *Curr Biol.* 15(23):2119-24
- Marshall FH, Jones KA, Kaupmann K, Bettler B (1999) GABAB receptors - the first 7TM Heterodimers. *Trends Pharmacol. Sci.* 20, 396-399
- Marty S, Berzaghi MdaP, Berninger B (1997) Neurotrophins and activity-dependent plasticity of cortical interneurons. *Trends Neurosci.* 20(5):198-202
- Marty S, Berninger B, Carroll P, Thoenen H (1996) GABAergic stimulation regulates the phenotype of hippocampal interneurons through the regulation of brain-derived neurotrophic factor. *Neuron.* 16(3):565-70
- Mason A, Larkman A (1990) Correlations between morphology and electrophysiology of pyramidal neurons in slices of rat visual cortex. II. Electrophysiology. *J Neurosci.* 10(5):1415-28
- Mathew SS, Pozzo-Miller L, Hablitz JJ (2008) Kainate modulates presynaptic GABA release from two vesicle pools. *J Neurosci.* 28(3):725-31
- Mayer ML, Westbrook GL, Guthrie PB (1984) Voltage-dependent block by Mg²⁺ of NMDA responses in spinal cord neurones. *Nature.* 309(5965):261-3
- Mayer ML, Westbrook GL (1987) The physiology of excitatory amino acids in the vertebrate central nervous system. *Prog Neurobiol.* 28(3):197-276
- McAllister AK, Katz LC, Lo DC (1996) Neurotrophin regulation of cortical dendritic growth requires activity. *Neuron.* 17(6):1057-64
- McAllister AK, Lo DC, Katz LC (1995) Neurotrophins regulate dendritic growth in developing visual cortex. *Neuron.* 15(4):791-803
- McAllister AK (1999) Subplate neurons: a missing link among neurotrophins, activity, and ocular dominance plasticity? *Proc Natl Acad Sci U S A.* 96(24):13600-2
- McAllister AK, Katz LC, Lo DC (1999) Neurotrophins and synaptic plasticity. *Annu Rev Neurosci.* 22:295-318

- McBain C, Dingledine R (1992) Dual-component miniature excitatory synaptic currents in rat hippocampal CA3 pyramidal neurons. *J Neurophysiol.* 68(1):16-27
- McBain CJ, Mayer ML (1994) N-methyl-D-aspartic acid receptor structure and function. *Physiol Rev.* 74(3):723-60
- McCormick DA, Prince DA (1987) Post-natal development of electrophysiological properties of rat cerebral cortical pyramidal neurones. *J Physiol.* 393:743-62
- McDonald RL, Olsen RW (1994) GABAA receptor channels. *Annu. Rev. Neurosci.* 17,569-602 8
- McGurk JF, Bennett MV, Zukin RS (1990) Polyamines potentiate responses of N-methyl-D-aspartate receptors expressed in xenopus oocytes. *Proc Natl Acad Sci U S A.* 87(24):9971-4
- Ming GL, Wong ST, Henley J, Yuan XB, Song HJ, Spitzer NC, Poo MM (2002) Adaptation in the chemotactic guidance of nerve growth cones. *Nature.* 417(6887):411-8
- Molnár P, Nadler JV (1999) Mossy fiber-granule cell synapses in the normal and epileptic rat dentate gyrus studied with minimal laser photostimulation. *J Neurophysiol.* 82(4):1883-94
- Monyer H, Burnashev N, Laurie DJ, Sakmann B, Seeburg PH (1994) Developmental and regional expression in the rat brain and functional properties of four NMDA receptors. *Neuron.* 12(3):529-40
- Mori H, Mishina M (1995) Structure and function of the NMDA receptor channel. *Neuropharmacology.* 34(10):1219-37
- Morishita W, Malenka RC (2008) Mechanisms Underlying Dedepression of Synaptic NMDA Receptors in the Hippocampus. *J Neurophysiol.* 99(1):254-63
- Mountcastle VB (1997) The columnar organization of the neocortex. *Brain.* 120 (Pt 4):701-22
- Mozhayeva MG, Sara Y, Liu X, Kavalali ET (2002) Development of vesicle pools during maturation of hippocampal synapses. *J Neurosci.* 22(3):654-65
- Nakanishi S (1994) The molecular diversity of glutamate receptors. *Prog Clin Biol Res.* 390:85-98
- Nakanishi S, Masu M, Bessho Y, Nakajima Y, Hayashi Y, Shigemoto R (1994) Molecular diversity of glutamate receptors and their physiological functions. *EXS.* 71:71-80
- Nakayama K, Kiyosue K, Taguchi T (2005) Diminished neuronal activity increases neuron-neuron connectivity underlying silent synapse formation and the rapid conversion of silent to functional synapses. *J Neurosci.* 25(16):4040-51
- Nicoll RA, Mellor J, Frerking M, Schmitz D (2000) Kainate receptors and synaptic plasticity. *Nature.* 406(6799):957

- Ninan I, Liu S, Rabinowitz D, Arancio O (2006) Early presynaptic changes during plasticity in cultured hippocampal neurons. *EMBO J.* 25(18):4361-71
- Nowak L, Bregestovski P, Ascher P, Herbet A, Prochiantz A (1984) Magnesium gates glutamate-activated channels in mouse central neurones. *Nature.* 307(5950):462-5
- Otmakhov N, Griffith LC, Lisman JE (1997) Postsynaptic inhibitors of calcium/calmodulin-dependent protein kinase type II block induction but not maintenance of pairing-induced long-term potentiation. *J Neurosci.* 17(14):5357-65
- Palmer MJ, Isaac JT, Collingridge GL (2004) Multiple, developmentally regulated expression mechanisms of long-term potentiation at CA1 synapses. *J Neurosci.* 24(21):4903-11
- Pandis C, Sotiriou E, Kouvaras E, Asproдини E, Papatheodoropoulos C, Angelatou F (2006) Differential expression of NMDA and AMPA receptor subunits in rat dorsal and ventral hippocampus. *Neuroscience.* 140(1):163-75
- Paoletti P, Ascher P, Neyton J (1997) High-affinity zinc inhibition of NMDA NR1-NR2A receptors. *J Neurosci.* 17(15):5711-25
- Pasternack M, Boller M, Pau B, Schmidt M (1999) GABA(A) and GABA(C) receptors have contrasting effects on excitability in superior colliculus. *J. Neurophysiol.* 82(4):2020-3
- Patapoutian A, Reichardt LF (2001) Trk receptors: mediators of neurotrophin action. *Curr Opin Neurobiol.* 11(3):272-80
- Patneau DK, Mayer ML (1990) Structure-activity relationships for amino acid transmitter candidates acting at N-methyl-D-aspartate and quisqualate receptors. *J Neurosci.* 10(7):2385-99
- Patterson SL, Grover LM, Schwartzkroin PA, Bothwell M (1992) Neurotrophin expression in rat hippocampal slices: a stimulus paradigm inducing LTP in CA1 evokes increases in BDNF and NT-3 mRNAs. *Neuron.* 9(6):1081-8
- Pérez-Otaño I, Ehlers MD (2005) Homeostatic plasticity and NMDA receptor trafficking. *Trends Neurosci.* 28(5):229-38
- Pérez-Otaño I, Ehlers MD (2004) Learning from NMDA receptor trafficking: clues to the development and maturation of glutamatergic synapses. *Neurosignals.* 13(4):175-89
- Peters A, Kara DA (1985) The neuronal composition of area 17 of rat visual cortex. II. The nonpyramidal cells. *J Comp Neurol.* 234(2):242-63
- Peters A, Kara DA (1985) The neuronal composition of area 17 of rat visual cortex. I. The pyramidal cells. *J Comp Neurol.* 234(2):218-41
- Pin JP, Duvoisin R (1995) The metabotropic glutamate receptors: structure and functions. *Neuropharmacology.* 34(1):1-26

- Pinheiro PS, Rodrigues RJ, Rebola N, Xapelli S, Oliveira CR, Malva JO (2005) Presynaptic kainate receptors are localized close to release sites in rat hippocampal synapses. *Neurochem Int.* 47(5):309-16
- Pizzorusso T, Maffei L (1996) Plasticity in the developing visual system. *Curr Opin Neurol.* 9(2):122-5
- Poo MM (2001) Neurotrophins as synaptic modulators. *Nat Rev Neurosci.* 2(1):24-32
- Prakash N, Cohen-Cory S, Frostig RD (1996) RAPID and opposite effects of BDNF and NGF on the functional organization of the adult cortex in vivo. *Nature.* 381(6584):702-6
- Premkumar LS, Auerbach A (1997) Stoichiometry of recombinant N-methyl-D-aspartate receptor channels inferred from single-channel current patterns. *J Gen Physiol.* 110(5):485-502
- Rakic P (1972) Mode of cell migration to the superficial layers of fetal monkey neocortex. *J Comp Neurol.* 145(1):61-83
- Ramming, M., Kins, S., Werner, N., Hermann, A., Betz, H., Kirsch, J (2000) Diversity and phylogeny of gephyrin: tissue-specific splice variants, gene structure, and sequence similarities to molybdenum cofactor-synthesizing and cytoskeleton-associated proteins. *Proc. Natl. Acad. Sci. U S A.* 10266-10271
- Redman S (1990) Quantal analysis of synaptic potentials in neurons of the central nervous system. *Physiol Rev.* 70(1):165-98
- Rivera C, Voipio J, Payne JA, Ruusuvuori E, Lahtinen H, Lamsa K, Pirvola U, Saarma M, Kaila K (1999) The K⁺/Cl⁻ co-transporter KCC2 renders GABA hyperpolarizing during neuronal maturation. *Nature.* 397(6716):251-5
- Rocamora N, Welker E, Pascual M, Soriano E (1996) Upregulation of BDNF mRNA expression in the barrel cortex of adult mice after sensory stimulation. *J Neurosci.* 16(14):4411-9
- Rodríguez-Moreno A (2006) [The role of kainate receptors in the regulation of excitatory synaptic transmission in the hippocampus] *Rev Neurol.* 42(5):282-7
- Rosenmund C, Stern-Bach Y, Stevens CF (1998) The tetrameric structure of a glutamate receptor channel. *Science.* 280(5369):1596-9
- Rumpel S, Hatt H, Gottmann K (1998) Silent synapses in the developing rat visual cortex: evidence for postsynaptic expression of synaptic plasticity. *J Neurosci.* 18(21):8863-74
- Rüschenschmidt C, Koch PG, Brüstle O, Beck H (2005) Functional properties of ES cell-derived neurons engrafted into the hippocampus of adult normal and chronically epileptic rats. *Epilepsia.* 46 Suppl 5:174-83
- Sansom MS, Usherwood PN (1990) Single-channel studies of glutamate receptors. *Int Rev Neurobiol.* 32:51-106

- Scheffler B, Edenhofer F, Brüstle O (2006) Merging fields: stem cells in neurogenesis, transplantation, and disease modeling. *Brain Pathol.* 16(2):155-68
- Schikorski T, Stevens CF (1997) Quantitative ultrastructural analysis of hippocampal excitatory synapses. *J Neurosci.* 17(15):5858-67
- Schinder AF, Poo M (2000) The neurotrophin hypothesis for synaptic plasticity. *Trends Neurosci.* 23(12):639-45
- Schmidt M, Boller M, Ozen G, Hall WC (2001) Disinhibition in rat superior colliculus mediated by GABA_A receptors. *J. Neurosci.* 21(2):691-9
- Schmitz D, Frerking M, Nicoll RA (2000) Synaptic activation of presynaptic kainate receptors on hippocampal mossy fiber synapses. *Neuron.* 27(2):327-38
- Schneggenburger R, Neher E (2000) Intracellular calcium dependence of transmitter release rates at a fast central synapse. *Nature.* 406(6798):889-93
- Schnell E, Sizemore M, Karimzadegan S, Chen L, Brecht DS, Nicoll RA (2002) Direct interactions between PSD-95 and stargazin control synaptic AMPA receptor number. *Proc Natl Acad Sci U S A.* 99(21):13902-7
- Schubert D, Staiger JF, Cho N, Kötter R, Zilles K, Luhmann HJ (2001) Layer-specific intracolumnar and transcolumar functional connectivity of layer V pyramidal cells in rat barrel cortex. *J Neurosci.* 21(10):3580-92
- Schubert D, Kötter R, Zilles K, Luhmann HJ, Staiger JF (2003) Cell type-specific circuits of cortical layer IV spiny neurons. *J Neurosci.* 23(7):2961-70
- Schuman EM (1999) Neurotrophin regulation of synaptic transmission. *Curr Opin Neurobiol.* 9(1):105-9
- Sedman GL, Jeffrey PL, Austin L, Rostas JA (1986) The metabolic turnover of the major proteins of the postsynaptic density. *Brain Res.* 387(3):221-30
- Sheng M, Pak DT (2000) Ligand-gated ion channel interactions with cytoskeletal and signaling proteins. *Annu Rev Physiol.* 62:755-78
- Sheng M, Wyszynski M (1997) Ion channel targeting in neurons. *Bioessays.* 19(10):847-53
- Shepherd GM (2005) Perception without a thalamus how does olfaction do it? *Neuron.* 46(2):166-8
- Shepherd GM, Svoboda K (2005) Laminar and columnar organization of ascending excitatory projections to layer 2/3 pyramidal neurons in rat barrel cortex. *J Neurosci.* 25(24):5670-9
- Shi SH, Hayashi Y, Petralia RS, Zaman SH, Wenthold RJ, Svoboda K, Malinow R (1999) Rapid spine delivery and redistribution of AMPA receptors after synaptic NMDA receptor activation. *Science.* 284(5421):1811-6

- Sivilotti L, Nistri A (1991) GABA receptor mechanisms in the central nervous system. *Prog Neurobiol.* 36(1):35-92
- Skibinska-Kijek A, Radwanska A, Kossut M (2007) Alpha calcium/calmodulin dependent protein kinase II in learning-dependent plasticity of mouse somatosensory cortex. *Neuroscience.* Epub
- Snider WD, Lichtman JW (1996) Are neurotrophins synaptotrophins? *Mol Cell Neurosci.* 7(6):433-42
- Sokolov MV, Rossokhin AV, Astrelin AV, Frey JU, Voronin LL (2002) Quantal analysis suggests strong involvement of presynaptic mechanisms during the initial 3 h maintenance of long-term potentiation in rat hippocampal CA1 area in vitro. *Brain Res.* 957(1):61-75
- Song I, Huganir RL (2002) Regulation of AMPA receptors during synaptic plasticity. *Trends Neurosci.* 25(11):578-88
- Stevens CF, Wang Y (1994) Changes in reliability of synaptic function as a mechanism for plasticity. *Nature.* 371(6499):704-7
- Stoppini L, Buchs PA, Muller D (1991) A simple method for organotypic cultures of nervous tissue. *J Neurosci Methods.* 37(2):173-82
- Supèr H, Uylings HB (2001) The early differentiation of the neocortex: a hypothesis on neocortical evolution. *Cereb Cortex.* 11(12):1101-9
- Sur M, Cowey A (1995) Cerebral cortex: function and development. *Neuron.* 15(3):497-505
- Takahashi T, Goto T, Miyama S, Nowakowski RS, Caviness VS Jr (1999) Sequence of neuron origin and neocortical laminar fate: relation to cell cycle of origin in the developing murine cerebral wall. *J Neurosci.* 19(23):10357-71
- Tanabe Y, Masu M, Ishii T, Shigemoto R, Nakanishi S (1992) A family of metabotropic glutamate receptors. *Neuron.* 8(1):169-79
- Tanaka K (2003) Columns for complex visual object features in the inferotemporal cortex: clustering of cells with similar but slightly different stimulus selectivities. *Cereb Cortex.* 13(1):90-9
- Thoenen H (1995) Neurotrophins and neuronal plasticity. *Science.* 270(5236):593-8
- Vallano ML, Lambolez B, Audinat E, Rossier J (1996) Neuronal activity differentially regulates NMDA receptor subunit expression in cerebellar granule cells. *J Neurosci.* 16(2):631-9
- Volgushev M, Balaban P, Chistiakova M, Eysel UT (2000) Retrograde signalling with nitric oxide at neocortical synapses. *Eur J Neurosci.* 12(12):4255-67
- Voronin LL, Altinbaev RS, Bayazitov IT, Gasparini S, Kasyanov AV, Saviane C, Savtchenko L, Cherubini E (2004) Postsynaptic depolarisation enhances transmitter release and causes the appearance of responses at "silent" synapses in rat hippocampus. *Neuroscience.* 126(1):45-59

- Voronin LL, Cherubini E (2004) 'Deaf, mute and whispering' silent synapses: their role in synaptic plasticity. *J Physiol.* 557(Pt 1):3-12
- Walz C, Jüngling K, Lessmann V, Gottmann K (2006) Presynaptic plasticity in an immature neocortical network requires NMDA receptor activation and BDNF release. *J Neurophysiol.* 96(6):3512-6
- Wang H, Bedford FK, Brandon NJ, Moss SJ, Olsen RW (1999) GABAA-receptor-associated protein links GABAA receptors and the cytoskeleton. *Nature.* 7, 69-72
- Wang H, Olsen RW (2000) Binding of the GABAA-receptor-associated protein (GABARAP) to microtubules and microfilaments suggests involvement of the cytoskeleton in GABARAP GABAA-receptor interaction. *J. Neurochem.* 75, 644-55
- Wardle RA, Poo MM (2003) Brain-derived neurotrophic factor modulation of GABAergic synapses by postsynaptic regulation of chloride transport. *J Neurosci.* 23(25):8722-32
- Watkins JC, Krogsgaard-Larsen P, Honoré T (1990) Structure-activity relationships in the development of excitatory amino acid receptor agonists and competitive antagonists. *Trends Pharmacol Sci.* 11(1):25-33
- Welker C (1971) Microelectrode delineation of fine grain somatotopic organization of (Sml) cerebral neocortex in albino rat. *Brain Res.* 26(2):259-75
- Westbrook GL, Mayer ML (1987) Micromolar concentrations of Zn²⁺ antagonize NMDA and GABA responses of hippocampal neurons. *Nature.* 328(6131):640-3
- Wirth MJ, Brun A, Grabert J, Patz S, Wahle P (2003) Accelerated dendritic development of rat cortical pyramidal cells and interneurons after biolistic transfection with BDNF and NT4/5. *Development.* 130(23):5827-38
- Wisden W, Seeburg PH (1993) Mammalian ionotropic glutamate receptors. *Curr Opin Neurobiol.* 3(3):291-8
- Woolsey TA, Van der Loos H (1970) The structural organization of layer IV in the somatosensory region (SI) of mouse cerebral cortex. The description of a cortical field composed of discrete cytoarchitectonic units. *Brain Res.* 17(2):205-42
- Wu LJ, Xu H, Ren M, Zhuo M (2007) Genetic and pharmacological studies of GluR5 modulation of inhibitory synaptic transmission in the anterior cingulate cortex of adult mice. *Dev Neurobiol.* 67(2):146-57
- Yan Q, Rosenfeld RD, Matheson CR, Hawkins N, Lopez OT, Bennett L, Welcher AA (1997) Expression of brain-derived neurotrophic factor protein in the adult rat central nervous system. *Neuroscience.* 78(2):431-48
- Zafra F, Hengerer B, Leibrock J, Thoenen H, Lindholm D (1990) Activity dependent regulation of BDNF and NGF mRNAs in the rat hippocampus is mediated by non-NMDA glutamate receptors. *EMBO J.* 9(11):3545-50

Zhang X, Poo MM (2002) Localized synaptic potentiation by BDNF requires local protein synthesis in the developing axon. *Neuron*. 36(4):675-88

Zhong J, Carrozza DP, Williams K, Pritchett DB, Molinoff PB (1995) Expression of mRNAs encoding subunits of the NMDA receptor in developing rat brain. *J Neurochem*. 64(2):531-9

Zhou Y, Takahashi E, Li W, Halt A, Wiltgen B, Ehninger D, Li GD, Hell JW, Kennedy MB, Silva AJ (2007) Interactions between the NR2B receptor and CaMKII modulate synaptic plasticity and spatial learning. *J Neurosci*. 27(50):13843-53

Zhuo M (2000) Silent glutamatergic synapses and long-term facilitation in spinal dorsal horn neurons. *Prog Brain Res*. 129:101-13

Zucker RS (1989) Short-term synaptic plasticity. *Annu Rev Neurosci*. 12:13-31

6. Appendix

6.1 Abbreviations

ACSF	artificial cerebro-spinal fluid
AMPA	α -amino-3-hydroxy-5-methylisoxazol-4-propionacid
ARAC	cytosin- β -D-arabinofuranosid-hydrochloride
BDNF	<i>“brain-derived neurotrophic factor”</i>
Bicuculline	([R-(R*,S*)]-6-(5,6,7,8-Tetrahydro-6-methyl-1,3-dioxolo[4,5-g]isoquinolin-5-yl)furo[3,4-e]-1,3-benzodioxol-8(6H)-one)
BSA	<i>“bovine serum albumine”</i>
(X) $^{\circ}$ C	(X) degree Celsius
CaMKII	Calcium-Calmodulin-dependent proteinkinase II
CO ₂	Carbon dioxide
D-AP5	D(-)-2-amino-5-phosphonopentanacid
DIV	<i>„day in vitro“</i>
DNQX	6,7-dinitroquinoxalin-2,3-dion
E(x)	Day x of embryonic development
EDTA	Ethylenediamine-tetraacetic acid
EGFP	<i>„enhanced green fluorescent protein“</i>
EGTA	Ethylenbis(oxyethylen-nitrilo-)tetraaceticacid
EPSC	<i>“excitatory postsynaptic current”</i>
G-Protein	Guanosinnukeotid-dependent protein
GABA	γ -aminobutanoic acid
GABA _A	γ -aminobutanoic acid receptor type A
GABA _B	γ -aminobutanoic acid receptor type B
GABA _C	γ -aminobutanoic acid receptor type C
GFP	<i>„green fluorescent protein“</i>
h	hour
HEPES	N-2-hydroxyethylpiperazin-N`-2-ethansulfonacid
IPSC	<i>„inhibitory postsynaptic current“</i>
IR	infrared
KA	Kainat
KO	<i>„knockout“</i>
LTD	<i>„long-term depression“</i>
LTP	<i>„long-term potentiation“</i>
min	minutes
mPSC	<i>“miniature postsynaptic current”</i>
n	number of experiments
NGF	<i>„nerve growth factor“</i>
NMDA	N-Methyl-D-Aspartat
NR(X)	NMDA-receptor subunti (X)
NT-3, 4/5	Neurotrophin 3, 4/5
OPA	Operational amplifier
P(X)	postnatal day (X)
PBS	<i>„phosphate buffered saline“</i>
PCR	<i>“Polymerase Chain Reaction”</i>
PSC	<i>“postsynaptic current”</i>
PSD	<i>“postsynaptic density”</i>

PSP	„postsynaptic potential“
RP	“reserve pool”
rpm	“rounds per minute”
RRP	“readily releasable pool”
RT	room temperature
s	second
SD	“standard deviation”
SEM	“standard error of means”
SNAP	“synaptosome-associated protein”
SNARE	„soluble N-ethylmaleinide-sensitive factor [NSF] –attachment protein receptor“
t	time
TEA	Tetraethylammoniumchloride
TTX	Tetrodotoxin
U	„unit“
UV	Ultraviolet
WT	Wildtype
CNS	Central nervous system

6.2 List of figures and tables

Fig. 1.1:	Development of the cerebral cortex.....	4
Fig. 1.2:	Summary of some main mechanisms involved in immediate signaling at the synapse.....	6
Fig. 1.3:	Model of different intracellular interactions of the NMDA-receptor.....	9
Fig. 1.4:	Schematic illustration of the GABA _A -receptor and its binding sites.....	11
Fig. 1.5:	Models of silent synapses.....	14
Fig. 1.6:	Simplified model of the signal transduction of neurotrophins.....	16
Fig. 2.1:	Genotyping of genetically modified mice using PCR.....	24
Fig. 2.2:	Preparation and storage of in vitro slice preparations.....	25
Fig. 2.3:	Different configurations of the patch clamp technique.....	28
Fig. 2.4:	Simplified circuit diagram of patch clamp recording.....	30
Fig. 2.5:	Diagram of the experimental setup.....	31
Fig. 2.6:	Electrophysiological recordings of evoked PSCs in mouse somatosensory cortex.....	32
Fig. 2.7:	Photolysis of <i>caged</i> -glutamate.....	35
Fig. 2.8:	Diagram of the optic components.....	36
Fig. 2.9:	Differentiation between spontaneous activity and photolysis induced activity.....	38

Fig. 3.1:	Morphology and electrophysiology of immature layer Vb pyramidal neurons.....	43
Fig. 3.2:	Presynaptic properties of immature synapses on layer Vb pyramidal neurons.....	45
Fig. 3.3:	Quantification of evoked AMPA-receptor mediated EPSCs of immature layer Vb pyramidal neurons.....	46
Fig. 3.4:	Dependence of paired-pulse behavior on interstimulus interval.....	47
Fig. 3.5:	Classification of AMPA-receptor mediated EPSCs of immature layer Vb pyramidal neurons.....	48
Fig. 3.6:	Morphology and basic electrophysiology of mature layer Vb pyramidal neurons at P14.....	49
Fig. 3.7:	Presynaptic properties of glutamatergic synapses on layer Vb pyramidal neurons at P14.....	51
Fig. 3.8:	Comparison of presynaptic properties of immature and mature layer Vb pyramidal neurons.....	52
Fig. 3.9:	Properties of NMDA-receptor mediated PSCs at P7.....	53
Fig. 3.10:	Postsynaptically silent synapses on immature layer Vb pyramidal neurons.....	55
Fig. 3.11:	Pharmacological analysis of NMDA-receptors using a NR2B subunit selective blocker.....	57
Fig. 3.12:	Pharmacological analysis of NMDA-receptors using a NR2A subunit selective blocker.....	58
Fig. 3.13:	Changes of NMDA-receptor kinetics at different maturational stages.....	59
Fig. 3.14:	Progressive block of NMDA-receptor mediated PSCs with MK-801.....	60
Fig. 3.15:	Functional potentiation of presynaptically immature synapses.....	62
Fig. 3.16:	Potentiation of immature synapses depends on NMDA-receptor activation	63
Fig. 3.17:	Morphology of transplanted EGFP expressing neurons.....	65
Fig. 3.18:	Electrophysiological properties of transplanted EGFP expressing neurons.....	67
Fig. 3.19:	Properties of photolysis induced direct and synaptic activity.....	69
Fig. 3.20:	Topographic map of synaptic inputs onto an endogenous neuron in an organotypic slice culture.....	71

Fig. 3.21:	Topographic map of synaptic inputs onto a transplanted wildtype neuron in an organotypic slice culture.....	72
Fig. 3.22:	Topographic map of synaptic inputs onto a transplanted heterozygous BDNF knockout neuron in an organotypic slice culture.....	73
Fig. 3.23:	Topographic map of synaptic inputs onto a transplanted homozygous BDNF knockout neuron in an organotypic slice culture.....	74
Fig. 3.24:	Quantification of synaptic inputs onto endogenous and transplanted neurons in organotypic slice cultures.....	76
Fig. 3.25:	Quantification of synaptic inputs onto transplanted BDNF knockout neurons in organotypic slice cultures.....	78
Fig. 3.26:	Reduction in the frequency of GABA _A mPSCs in transplanted BDNF knockout neurons.....	80
Fig. 4.1:	Different maturational states of glutamatergic synapses on layer Vb pyramidal neurons.....	91
Fig. 4.2:	Retrograde action of BDNF onto inhibitory GABAergic synapses.....	99
Table 1:	Basic electrophysiological properties of immature layer Vb pyramidal neurons.....	43
Table 2:	Properties of AMPA-receptor mediated EPSCs at P7.....	45
Table 3:	Basic electrophysiological parameters of layer Vb pyramidal neurons at P14.....	50
Table 4:	Properties of AMPA-receptor mediated EPSCs at P14.....	51
Table 5:	Properties of NMDA-receptor mediated PSCs at P7.....	54
Table 6:	Basic electrophysiological properties of EGFP expressing neurons.....	66
Table 7:	Excitatory inputs onto endogenous and transplanted neurons.....	77
Table 8:	Inhibitory inputs onto endogenous and transplanted neurons.....	78

6.3 TIDA Macrofunktionen

REM DS Jan. 1999

REM modified Apr 2006

REM set no. of triggered sweeps

REM interval: trigger dependent

REM Stim. pulse on analog #1 (5 Volt)
REM Loop triggered externally, use c:\mpc\%11.nc etc.

CHANNELS 4 1;2;3;4
PPS 10000
OWR
rem 15x25 375; 15x30 450 ; 8x30 240 ; 15x35 525

For 525

Trigger X

rem First Flash cycle at $V_h = -60$ mV
ACQ

WAIT 10

rem Testpulse for Rm
DA 2 -0.1
DA 3 -0.1
wait 20
DA 2 0
DA 3 0
wait 60

rem Stim Flash
DI 2 1
wait 10
DI 2 0

WAIT 300
SACQ

rem Second Flash cycle at $V_h = -50$ mV
rem shift V_h
DA 1 0.2
DA 4 0.2
WAITSEC 3

ACQ

WAIT 10
rem Testpulse for Rm
DA 2 -0.1
DA 3 -0.1
WAIT 20
DA 2 0
DA 3 0
WAIT 60

```

    rem Stim Flash
DI 2 0
DI 2 1
wait 10
DI 2 0

WAIT 300

SACQ
DA 1 0
DA 4 0
rem waitsec 3

next
END

```

6.4 Rasterprogramm

```

(RASTER-PROGRAMM FUER TRIGSTIF.STM; ROLF KOETTER 6.9.96, Dirk Schubert
ab 99)
(ADAPTIERT FUER MULTIELEKTRODE 7.5.97,FUER INTRACELL 19.2.99)
(ADAPTIERT FUER FLASH-WIEDERHOLUNG 29.4.99)
(ADAPTIERT Y-VERSCHIEBUNG UND GESCHWINDIGKEIT SEPT 2000)
(ADAPTIERT BEI UNTERSCH HALTEPOTENTIALEN 10.05.06)
(LAEUFT IN X-RICHTUNG HIN UND HER: LINKS - RECHTS - USW.)
(VERSCHIEBT NACH JEDEM LAUF EINEN SCHRITT IN Y-RICHTUNG)
(BIS ALLE Y ABGEARBEITET SIND)
N10 G01 G31 G91 (SCHLEICHGANG, RELATIV)
N11 G31 I0J0 (GESCHWINDIGKEIT SCHLEICHGANG MIKROSKOP 0=MIN)
N20 M41 (HILFSEINGANG AUS)
N30 R0=1 (R0=STARTPUNKT)
(DIE FOLGENDEN PARAMETER SIND EINZUSTELLEN:)
N40 R1=10 (R1=ANZAHL DER PUNKTE IN X-RICHTUNG)
N41 R2=35 (R2=ANZAHL DER PUNKTE IN Y-RICHTUNG)
N42 R6=2 (R6=ANZAHL PUNKTE MIT X LINKS+AUF ELEK-ENDE)
N43 R7=1 (R7=ANZAHL DER FLASH-WIEDERHOLUNGEN AM ORT)
N44 G79 T(ANZAHL DER FELDER OBERHALB DER ZELLE?) R8 3
N45 R14=4 (WARTEZEIT FUER TIDA AUFZEICHNUNG)
N50 R3=0.05 (SCHRITTWEITE NACH X IN MM)
N51 R4=0.05 (SCHRITTW. IN Y NACH U IN MM, NEG. VALUES OK!)
N52 R5=20 (NOMINELLE WARTEZEIT ZWISCHEN FLASHS)
(WARTEZEIT STIMMT ZWISCHEN WIEDERHOLUNGEN, SONST ZEIT+MOVE)
N53 R6=R6*R3
N54 R8=R8*R4
N55 I-R6 (ABZIEHEN DES UEBERLAPP X ACHSE)
N56 J-R8 (ABZIEHEN DES UEBERLAPP Y ACHSE)
N57 G77 T(GENAU HIER RASTERN BEGINNEN?) N80
(UMFAHREN DES ZU RASTERNDEN BEZIRKS:)
(STARTPUNKT PIA OBERHALB DER SPITZE DER ELEKTRODEN)

```

(MPC FUEHRT NUR EINE OPERATION JE ZEILE AUS!)

N64 R12=R1*R3 (MAXX = RECHTS OBEN)

N65 IR12

N66 R12=R2*R4 (MAXY = RECHTS UNTEN)

N67 JR12

N68 R12=R1*R3 (-MAXX=LINKS UNTEN)

N69 I-R12

N70 R12=R2*R4 (-MAXY = LINKS OBEN)

N71 J-R12 (AM RASTERSTARTPUNKT ANKOMMEN)

N80 G78 T(TRIGSTIF + STARTPUNKT OK?) N999
(RASTERN BEGINNT)

N81 G94 I J K (ACHSEN AUF NULL SETZEN)

N90 R11=R0 (ZAEHLER FUER Y-RICHTUNG INITIALISIEREN)

N91 G79 T(FLASHINTERVALL IN S EINGEBEN) R5 5

N92 R5=R5-0.5 (ABZIEHEN DER PROGRAMMLAUFDAUER)

N100 R10=R0 (N100 USW. SCHLEIFE FUER X HIN)

N101 R13=0

N102 G4 X2.0

N103 M40

N104 G4 X0.001

N106 M41

N107 R13=R13+1

N108 G74 R13 R7 N102

N109 G4 XR14 (WARTEN AUF TIDA REGISTRIERUNG)

N110 IR3 (VERSCHIEBUNG IN X UM R3)

N114 R13=0 (REPETITION COUNTER)

N115 G4 XR5 (WARTEN ZUM AUFLADEN DES FLASH)

N120 M40 (HILFSEINGANG EIN)

N130 G4 X0.001 (WARTEN 0.001S)

N140 M41 (HILFSEINGANG AUS)

N141 R13=R13+1 (REPETITION COUNTER INCREMENT)

N142 G4 XR14 (WARTEN AUF TIDA REGISTRIERUNG)

N143 G74 R13 R7 N115

N150 R10=R10+1 (ZAEHLER IN X-RICHTUNG EINS HOCHSETZEN)

N160 G74 R10 R1 N110 (NAECHSTER PUNKT IN X)

N200 JR4 (VERSCHIEBUNG IN Y UM R4 MM)

N210 R11=R11+1

N220 G72 R11 R2 N440 (ABBRUCH FALLS MAX Y ERREICHT)

N300 R10=R0 (N300 SCHLEIFE FUER X HER)

N301 R13=0 (REPETITION COUNTER)

N302 G4 XR5 (WARTEN)

N303 M40 (TRIGGER ON)

N304 G4 X0.001 (TRIGGER WAIT)

N306 M41 (TRIGGER OFF)

N307 R13=R13+1 (REPETITION COUNTER INCREMENT)

N308 G4 XR14 (WARTEN AUF TIDA REGISTRIERUNG)

N309 G74 R13 R7 N302 (REPETITION LOOP)

N310 I-R3 (VERSCHIEBUNG IN X UM -R3 MM)

N311 R13=0 (REPETITION COUNTER)

N315 G4 XR5 (WARTEN)

N320 M40 (TRIGGER ON)

N330 G4 X0.001 (TRIGGER WAIT)
 N340 M41 (TRIGGER OFF)
 N341 R13=R13+1 (REPETITION COUNTER INCREMENT)
 N342 G4 XR14 (WARTEN AUF TIDA REGISTRIERUNG)
 N343 G74 R13 R7 N315 (REPETITION LOOP)
 N350 R10=R10+1
 N360 G74 R10 R1 N310
 N400 JR4 (VERSCHIEBUNG IN Y UM R4 MM)
 N410 R11=R11+1
 N420 G75 R11 R2 N100 (NAECHSTER PUNKT IN Y)
 N430 G70 N470
 N440 R12=R1-1 (EVTL. X ZURUECK ZUM BEGINN DES FELDES)
 N450 R12=R12*-R3
 N460 IR12
 N470 R12=R2*-R4 (Y ZURUECK ZUR AUSGANGSPOSITION)
 N480 JR12
 N500 G77 T(DEN BEREICH ERNEUT RASTERN?) N80
 N510 IR6 (ZURUECK ZUR INITIALPOSITION X)
 N520 JR8 (ZURUECK ZUR INITIALPOSITION Y)
 N999 M30
 □

6.5 Curriculum vitae

Name:	Corinna Gabriele Walz
Geburtsdatum:	21. November 1976
Geburtsort:	Castrop-Rauxel
Familienstand:	verheiratet
05.2004 – 04.2008	Promotion am Institut für Neurophysiologie
05.2004 – 12.2004	Wissenschaftliche Mitarbeiterin im SFB 509 -Neurovision
04.2004	Studienabschluss als Diplom-Biologin
05.2003 – 02.2004	Anfertigung der Diplomarbeit am Lehrstuhl für Zellphysiologie
10.1999 – 04.2003	Studium der Biologie an der Ruhr-Universität Bochum
04.1999 – 09.1999	Praktikum im Bereich der Physiologie und Meeresbiologie bei der „Estacion Costera de Investigaciones Marinas“ der Katholischen Universität in Santiago de Chile
03.1998 – 09.1998	Studium der Pharmazie an der Westfälischen-Wilhelms-Universität Münster
08.1996 – 02.1997	Praktikum im Bereich Chirurgie im Evangelischen Krankenhaus Castrop-Rauxel
08.1987 – 07.1996	Adalbert-Stifter Gymnasium in Castrop-Rauxel
08.1983 - 07.1987	Elisabeth-Grundschule in Castrop-Rauxel

6.6 Publications

articles:

Walz, C., Jüngling, K., Leßmann, V., Gottmann, K., Presynaptic Plasticity in an Immature Neocortical Network Requires NMDA Receptor Activation and BDNF Release, *J. Neurophysiol.*, 96:3512-3516, 2006

Walz, C., Schubert, D., Staiger, J.F., Gottmann, K., Developmental plasticity of glutamatergic synapses on layer Vb pyramidal neurons in the mouse barrel cortex.
(will be submitted in April 2008)

Walz, C., Gottmann, K., Leßmann, V., Staiger, J.F., Schubert, D., Spatial mapping of transplanted BDNF-deficient neurons reveals a local reduction of GABAergic inputs
(in preparation)

Contributions at congresses (poster):

Walz, C., Leßmann, V., Gottmann, K., Presynaptic long-term induction of immature glutamatergic synapses in cultured neocortical neurons, *Proc. 30th Göttingen Neurobiology Conference 2005*

Walz, C., Schubert, D., Staiger, J.F., Gottmann, K., Presynaptic properties of immature glutamatergic synapses in neocortical neurons, *SfN 35th Annual Meeting Washington 2005*

Walz, C., Schubert, D., Staiger, J.F., Gottmann, K., Presynaptically immature glutamatergic synapses in layer 5B of the mouse somatosensory cortex, *85th Annual Meeting of the DPG München 2006*

Walz, C., Schubert, D., Staiger, J.F., Gottmann, K., Developmental plasticity of layer 5B glutamatergic synapses in the mouse barrel cortex, *5th Forum of European Neuroscience Wien 2006*

Contributions at congresses (oral presentation):

Walz, C., Schubert, D., Staiger, J.F., Gottmann, K., Coupling of pre- and postsynaptic maturation of glutamatergic synapses on layer Vb pyramidal neurons in mouse somatosensory cortex *87th Annual Meeting of the DPG Köln 2008*

7. Acknowledgements

At this point I would like to convey my personal thanks to everyone who contributed to the success of this work:

First of all, I would like to thank Prof. Dr. Kurt Gottmann, not only for the time and effort teaching me the basics about electrophysiology, but also for his absolute support and lively discussions that essentially contributed to this work. I could not have had a better guide on my way into the scientific world. Furthermore, I would like to acknowledge Prof. Dr. Christine R. Rose for providing excellent support.

I am deeply indebted to Dr. Dirk Schubert for weeks of teaching me the basics about *caged* glutamate as well as active guidance and outstanding support in any way. Also, I would like to thank all my colleagues and former colleagues in Bochum for the great atmosphere in the lab: Dr. Gunnar Kattenstroth, Dr. Kay Jüngling, Dr. Andrea Copi, Martina Bohndorf, Dipl.-Biol. Adriana Stan, Dipl.-Biol. Kim Pielarski, Cand. Biol. Bastian Elßner-Beyer, Cand. Med. Andreas Fiederling and Cand. Med. Sebastian Flerus. Thank you for support, advices and having fun!

For excellent technical assistance I would like to thank Harry Bartel and Stefan Schätz.

Also, I would like to thank all my friends for supporting my work in different ways and staying with me, even though I am most often not there.

Above all, I would like to thank Chris for his unrestricted support during these not always easy times and my parents for their long lasting support, understanding and confidence. Last but not least I would like to thank the extended family and of course Ben!

THANK YOU!!!